

DEVELOPMENT OF A METHODOLOGY FOR PREDICTION OF SURFACE  
ROUGHNESS OF CURVED CAVITIES MANUFACTURED  
BY 5-AXES CNC MILLING

A THESIS SUBMITTED TO  
THE GRADUATE SCHOOL OF NATURAL AND APPLIED SCIENCES  
OF  
MIDDLE EAST TECHNICAL UNIVERSITY

BY

KÂZIM ARDA ÇELİK

IN PARTIAL FULFILLMENT OF THE REQUIREMENTS  
FOR  
THE DEGREE OF MASTER OF SCIENCE  
IN  
MECHANICAL ENGINEERING

MAY 2007

Approval of the Graduate School of Natural and Applied Sciences

---

Prof. Dr. Canan ÖZGEN  
Director

I certify that this thesis satisfies all the requirements as a thesis for the degree of  
Master of Science

---

Prof. Dr. Kemal İDER  
Head of the Department

This is to certify that we have read this thesis and that in our opinion it is fully  
adequate, in scope and quality, as a thesis for the degree of Master of Science

---

Prof. Dr. Mustafa İlhan GÖKLER  
Supervisor

Examining Committee Members:

Prof. Dr. Demir BAYKA (METU, ME)

Prof. Dr. Mustafa İlhan GÖKLER (METU, ME)

Prof. Dr. R.Orhan YILDIRIM (METU, ME)

Prof. Dr. M.A.Sahir ARIKAN (METU, ME)

Prof. Dr. Can ÇOĞUN (GAZİ UNV., ME)

I hereby declare that all information in this document has been obtained and presented in accordance with academic rules and ethical conduct. I also declare that, as required by these rules and conduct, I have fully cited and referenced all material and results that are not original to this work.

Kâzım Arda ÇELİK

## **ABSTRACT**

### **DEVELOPMENT OF A METHODOLOGY FOR PREDICTION OF SURFACE ROUGHNESS OF CURVED CAVITIES MANUFACTURED BY 5-AXES CNC MILLING**

**ÇELİK, Kâzım Arda**

M.Sc., Department of Mechanical Engineering

Supervisor: Prof. Dr. Mustafa İlhan GÖKLER

May 2007, 97 pages

The surface quality is identified by surface roughness parameters. The average surface roughness (Ra) is used in this study, as it is the most commonly used roughness parameter in the industry. A particular curved cavity of a forging die is selected for the experimental study. Different milling methods are tested. The comparison studies are conducted between 3-axes and 5-axes milling, linear and circular tool path strategies and down and up milling. According to the experimental study, appropriate method is determined for the milling of a particular curved cavity of a forging die.

The experimental analysis based on design of experiments (DOE) has been employed by considering cutting speed, feed per tooth and stepover parameters. Multiple linear regression technique is used by which a mathematical formula has been developed to predict the Ra values for milling parameters. The results of the mathematical formula are controlled by conducting test experiments and good correlations are observed between the results of the formula and the results of test experiments.

**Keywords:** CNC Milling, Milling process parameters, Surface Roughness, Design of Experiment, Multiple linear regression.



## ÖZ

### BEŞ-EKSEN CNC FREZE TEZGAHI İLE ÜRETİLEN EĞRİSEL KAVİTELERİN YÜZEY PÜRÜZLÜLÜĞÜNÜN KESTİRİMİ İÇİN BİR YÖNTEM GELİŞTİRİLMESİ

ÇELİK, Kâzım Arda

Yüksek Lisans, Makina Mühendisliği Bölümü

Tez Yöneticisi: Prof. Dr. Mustafa İlhan GÖKLER

Mayıs 2007, 97 sayfa

Yüzey pürüzlük parametreleri yüzey kalitesini tanımlamak için kullanılırlar. Endüstride en sık kullanılan parametre ortalama yüzey pürüzlüğüdür (Ra) ve bu nedenle bu çalışmada kullanılmıştır. Denesel çalışma için eğrisel bir dövme kalıp kavitesi seçilmiştir. Değişik frezeleme metotları test edilmiştir. 3-eksen ve 5-eksen frezeleme, doğrusal ve dairesel takım yolu stratejileri ve yukarı ve aşağı frezeleme metotları kıyaslanmıştır. Bu deneysel çalışma doğrultusunda eğrisel bir dövme kalıp kavitesinin freze ile işlenmesi için uygun bir metot belirlenmiştir.

Deney tasarımı metodu temel alınarak ve kesme hızı, diş başı ilerleme ve yanal ilerleme parametreleri dikkate alınarak deneysel bir çalışma gerçekleştirilmiştir. Çoklu doğrusal regresyon tekniği kullanılarak frezeleme parametrelerine göre Ra değerini tahmin etmeye yönelik matematiksel bir formül geliştirilmiştir. Matematiksel denklemden elde edilen sonuçlar test deneyleriyle kontrol edilmiş ve iyi neticeler alınmıştır.

**Anahtar Sözcükler:** CNC frezeleme, Freze işlemi parametreleri, Yüzey pürüzlüğü, Çoklu doğrusal regresyon, Deney Tasarımı

To My Family,

## ACKNOWLEDGEMENTS

I express sincere appreciation to Prof. Dr. Mustafa İlhan Gökler for his guidance, advice, criticism, systematic supervision, encouragements, and insight throughout the study.

I also would like to thank to METU-BİLTİR Research & Application Center, ORTADOĞU RULMAN SANAYİ (ORS), ASELSAN and AKSAN Steel Forging Company for the facilities provided for my work.

I wish to thank to Mr. Özcan Kahramangil, Mr. İhsan Özsoy, Mr. Serdal Çalı, Mr. Selahattin Çetin and Ms. Meltem Yıldız, for their support and help.

Special thanks go to my colleagues, Arda Özgen, Hüseyin Öztürk, Özgür Cavbozar, İlker Durukan, Mehmet Maşat, Sevgi Saraç and Halit Şahin for their valuable support and aid.

I offer sincere thanks to my wife Göknur Çelik and my parents, Nesrin and Zafer Çelik and my brother Gökhan Çelik, for their encouragement and faith in me.

## TABLE OF CONTENTS

ABSTRACT .....	iv
ÖZ .....	v
ACKNOWLEDGEMENTS .....	vii
TABLE OF CONTENTS .....	viii
LIST OF TABLES.....	xi
LIST OF FIGURES .....	xiii
LIST OF SYMBOLS .....	xv
CHAPTERS	
1.INTRODUCTION .....	15
1.1 Importance of surface quality of curved surfaces .....	15
1.2 Forging Die Manufacturing .....	15
1.3 Using of CNC Milling Machines in Die Manufacturing.....	15
1.4 Previous Studies .....	15
1.5 Scope of the Thesis.....	15
2.MEASUREMENT OF SURFACE QUALITY .....	15
2.1 Surface Imperfections.....	15
2.2 Common Parameters of Roughness .....	15
2.3 Roughness Measurement .....	15
2.4 Filtering.....	15

3.DESIGN OF EXPERIMENT .....	15
3.1 The Two Factor Factorial Design.....	15
3.2 The 2 <sup>3</sup> Factorial Design .....	15
3.3 Deriving the Formula .....	15
3.3.1 Linear Regression Models.....	15
3.3.2 Linear Regression Models for 2 <sup>3</sup> Factorial Design .....	15
3.3.3 Estimation of the Parameters in Linear Regression Models .....	15
4.MILLING PARAMETERS IN MANUFACTURING .....	15
4.1 Determining the Test Specimen.....	15
4.2 Milling Tool Selection.....	15
4.3 Three and Five Axes CNC Milling .....	15
4.4 Determination of the Value of Depth of Cut in Rough Cutting.....	15
4.5 Cutting Path .....	15
4.6 Down (Climb) and Up (Conventional) milling.....	15
4.7 Cutting Parameters in CNC Milling.....	15
4.8 Other Parameters .....	15
5.MACHINING EXPERIMENTS ON CNC MILLING MACHINE.....	15
5.1 Test Specimen and Cutting Parameters .....	15
5.2 The Milling Experiments for Comparison.....	15
5.3 Comparison of 3-Axes and 5-Axes Milling.....	15
5.3.1 3-Axes Milling .....	15
5.3.2 5-Axes Milling .....	15
5.3.3 Discussion of Results.....	15
5.4 Comparison of Down and Up Milling.....	15
5.5 Comparison of Cutting Paths.....	15
5.6 General Discussion of the Experiments.....	15
6.ANALYSIS OF THE EXPERIMENTS AND DERIVATION OF Ra PREDICTION FORMULAS .....	15
6.1 Ra Analysis for Down Milling.....	15
6.1.1 Effect Estimation .....	15

6.1.2	Ra Prediction Formula .....	15
6.2	Ra Analysis When Down and Up Milling is Used Together.....	15
6.2.1	Effect Estimation .....	15
6.2.2	Ra Prediction Formula .....	15
7.	CONCLUSIONS AND FUTURE WORK .....	15
7.1	Conclusions.....	15
7.2	Future work.....	15
	REFERENCES .....	15
	APPENDICES	
	A.MATERIAL LEFT THICKNESSES AT THE STAIRCASE TIPS.....	15
	B.EXAMPLES OF MILLING REPORTS OF VERICUT .....	15
	C.MAZAK VARIAXIS 630-5X CNC MILLING CENTER.....	15
	D.PROPERTIES OF DIE MATERIAL.....	15
	E.CALCULATION OF VARIABLE COEFFICIENTS.....	15

## LIST OF TABLES

Table 3.1 Signs of factorial effects [22].....	15
Table 5.1 Cutting parameters used in the first set of experiments .....	15
Table 5.2 The methods used during the first set of experiments.....	15
Table 5.3 The Ra measurement results of the first set of experiments.....	15
Table 5.4 The Ra values of the 3 axes milling experiments .....	15
Table 5.5 The Ra results of 5-axes milling with 15 degree inclination angle.....	15
Table 5.6 Ra Comparison of manufacturing by 3-axes and 5-axes milling.....	15
Table 5.7 Results of manufacturing by down and up milling .....	15
Table 5.8 Ra values for linear and circular cutting paths when down milling was used.....	15
Table 5.9 Ra values for linear and circular cutting paths when down and up milling were used together .....	15
Table 6.1 Limits of milling parameters for Ra prediction experiments.....	15
Table 6.2 The results of second set of experiments for Ra prediction.....	15
Table 6.3 Main and Interaction Effects on Ra ( $\mu\text{m}$ ) value when down milling is used.....	15
Table 6.4 Measurement results of Ra values for second set of experiments .....	15
Table 6.5 Calculated error and error percentage values for second set of experiment of Ra prediction .....	15
Table 6.6 The observed Ra values used to test the accuracy of Ra prediction formula.....	15
Table 6.7 Calculated error and error percentage values for test experiments .....	15
Table 6.8 The result of the third set of Ra prediction experiments .....	15
Table 6.9 Main and Interaction Effects on Ra ( $\mu\text{m}$ ) value when both of the down and up milling used together .....	15
Table 6.10 Measurement results of average Ra values for third set of experiments when down and up milling used together .....	15

Table 6.11 Calculated error and error percentage values for Ra prediction when down and up milling is used together .....	15
Table 6.12 The observed Ra values used to test the accuracy of Ra prediction formula.....	15
Table 6.13 Calculated error and error percentage values for test experiments .....	15
Table A.1 Material left thicknesses at the staircase tips when the tool is cutting with 15° inclination angle.....	15
Table D.1 Material category.....	15
Table D.2 Material composition.....	15
Table D.3 Material mechanical properties.....	15
Table D.4 Material thermal properties.....	15



## LIST OF FIGURES

Figure 1.1 General steps of production of forging dies in Aksan Steel Forging Company, Ankara [8].....	15
Figure 1.2 EDM working with a dielectric liquid [8] .....	15
Figure 1.3 Picture of cracks in the layer [6].....	15
Figure 1.4 The surface manufactured by using EDM [8] .....	15
Figure 1.5 Manual polishing on die surface [8].....	5
Figure 1.6 Manual polishing on die surface [8].....	15
Figure 1.7 Proposed steps of production of a forging die .....	15
Figure 1.8 Example of the structure of a 3-axes milling machine [11] .....	15
Figure 1.9 Rotary Axis Labeling [10].....	15
Figure 1.10 Example of the structure of a 4-axes milling machine [11] .....	15
Figure 1.11 Example of the structure of a 5-axes milling machine [11] .....	15
Figure 2.1 Example of a surface profile [3] .....	15
Figure 2.2 Lay types [16] .....	15
Figure 2.3 $R_a$ and $R_q$ shown on a surface profile [20] .....	15
Figure 2.4 $R_z$ and $R_{max}$ shown on a surface profile [20] .....	15
Figure 2.5 Stylus type surface roughness measurement machine [21].....	15
Figure 2.6 The lengths of roughness measurement [21].....	15
Figure 2.7 Tracing of a stylus tip [19] .....	15
Figure 2.8 Sample lengths smaller than wave length [19] .....	15
Figure 2.9 Redrawing of Figure 2.8 using the axis line [19] .....	15
Figure 2.10 Sample lengths bigger than wave length [19] .....	15
Figure 2.11 Skid movement on a profile [19] .....	15
Figure 2.12 2RC Filter [19].....	15
Figure 2.13 2RC filter effect [19] .....	15

Figure 3.1 A two factor factorial experiment [22].....	15
Figure 3.2 A two factor factorial experiment with the response values .....	15
Figure 3.3 A two factor factorial experiment with interaction.....	15
Figure 3.4 The Geometric View of the $2^3$ factorial design [22].....	15
Figure 4.1 CAD model of M24 forged eye bolt .....	15
Figure 4.2 Die of the eye bolt.....	15
Figure 4.3 Designed model of the test specimen.....	15
Figure 4.4 Edge fillet of the shank section of die of eye bolt .....	15
Figure 4.5 Endmill [25].....	15
Figure 4.6 Ball endmill [25].....	15
Figure 4.7 3-axes milling .....	15
Figure 4.8 Cutting Points in 5-axes milling .....	15
Figure 4.9 5-axes milling with an inclination angle .....	15
Figure 4.10 Lead angle .....	15
Figure 4.11 Tilt angle.....	15
Figure 4.12 Die surface geometry after rough cut.....	15
Figure 4.13 Material thickness that is left after rough cut .....	15
Figure 4.14 The position of the stair tips with respect to the radius center .....	15
Figure 4.15 Radius profile after the finish cut.....	15
Figure 4.16 Circular tool path.....	43
Figure 4.17 Linear tool path.....	15
Figure 4.18 The CAD model of die surface .....	15
Figure 4.19 NC programming .....	15
Figure 4.20 Simulation of MANUS post processor program.....	15
Figure 4.21 Simulation result of Vericut when circular tool paths were used .....	15
Figure 4.22 Simulation result of Vericut when linear tool paths were used .....	15
Figure 4.23 Down milling and up milling [9] .....	15
Figure 4.24 Stepover.....	15
Figure 5.1 The test specimen.....	15
Figure 5.2 Test specimen after rough cut.....	15
Figure 5.3 Test specimen during finish cut.....	15
Figure 5.4 Taylor Hobson's Talysurf PGI stylus type surface roughness measuring machine .....	15

Figure 5.5 The photographs of test specimen surfaces of first set of experiments used for comparison study .....	15
Figure 5.6 The Photographs of the surfaces that are machined by using 3-axes CNC milling .....	15
Figure 5.7 The photograph of the surface that is machined by using 5-axes milling normal to surface .....	15
Figure 5.8 5-axes machining of the radial die cavity with an inclination angle....	15
Figure 5.9 Tool tip of a ball endmill.....	15
Figure 5.10 Photographs of Surfaces that are machined using 5-axes milling .....	15
Figure 5.11 5-axes machining with an inclination angle .....	15
Figure 5.12 The photographs of the surfaces that are machined for the comparison of down and up milling .....	15
Figure 5.13 Simulation of down milling.....	62
Figure 5.14 Simulation of down and up milling used together.....	15
Figure 5.15 Photographs of the surfaces, machined for the comparison of tool path strategies when down milling was used.....	15
Figure 5.16 Photographs of the surfaces, machined for the comparison of tool path strategies when down and up milling were used together .....	15
Figure 6.1 The Geometric View of the $2^3$ factorial design for Ra prediction experiments .....	15
Figure 6.2 The photograph of the test specimen of the second set of experiments manufactured by down milling.....	15
Figure 6.3 Main effects plots on Ra value when down milling is used.....	15
Figure 6.4 Interaction effects plots on Ra value when down milling is used .....	15
Figure 6.5 The photograph of the test specimen of the third set of experiments manufactured by using down and up milling together .....	15
Figure 6.6 Main effects plots when both of the down and up milling used together.....	15
Figure 6.7 Interaction effects plots when both of the down and up milling used together.....	15
Figure C.1 Mazak Variaxes 630-5X milling center.....	15

## LIST OF SYMBOLS

### SYMBOL

$a_e$	: Stepmover
$D$	: Tool diameter
$d_{af-max}$	: Maximum value of allowable depth of cut in finish cut
$d_{af-min}$	: Minimum value of allowable depth of cut in finish cut
$d_{cp}$	: Distance of cutting point to the tool axis
$d_f$	: Depth of cut value in finish cut
$d_r$	: Depth of cut value in rough cut
$f_z$	: Feed per tooth
$N$	: Spindle speed
$r$	: Radius of die cavity
$r^*$	: Distance of stair tips to die radius center
$t_m$	: Minimum material left after rough cut
$t_s$	: Material thickness due to the height of the stairs
$V_c$	: Cutting speed
$V_f$	: Table feed
$X_1$	: Distance between the stair tip and the x-coordinate of the radius center
$X_2$	: Distance between the stair bottom and the x-coordinate of the radius center

$Y_1$  : Distance between the stair tip and the y-coordinate of the radius center

$Y_2$  : Distance between the stair bottom and the y-coordinate of the radius center

$z$  : Number of tool flutes

## **CHAPTER 1**

### **INTRODUCTION**

#### **1.1 Importance of surface quality of curved surfaces**

In milling process, obtaining desired surface quality is significant. The surfaces may be classified as planer, inclined and curved. Curved surfaces are more complex than the other surfaces. Because of this, obtaining desired surface quality is more difficult for these kinds of surfaces. 5-axes machining may be used for the milling of this type of surfaces to obtain better surface quality. Forging is a commonly used manufacturing process in industry and most of the dies used in forging process have curved cavities.

Forging may be defined as the plastic deformation of metals by applying compressive forces by manual or power hammers, presses or special forging machines. The forging operation can be done cold, warm or hot [1]. During this process open and closed forging dies can be used. In close die forging, as the forged material takes the shape of the die because of the pressure applied on it, the quality of the forging products highly depends on the surface quality of its die [2]. As a result, good surface quality for die surfaces is very important in close die forging process. Moreover, as the surface quality increases, the friction between the die and the working material decreases which results with lower forces in the process. Therefore, it may improve the life of the forging die and also decrease the energy consumption. Surface quality also affects several functional attributes of parts, such as wearing, heat transmission or ability of distributing and holding a lubricant [3]. Because of this, obtaining the desired surface quality is very essential in die manufacturing. In order to define the die surface quality, surface

roughness parameters are used. Consequently, obtaining better surface roughness values is an advantage for die forging.

## **1.2 Forging Die Manufacturing**

The common way of manufacturing of forging die, which is also used in the Aksan Steel Forging Company in Ankara, is shown in Figure 1.1. Firstly, the forging part geometry is examined. According to the part geometry forging die geometry and copper electrode, which will be used in die manufacturing process, is designed. Computer Aided Design (CAD) systems are used to obtain the 3D models of die and copper electrode. Then using Computer Aided Manufacturing (CAM) system, manufacturing tool paths are formed on the CAD model of the designed parts [4]. These tool paths are converted into Numerical Control (NC) codes by postprocessors, which are used to program CNC milling centers. Milling operation is done separately on the die material and copper electrode. After milling operations are conducted, to obtain the desired surface quality on die material, a finish operation is done in Electro Discharge Machine (EDM) using the copper electrode.

EDM removes electrically conductive material by means of rapid and repetitive spark discharges resulting from local explosion of a dielectric liquid shown in Figure 1.2. This explosion is produced by applying a voltage between copper electrode and a workpiece [5]. EDM process formed a layer as a result of the solidification of a melted zone and is known to exhibit high hardness also as a consequence of the rapid quenching process, micro- and nanocracks are formed at the surface of the layer (Figure 1.3) [6]. As the hardness is higher in this layer, this layer become more brittle and the micro cracks may lead to crack propagation during forging process on die surfaces. Also the roughness of the surface formed after EDM process is poor in surface quality as seen in Figure 1.4. Because of these effects, polishing should be used after EDM processes on die surfaces to remove this hardened layer and to reduce the surface roughness until the required condition is achieved.

Polishing process is done manually by using a portable grinding machine as shown in Figure 1.5 and Figure 1.6. The surface roughness to be achieved

mainly depends on the choice of abrasives and in particular on the grain size. Polishing for molds and dies is expensive, time consuming, labor intensive, and error prone. Mistakes committed by a human operator at a later stage may result in expensive re-working [7].

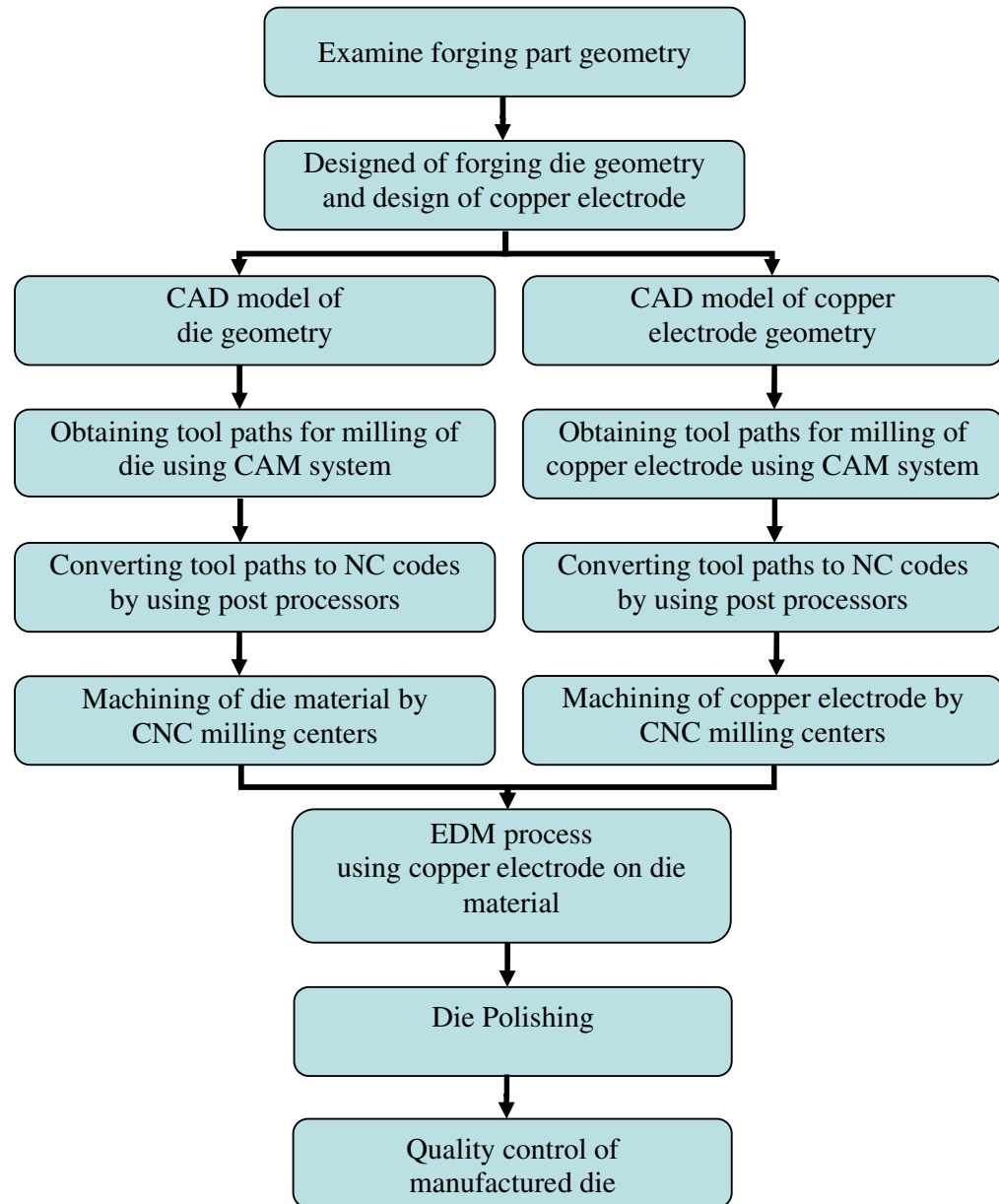


**Figure 1.1 General steps of production of forging dies in Aksan Steel Forging Company, Ankara [8]**



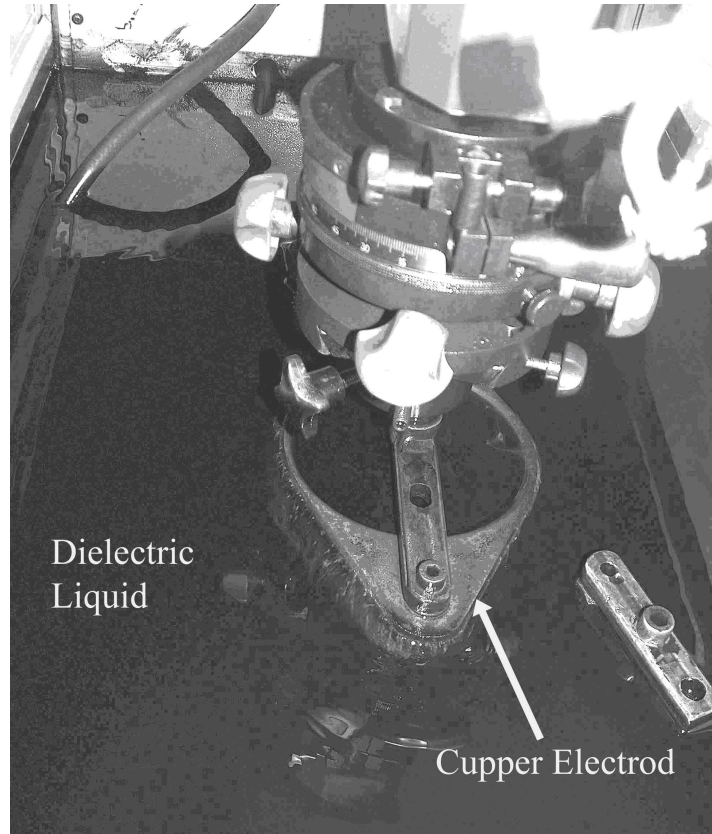


**Figure 1.2 EDM working with a dielectric liquid [8]**

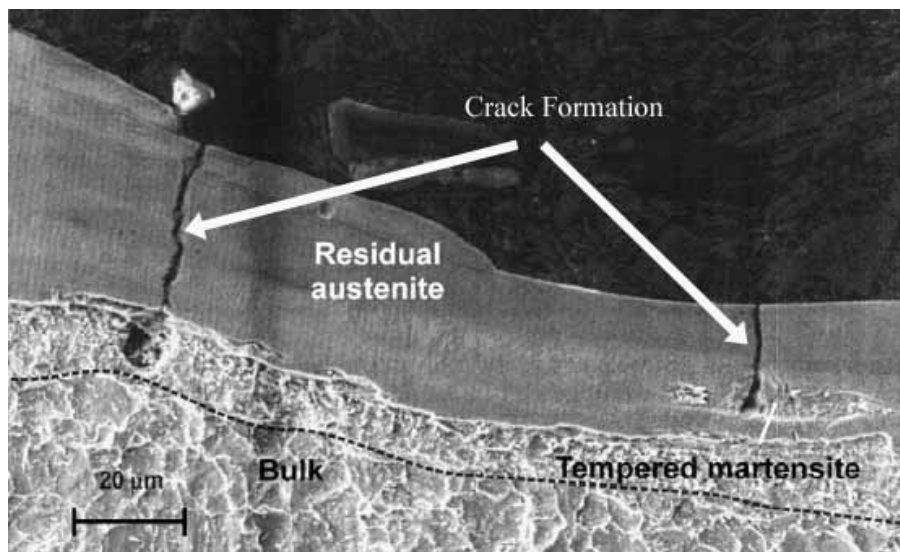


**Figure 1.3 Picture of cracks in the layer [6]**



**Figure 1.4 The surface manufactured by using EDM [8]**



**Figure 1.5 Manual polishing on die surface [8]**



**Figure 1.6 Manual polishing on die surface [8]**

If the die is produced in desired surface quality after milling process, it is possible to use die without any additional processes. By this way, manufacturing of copper electrode and EDM and polishing processes may be totally eliminated as seen in Figure 1.7, which will decrease the cost of forging die production.

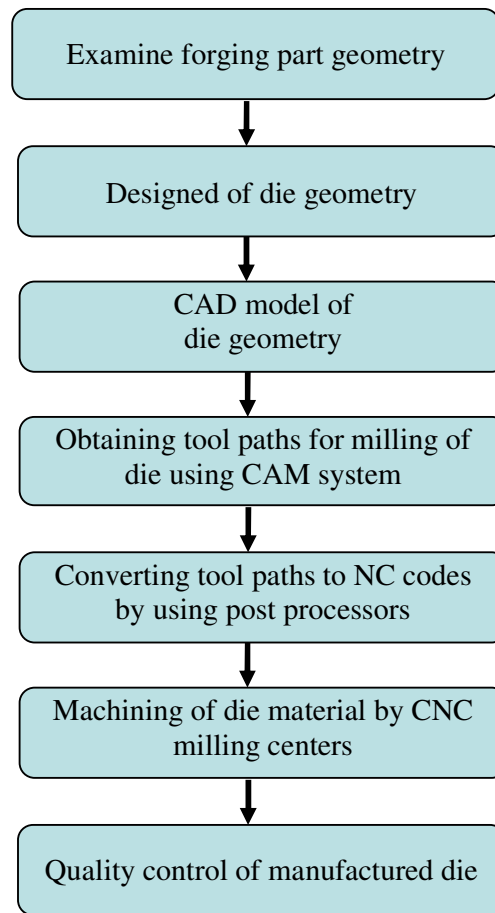


**Figure 1.7 Proposed steps of production of a forging die**

### **1.3 Using of CNC Milling Machines in Die Manufacturing**

As the milling process is versatile and highly productive, a variety of machines have been developed to employ the milling principle [9]. The CNC milling machines which can be used in forging die machining may be classified as 3-axes, 4-axes and 5-axes according to the number of simultaneous motion achieved with independently working motors of the machine tool.

The motion of the 3-axes milling machines are in three linear axes (X, Y and Z) as seen in Figure 1.8. The orientation of these linear axes may depend on the machine tool configurations. In some machine tools, all of these linear

motions are activated by spindle head, while in some other machine tools; some or all linear motions can be performed by the table instead [10].

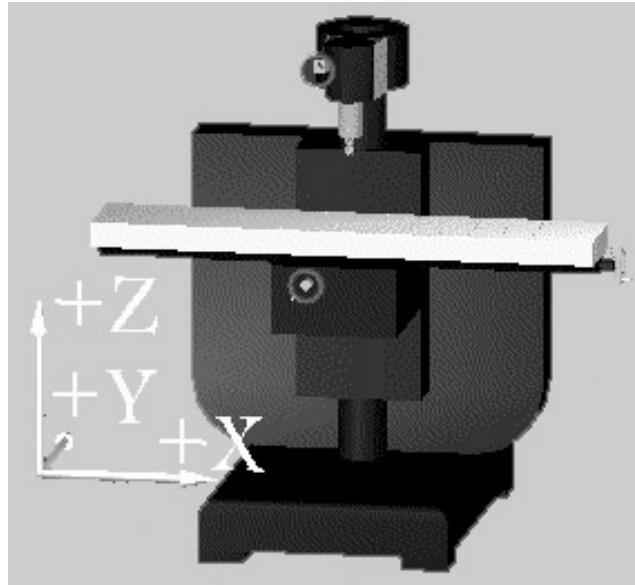


**Figure 1.8** Example of the structure of a 3-axes milling machine [11]

4-axes milling machines have one rotational axis and 5-axes milling machines have two rotational axes in addition to three linear axes (X, Y and Z). The variations in 4-axes and 5-axes milling machines mainly depend on the differences in rotary axes. By convention, rotary axes are labeled according to the orientation of the rotation axes as shown in Figure 1.9 [10]. The examples of the structures of 4-axes and 5-axes milling machines are demonstrated in Figure 1.10 and Figure 1.11, respectively.

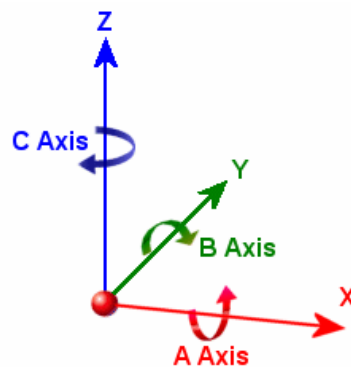


**Figure 1.9** Rotary axis labeling [10]

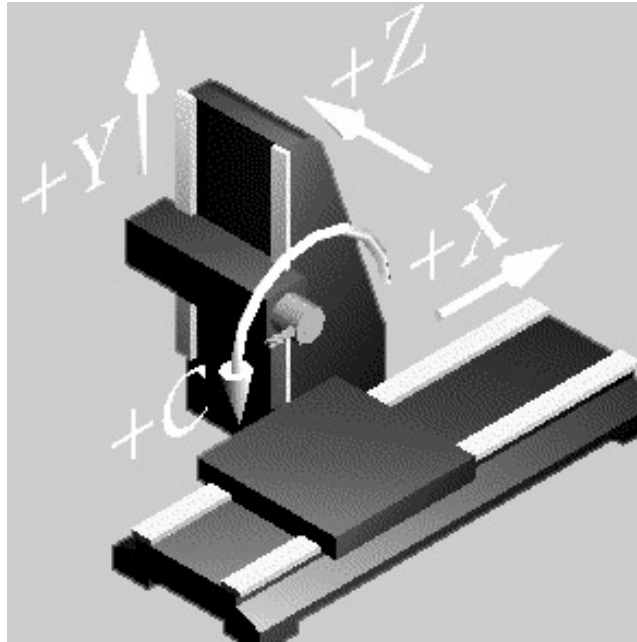


**Figure 1.10** Example of the structure of a 4-axes milling machine [11]

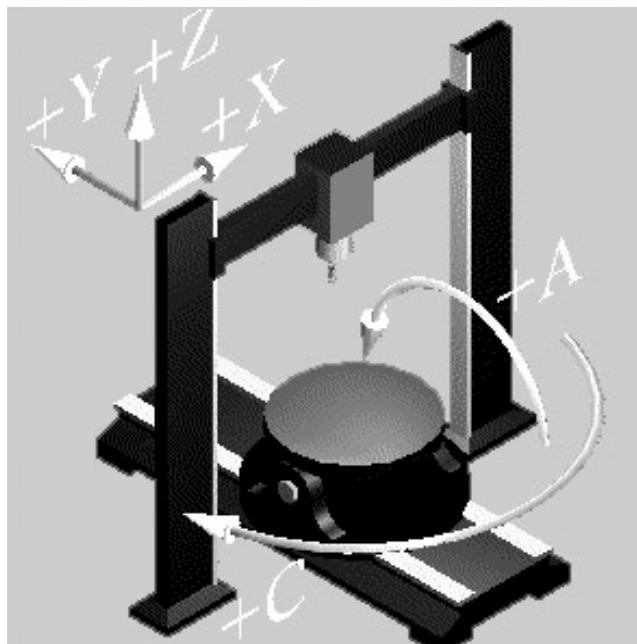


**Figure 1.11** Example of the structure of a 5-axes milling machine [11]

## 1.4 Previous Studies

In forging die manufacturing, it is very important to obtain desired surface quality. Forging dies are commonly produced by milling process and choosing the right milling conditions and parameters is very critical in determining the surface quality which is defined by surface roughness and mostly by Ra values as it is the most common used roughness parameter.

The chosen cutting methods have an important effect on surface roughness and studies are done for comparison of cutting strategies and parameters. The effects of 3-axes and 5-axes milling on surface roughness is compared by study of R. Baptista and J.F. Antune Simoes [12]. Moreover, the effects of different tool inclination angle in 5-axes milling on surface roughness, is studied by T. J. Ko, H. S. Kimi and S. S. Lee [13].

A study has been done in METU BİLTİR Research and Development Center to develop a post processor and simulation program for five axes CNC milling machines available in the Center [10].

The important goal may be considered about surface roughness is to predict the roughness value before milling process. There are studies conducted to achieve this. K.D. Bouzakis, K. Efstathiou, P. Aichouh [14] performed experiments with different parameters and according to the results of these experiments, develop a program that will predict surface quality. In the studies of Dr. Mike S. Lou, Dr. Joseph C. Chen & Dr. Caleb M. Li [3], a prediction formula of Ra value was derived for milling processes by using an endmill type of cutting tool, over a flat surface using statistical programs.

J. Vivancos , C.J. Luis , L. Costa and J.A. Ortiz [15] also studied to predict the Ra value according to the input parameters. They use design of experiment method, which is a powerful tool to analyze the effect of the input parameters and their interactions on the results by performing small number of experiments, to derive a prediction formula, according to the experimental results. They also analyze the effects of up and down milling methods on Ra value.

The above literature review shows that different researches conducted on the effects of milling methods on surface roughness and prediction techniques have been tried to be developed for Ra values, before milling process.

### **1.5 Scope of the Thesis**

Changing the milling parameters; cutting speed, feed per tooth and stepover, different roughness values can be obtained at the end of milling operations. Design of experiment methods can be used to analyze their effect on roughness value. Moreover, by using multiple linear regression technique a mathematical model may be developed by which surface roughness may be predicted in the limits of selected parameters.

Main scope of this thesis is, to develop a methodology for prediction of surface roughness of curved cavities manufactured by 5-axes CNC milling. The study includes comparison of the milling approaches of a particular curved surface and also according to comparison results, an appropriate milling approach is chosen to conduct experiments to analyze the influence of the milling parameters on the average surface roughness (Ra) and derive a mathematical formula for Ra prediction within the defined parameters limits for the chosen milling method. As a case study, surface roughness of curved cavity of a particular forging die is examined.

In Chapter 1, general information about die manufacturing and the importance of the surface quality of die cavities has been presented. In Chapter 2, the measurement of surface quality is described.

The method of design of experiment with the multiple linear regression technique is explained in Chapter 3.

In Chapter 4, the geometry of a particular forging die cavity, milling conditions and the milling parameters, which will be studied, are determined and explained. In Chapter 5, an experimental study is conducted to decide a proper method for milling of a particular curved surface.

In Chapter 6, design of experiment analysis is used for the cutting methods which are decided in Chapter 5. Different cutting speed, feed per tooth and

stepover values are used in the experiments to understand the effects of these parameters on Ra value and a formula is derived for the methods which will be used to predict the Ra values within the defined limits of milling parameters and for the selected milling conditions.

In Chapter 7, conclusion and final remarks are presented.



## **CHAPTER 2**

### **MEASUREMENT OF SURFACE QUALITY**

#### **2.1 Surface Imperfections**

During machining operations, inevitably some imperfections are left over the material.

a) Roughness includes the finest (shortest wavelength) imperfections of a surface (Figure 2.1) [16]. It can be a result of a normal manufacturing process or because of the structure of the material.

b) Waviness is that deviation from a nominal surface which ordinarily takes the form of smoothly rounded waves. It is an imperfection brought about by the deflection of the finishing machine or tool, by vibration or as the result of similar inaccuracies [17]. The wavelength of waviness is longer than roughness as demonstrated in Figure 2.1.

c) Surface texture is simply the combination of the surface imperfections which are the roughness and waviness formed on the surface.

d) Lay is the term used to refer to the direction of the predominant tool marks, grain, or pattern of the surface roughness. All surface roughness measurements or comparisons are normally taken across the lay, as this direction gives the best comparative value [17]. The machining processes like turning, grinding, milling and drilling causes lays on the machined surface. These lays can be named according to their shapes. Some examples to the lay types are given in Figure 2.2.

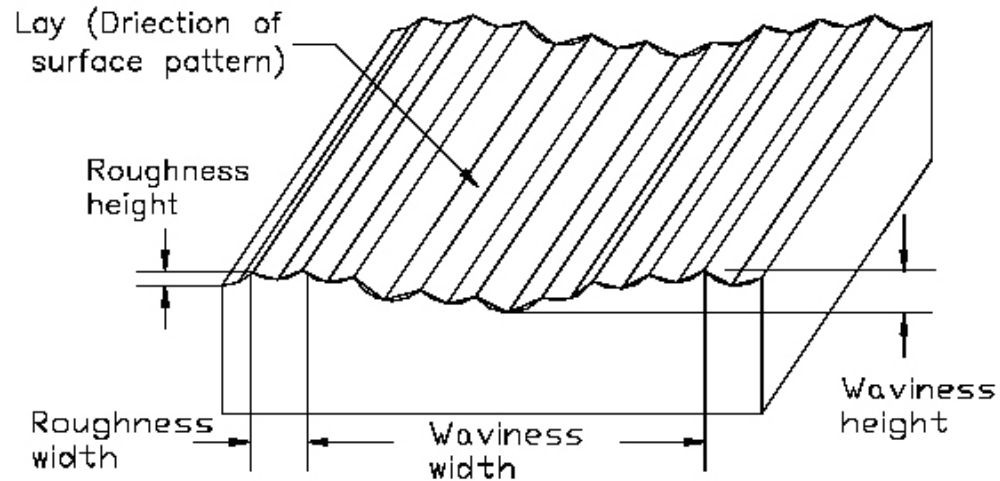


**Figure 2.1 Example of a surface profile [3]**

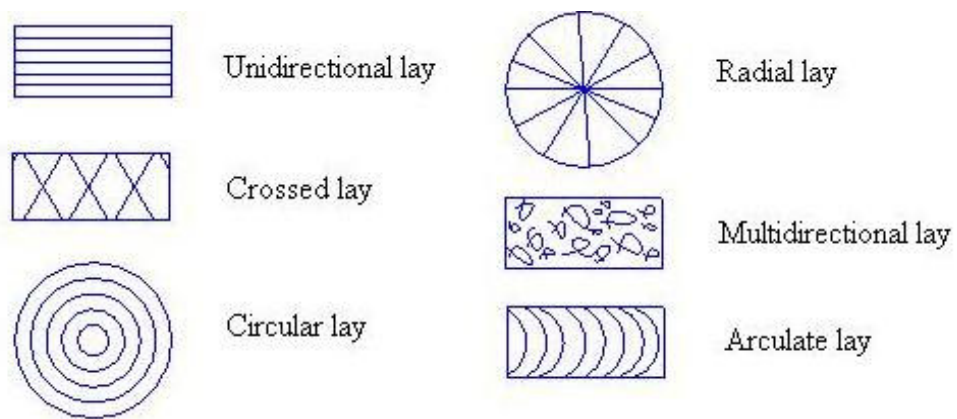


**Figure 2.2 Lay types [16]**

## **2.2 Common Parameters of Roughness**

In order to describe surface roughness, using the mean line to provide a datum, it is possible to give the surface finish profile a numerical value. The followings are the most commonly used values.

a) Average Roughness ( $R_a$ ): It is the arithmetic mean of the departures of the profile from the mean line and shown in Figure 2.3.  $R_a$  value is the most used, and universally known, international parameter of roughness [18]. The formula of  $R_a$  is as fallows [19];

$$R_a = \frac{1}{l} \int_0^l |Z(x)| dx \quad (2.1)$$

Where  $Z(x)$  is the profile ordinates of the roughness profile and  $l$  is the evaluation length.

b) Root mean square (RMS) roughness ( $R_q$ ): It is the root mean square average of the roughness profile ordinates (Figure 2.3) [20]. The formula of  $R_q$  is as follows [19];

$$R_q = \sqrt{\frac{1}{l} \int_0^l Z^2(x) dx} \quad (2.2)$$

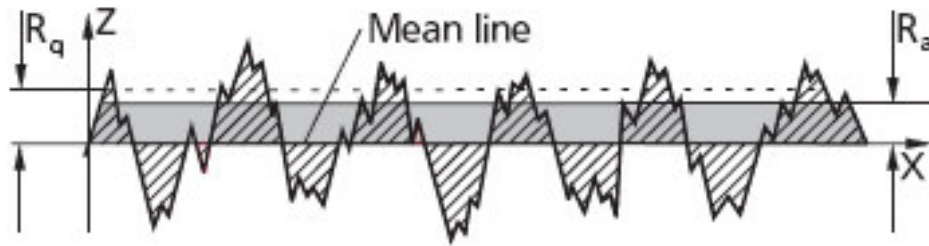


**Figure 2.3  $R_a$  and  $R_q$  shown on a surface profile [20]**

c) Mean roughness depth ( $R_z$ ): It is the average of single peak to valley heights from five adjoining sampling lengths [19].

$$R_z = \frac{1}{n} (R_{z1} + R_{z2} + \dots + R_{zn}) \quad (2.3)$$

d) Maximum roughness depth ( $R_{max}$ ): It is the largest single peak to valley height in five adjoining sampling lengths as shown in Figure 2.4 [19].

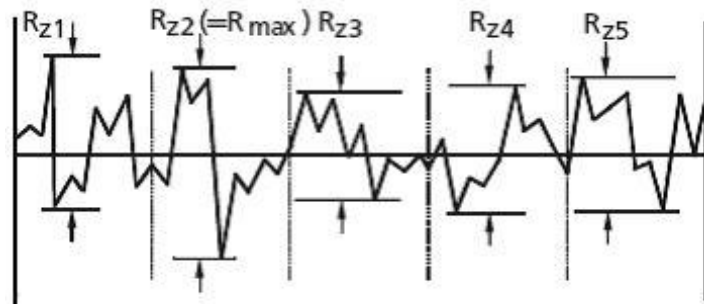


**Figure 2.4  $R_z$  and  $R_{max}$  shown on a surface profile [20]**

## 2.3 Roughness Measurement

The roughness measurement machines are the converters of the surface profiles into electrical (analog or digital) representation of the profile [16]. The stylus moves in up and down direction according to the surface texture when it is moved in the x direction as shown in Figure 2.5.

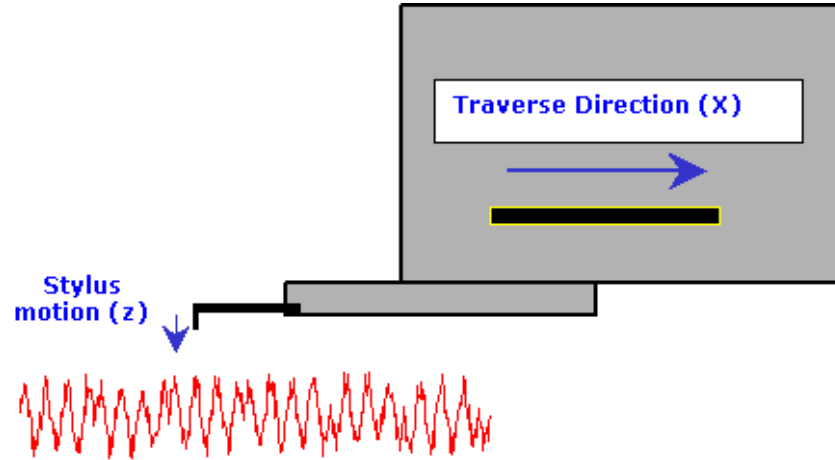


**Figure 2.5 Stylus type surface roughness measurement machine [21]**

The stylus of the measuring machine traces a path which is divided into divisions to collect data over the surface as follows;

a) Traverse length: It is the overall length traveled by the stylus when acquiring the traced profile. It is the sum of pre-travel, evaluation length, and post-travel as given in Figure 2.6.

b) Pre-travel (Run-up): It is the first part of traverse length and demonstrated in Figure 2.6 [20].

c) Post-Travel (Over Travel): It is the last part of the traverse length and shown in Figure 2.6. Pre-travel and Post-Travel are required for phase correcting filtering [20].

d) Evaluation length: It is the part of the traversing length over which the values of surface parameters are determined (Figure 2.6). The standard roughness evaluation length comprises five consecutive sampling lengths [20].

e) Cut-off: It is a profile filter, determines which wavelengths belong to roughness and which ones to waviness. There are internationally recognized cut-offs of varying lengths which are standardized in ISO , TSE (971) at 0.08mm, 0.25mm, 0.8mm, 2.5mm and 8mm dependent on the surface being checked [18]. Choosing the right cut-off value is very important in order to determine the true roughness value.

f) Sampling length: Sampling is done by breaking the data into equal sample lengths like in Figure 2.6. The sample lengths have the same numeric value as the cut-off. In other words, if you use a 0.8mm cut-off, then the filtered data will be broken down into 0.8mm sample lengths. These sample lengths are chosen in such a way that a good statistical analysis can be made of the surface. In most cases, five sample lengths are used for analysis [21].

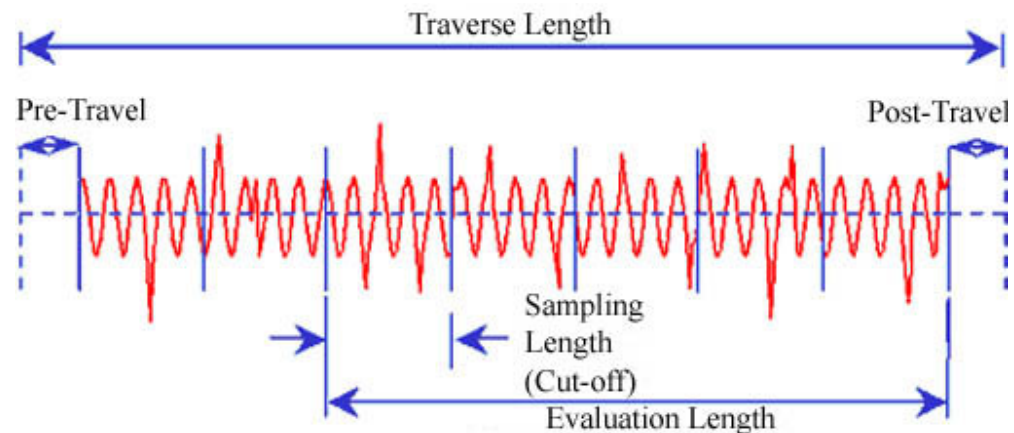


**Figure 2.6 The lengths of roughness measurement [21]**

According to the international standard (ISO 3274-1975) a stylus may have an included angle of  $60^\circ$  or  $90^\circ$  and a tip radius of curvature of 2, 5 or  $10\mu\text{m}$  [19]. Because of this the stylus tip can not reach to the every details of the profile surface like Figure 2.7 which cause errors. However, experience indicates that errors due to the finite radius of the stylus are not serious [18].

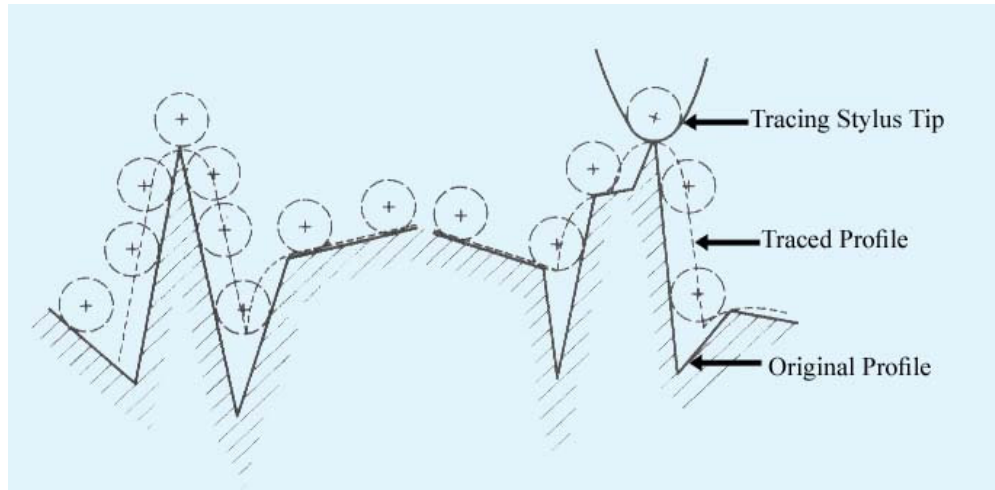


**Figure 2.7 Tracing of a stylus tip [19]**

## 2.4 Filtering

The roughness and waviness to be measured can be segregated by graphical, mechanical, electrical or digital filters during the roughness measurement.

a) Graphical filter: The value of sample length defines the graphical filter. If the sample length is smaller than the wave length of the surface texture, only the imperfections caused by roughness are included to the measuring. In Figure 2.8, the sample length  $L$  is chosen smaller than wave length and when the sections are redrawn using their axes in a line, the result profile shown in Figure 2.9 is obtained, which eliminates the waviness. However if the sample length is bigger than the waviness, the waviness is not filtered out and included to the measurement like in Figure 2.10.

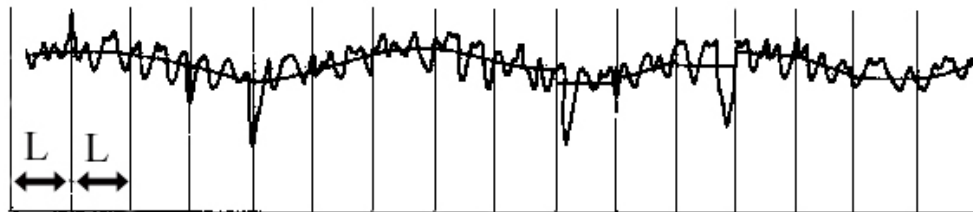


**Figure 2.8 Sample lengths smaller than wave length [19]**

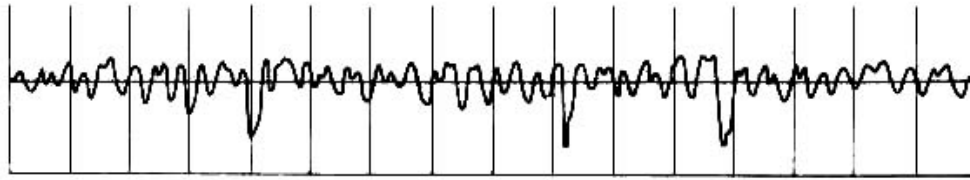


**Figure 2.9 Redrawing of Figure 2.8 using the axis line [19]**

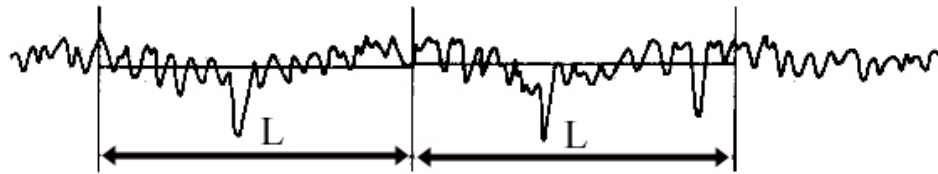


**Figure 2.10 Sample lengths bigger than wave length [19]**

b) Mechanical filter: Using skid is a good way to establish a reference line from which profile height can be measured. The measurement machine measures the difference in height between the skid height and the stylus tip height. The skid rides over imperfections in the surface and acts as a mechanical filter for waviness. This approach is therefore suitable for roughness profile measurement only [16]. The rounded skid shown in Figure 2.11 which is sliding over the imperfections tends to follow and thus eliminate the more widely spaced undulations [19].

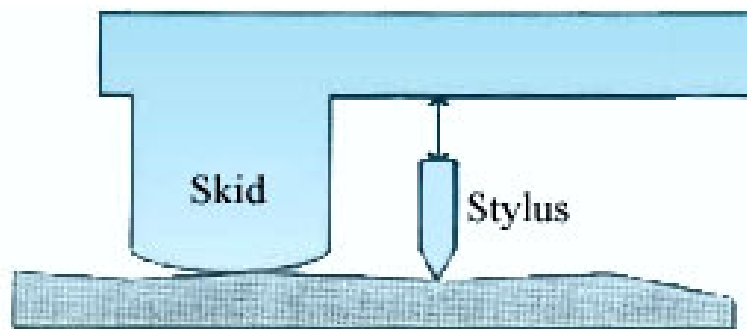


**Figure 2.11 Skid movement on a profile [19]**

c) Electrical filter: It is accomplished by passing the alternating voltage representing the profile through an electric wave filter. It is called 2-RC filter because it contains two capacitors and two resistances like in Figure 2.12. The effect of such a filter on a profile is shown in Figure 2.13 [19].

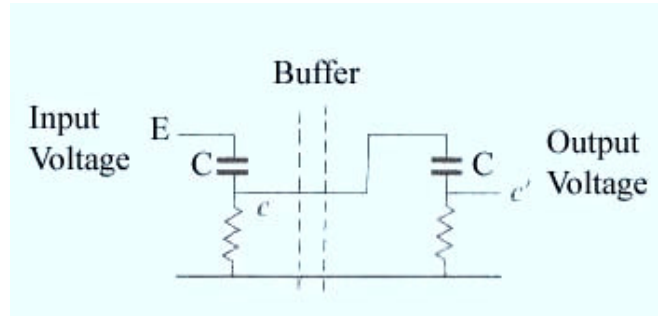


**Figure 2.12 2RC Filter [19]**

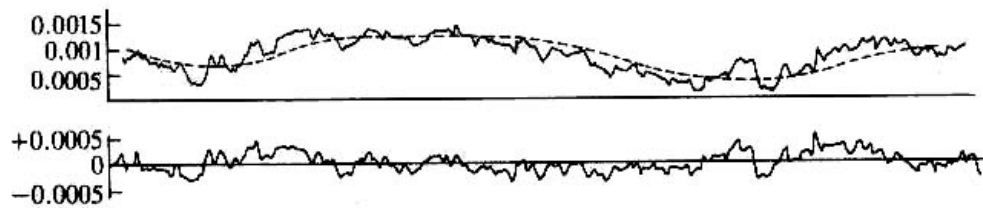


**Figure 2.13 2RC filter effect [19]**

d) Digital Filters: Modern surface finish measuring instruments mostly digitize the raw trace of the surface and mathematically (computationally) filter this raw data after it has been collected and stored in a computer memory to do the roughness filtering. The advantage of this approach is that the same raw data can be filtered multiple times with different cut-offs to compare the results [16].



## **CHAPTER 3**

### **DESIGN OF EXPERIMENT**

Sir Ronald A. Fisher was the innovator of the use of statistical methods in experimental design. The early application of experimental design methods were in the agricultural and biological sciences, and the first industrial applications of this method is appear in 1930s in the British textile and woolen industry [22].

Design of experiment is used to plan and conduct experiments and analyze the resulting data to obtain a solution for optimizing the problem. In engineering, experimental strategies are widely used in practice like one factor at a time approach. In this method a starting point and a range for each factor is selected. Then each factor is applied in different values while other factors kept constant at their starting point values to find out the effect of that factor in the process. However the one factor at a time strategy is not considering the interactions between the factors and their effect on the process when they are changed together. As the one factor at a time strategy is fails to consider any possible interaction between the factors, it may give poor results. Therefore, the factorial experiment method is used which also consider the interaction effects [23]. In the following sections this method is explained.

#### **3.1 The Two Factor Factorial Design**

The correct approach to deal with several factors is to conduct a factorial experiment. This is an experimental strategy in which factors are varied together, instead of one at a time [22]. In fractional design, all possible combinations of the levels of the factors are investigated. The interactions are included so poor results are avoided. Moreover, the effect of a factor can be estimated at the different values of other factors.

The effect of a factor is defined to be the change in response produced by a change in the level of the factor. This is called main effect because it refers to the primary factors of interest in the experiment [22].

In Figure 3.1 the lowercase letter denotes that, during the application that factor is in its higher level and the one which is absent means that factor is in its lower level. For example “b” denotes that the Factor B is at higher level and Factor A is at lower level. Also “1” is used to denote that all the factors are in their lower level.

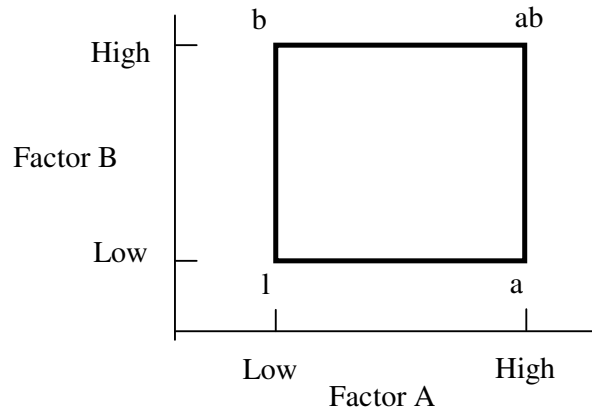


**Figure 3.1 A two factor factorial experiment [22]**

The main effect of factor A in this two level design is;

$$A = \frac{a + ab}{2} - \frac{1 + b}{2} \quad (3.1)$$

The main effect of factor B in this two level design can be similarly calculated.

$$B = \frac{b + ab}{2} - \frac{1 + a}{2} \quad (3.2)$$

The effect of the interaction between factors A and B (AB) is;

$$AB = \frac{(ab - b) - (a - 1)}{2} \quad (3.3)$$

For example, in Figure 3.2, a simple two-factor factorial design experiment is shown, with the response values shown at the corners.

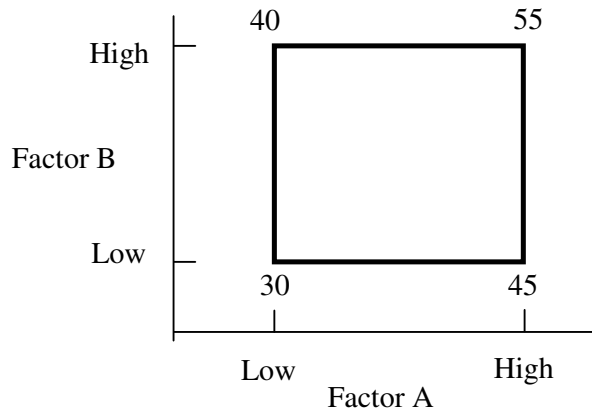


**Figure 3.2 A two factor factorial experiment with the response values**

In the experiment, each factor is designed with two levels. These levels are called “low” and “high”. The main effect of factor A in this two level design can be thought of as the difference between the average response at the high level of A and the average response at the low level of A [23].

$$A = \frac{45 + 55}{2} - \frac{30 + 40}{2} = 15 \quad (3.4)$$

An increase in the factor A from the low level to the high level causes an average response increase of 15 units.

Main effect of B can be similarly calculated,

$$B = \frac{40 + 55}{2} - \frac{30 + 45}{2} = 10 \quad (3.5)$$

From Figure 3.2, it is seen that, the effect of the increase in the level of Factor B from low to high level on the response does not depend on the level of Factor A. At the high level of Factor A, the increase in the level of Factor B from low to high level causes an increase of 10 units in the response which is the difference of 55 and 45, similarly, at the low level of Factor A, the levels of Factor B causes an increase of 10 units in the response which is the difference of 40 and 30. The same is also valid for factor A, when the effect of the increase in the level of Factor A from low to high on response is examined. In this case, there is no interaction between the factors in the designed experiment also seen in Equation 3.6 [23].

$$AB = \frac{(55 - 40) - (45 - 30)}{2} = 0 \quad (3.6)$$

In some experiments, it may be seen that the difference in response between the levels of one factor is not the same at all levels of the other factors. When this occurs there is an interaction between the factors [22]. For example, consider the two-factor factorial experiment shown below.

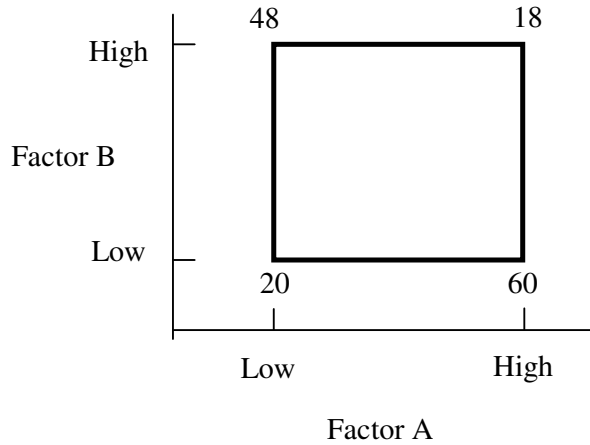


**Figure 3.3 A two factor factorial experiment with interaction**

In this case at the high level of factor A, the change in the level of factor B from low to high level is the difference of 18 and 60 which is -42. At the low level of factor A, the variation of B is 28 which is the difference of 48 and 20. When the results of effects of factor B, at low and high level of factor A is compared, it is seen that there is an interaction between factors A and B. The magnitude of the interaction effect of AB, which is the average of the difference between these two effects of B, is calculated as follow;

$$AB = \frac{(-42 - 28)}{2} = -35 \quad (3.7)$$

The main effect of factor A is;

$$A = \frac{60 + 18}{2} - \frac{48 + 20}{2} = 5 \quad (3.8)$$

The main effect of factor B is;

$$B = \frac{48 + 18}{2} - \frac{20 + 60}{2} = -7 \quad (3.9)$$

The result of this experiment indicates that, the effect of the interaction, AB, on the response is larger than the main effects, A and B. Thus, in designing the experiment and studying the effect of the factors on response, neglecting the interaction between the factors (one factor at a time approach) would result in a serious error [23].

### 3.2 The $2^3$ Factorial Design

The effects of feed per tooth, cutting speed and stepover (radial depth of cut) on surface roughness will be examined in this experimental study by fixing other parameters. Factorial design will be used to include the interaction effects of the parameters on the surface roughness. The  $2^k$  factorial design approach is chosen as it is simple and by performing small number of experiments good results may be obtained by including the interaction effects [23]. The number of the controlled parameters is 3 so the design is called a  $2^3$  factorial design and eight experiments will be used.

The geometric view of the  $2^3$  factorial design for the treatment combinations can be shown as a cube as illustrated in Figure 3.4. Lowercase letters denotes the factors that are at high level at that application.

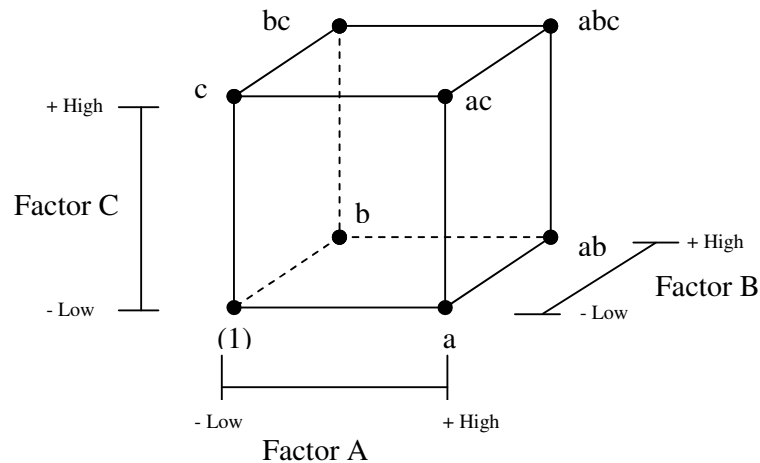


**Figure 3.4 The Geometric View of the  $2^3$  factorial design [22]**

In order to estimate the main effect of A, the effect of A in different conditions must be determined. The effect of A when B and C are at low level is  $[a-(1)]/n$ , where n is the number of replicates. Similarly the effect of A when B is at high level and C is at the low level is  $[ab-b]/n$ . The effect of A when C is at the high level and B is at the low level is  $[ac-c]/n$ . Finally, the effect of A, when B and C are at the high level is  $[abc-bc]/n$  [22].

The average of these calculations gives the average main effect of A

$$A = \frac{1}{4n} [a - (1) + ab - b + ac - c + abc - bc] \quad (3.10)$$

Similar calculations are done to calculate the average main effect of B and C.

$$B = \frac{1}{4n} [b + ab + bc + abc - (1) - a - c - ac] \quad (3.11)$$

$$C = \frac{1}{4n} [c + ac + bc + abc - (1) - a - b - ab] \quad (3.12)$$

The one-half difference between the averages A effects at the two levels of B gives the AB interaction formula.

At high level of B the A effects are  $[abc-bc]/n$  and  $[ab-b]/n$ . So the average A effect for the high levels of B is;

$$\frac{[(abc - bc) + (ab - b)]}{2n} \text{ (average A effect at high level B)} \quad (3.13)$$

In a similar way the A effect at low level B is;

$$\frac{[(ac - c) + (a - (1))]}{2n} \text{ (average A effect at low level B)} \quad (3.14)$$

The difference of average A effects is;

$$\frac{[abc - bc + ab - b - ac + c - a + (1)]}{2n} \quad (3.15)$$

As AB interaction is found by taking the one-half difference of average A effects which is;

$$AB = \frac{[abc - bc + ab - b - ac + c - a + (1)]}{4n} \quad (3.16)$$

Similar calculations are done to calculate the average main effect of AC and BC.

$$AC = \frac{[(1) - a + b - ab - c + ac - bc + abc]}{4n} \quad (3.17)$$

$$BC = \frac{[(1) + a - b - ab - c - ac + bc + abc]}{4n} \quad (3.18)$$

The ABC interaction is defined as the average differences between the AB interactions for the two different levels of C. The calculated ABC interaction is

$$ABC = \frac{1}{4n} [(abc - bc) - (ac - c) - (ab - b) + (a - (1))]$$

$$ABC = \frac{[abc - bc - ac + c - ab + b + a - (1)]}{4n} \quad (3.19)$$

The quantities in the brackets in numerators are called contrasts in the treatment combinations. Using these contrasts the Table 3.1 is developed with plus and minus signs [22].

**Table 3.1 Signs of factorial effects [22]**

Treatment Combination	Factorial Effect						
	A	B	AB	C	AC	BC	ABC
1	-	-	+	-	+	+	-
a	+	-	-	-	-	+	+
b	-	+	-	-	+	-	+
ab	+	+	+	-	-	-	-
c	-	-	+	+	-	-	+
ac	+	-	-	+	+	-	-
bc	-	+	-	+	-	+	-
abc	+	+	+	+	+	+	+

### 3.3 Deriving the Formula

#### 3.3.1 Linear Regression Models

Response surface methodology is a collection of statistical and mathematical techniques useful for developing, improving, and optimizing

process. In the practical application of response surface methodology, it is necessary to develop an approximating model for the true response surface. The underlying true response surface is typically driven by some unknown physical mechanism. The approximating model is based on observed data from the process or system and is an empirical model. Multiple regression is a collection of empirical models required in response surface methodology [24].

A first-order response surface model that might describe a relationship is

$$y = \beta_0 + \beta_1 x_1 + \beta_2 x_2 + \varepsilon \quad (3.20)$$

This is a multiple linear regression model with two independent variables  $x_1, x_2$  also in the equation  $y$  represents the response and  $\varepsilon$  is the error. Equation is a linear function of the unknown parameters  $\beta_0, \beta_1$  and  $\beta_2$ . The model describes a plane in the two dimensional  $x_1, x_2$  space. The parameter  $\beta_0$  defines the intercept of the plane [24]. The parameters,  $\beta_1$  and  $\beta_2$  are called the partial variable coefficients, because  $\beta_1$  measures the expected change in  $y$  per unit change in  $x_1$  when  $x_2$  is held constant, and  $\beta_2$  measures the expected change in  $y$  per unit change in  $x_2$  when  $x_1$  is held constant [23].

The response may be related to  $k$  independent variables and the model is

$$y = \beta_0 + \beta_1 x_1 + \beta_2 x_2 + \dots + \beta_k x_k + \varepsilon \quad (3.21)$$

This is called a multiple linear regression model with  $k$  variables. The parameter  $\beta_i$  represents the expected change in response  $y$  per unit change in  $x_i$  when all the independent variables are held constant [24].

When interaction terms are added to the first order model the new equation become more complex with respect to Equation 3.20.

$$y = \beta_0 + \beta_1 x_1 + \beta_2 x_2 + \beta_{12} x_1 x_2 + \varepsilon \quad (3.22)$$

Where  $x_1 x_2$  is an interaction term and  $\beta_{12}$  is the variable coefficient of it. If they are defined like  $x_3 = x_1 x_2$  and  $\beta_3 = \beta_{12}$ . The equation becomes

$$y = \beta_0 + \beta_1 x_1 + \beta_2 x_2 + \beta_3 x_3 + \varepsilon \quad (3.23)$$

This is also a standard multiple linear regression model with three independent variables.



### 3.3.2 Linear Regression Models for 2<sup>3</sup> Factorial Design

In order to form a model for a 2<sup>3</sup> Factorial Design, all the main terms and interaction terms have to be included in the equation. The main effects terms can be classified as  $x_1$ ,  $x_2$ ,  $x_3$  and the interaction effects terms are  $x_1x_2$ ,  $x_1x_3$ ,  $x_2x_3$  and  $x_1x_2x_3$ . The variable coefficients of these terms are  $\beta_1$ ,  $\beta_2$ ,  $\beta_3$ ,  $\beta_{12}$ ,  $\beta_{13}$ ,  $\beta_{23}$  and  $\beta_{123}$ . As a result the model is written as;

$$y = \beta_0 + \beta_1x_1 + \beta_2x_2 + \beta_3x_3 + \beta_{12}x_1x_2 + \beta_{13}x_1x_3 + \beta_{23}x_2x_3 + \beta_{123}x_1x_2x_3 + \varepsilon \quad (3.24)$$

By substituting the interaction effects like,  $x_1x_2=x_4$ ,  $x_1x_3=x_5$ ,  $x_2x_3=x_6$ ,  $x_1x_2x_3=x_7$  and substituting their variable coefficients such as  $\beta_{12}=\beta_4$ ,  $\beta_{13}=\beta_5$ ,  $\beta_{23}=\beta_6$  and  $\beta_{123}=\beta_7$  then equation becomes [23],

$$y = \beta_0 + \beta_1x_1 + \beta_2x_2 + \beta_3x_3 + \beta_4x_4 + \beta_5x_5 + \beta_6x_6 + \beta_7x_7 + \varepsilon \quad (3.25)$$

### 3.3.3 Estimation of the Parameters in Linear Regression Models

The method of least squares is typically used to estimate the regression coefficients in a multiple linear regression model. Suppose that  $n > k$  observations on the response variable are available. The model equation in terms of the observations is,

$$y_i = \beta_0 + \beta_1x_{i1} + \beta_2x_{i2} + \dots + \beta_kx_{ik} + \varepsilon_i$$

$$y_i = \beta_0 + \sum_{j=1}^k \beta_jx_{ij} + \varepsilon_i \quad i = 1, 2, 3, \dots, n \quad (3.26)$$

The sum of the squares of error is taken, so the error is minimized. The least squares function is [22],

$$L = \sum_{i=1}^n \varepsilon_i^2$$

$$L = \sum_{j=1}^n (y_i - \beta_0 - \sum_{j=1}^k \beta_jx_{ij})^2 \quad (3.27)$$

The function  $L$  is to be minimized with respect to  $\beta_0, \beta_1, \dots, \beta_k$ . The least squares estimators, say  $\hat{\beta}_0, \hat{\beta}_1, \dots, \hat{\beta}_k$ , must satisfy [22]

$$\left. \frac{\partial L}{\partial \beta_0} \right|_{\hat{\beta}_0, \hat{\beta}_1, \dots, \hat{\beta}_k} = -2 \sum_{j=1}^n (y_i - \hat{\beta}_0 - \sum_{j=1}^k \hat{\beta}_j x_{ij}) = 0 \quad (3.28a)$$

and

$$\left. \frac{\partial L}{\partial \beta_j} \right|_{\hat{\beta}_0, \hat{\beta}_1, \dots, \hat{\beta}_k} = -2 \sum_{j=1}^n (y_i - \hat{\beta}_0 - \sum_{j=1}^k \hat{\beta}_j x_{ij}) x_{ij} = 0 \quad j=1, 2, \dots, k \quad (3.28b)$$

Simplifying Equation 3.28,

$$\begin{aligned} n \hat{\beta}_0 + \hat{\beta}_1 \sum_{i=1}^n x_{i1} + \hat{\beta}_2 \sum_{i=1}^n x_{i2} + \dots + \hat{\beta}_k \sum_{i=1}^n x_{ik} &= \sum_{i=1}^n y_i \\ \hat{\beta}_0 \sum_{i=1}^n x_{i1} + \hat{\beta}_1 \sum_{i=1}^n x_{i1}^2 + \hat{\beta}_2 \sum_{i=1}^n x_{i1} x_{i2} + \dots + \hat{\beta}_k \sum_{i=1}^n x_{i1} x_{ik} &= \sum_{i=1}^n x_{i1} y_i \\ \cdot & \cdot \cdot \cdot \\ \cdot & \cdot \cdot \cdot \cdot \\ \cdot & \cdot \cdot \cdot \cdot \\ \hat{\beta}_0 \sum_{i=1}^n x_{ik} + \hat{\beta}_1 \sum_{i=1}^n x_{ik} x_{i1} + \hat{\beta}_2 \sum_{i=1}^n x_{ik} x_{i2} + \dots + \hat{\beta}_k \sum_{i=1}^n x_{ik}^2 &= \sum_{i=1}^n x_{ik} y_i \end{aligned} \quad (3.29)$$

These equations are called the least squares normal equations. It is seen that there are  $p=k+1$  normal equations, one for each of the unknown regression coefficients. The solutions to the normal equations will be the least square estimators of the regression coefficients  $\hat{\beta}_0, \hat{\beta}_1, \dots, \hat{\beta}_k$  [22].

Solving these normal equations in matrix notation is simpler. In matrix form the Equation may be written as

$$y = X\beta + \varepsilon \quad (3.30)$$

where

$$y = \begin{bmatrix} y_1 \\ y_2 \\ \cdot \\ \cdot \\ y_n \end{bmatrix}, \quad X = \begin{bmatrix} 1 & x_{11} & x_{12} & \dots & x_{1k} \\ 1 & x_{21} & x_{22} & \dots & x_{2k} \\ \cdot & \cdot & \cdot & \dots & \cdot \\ \cdot & \cdot & \cdot & \dots & \cdot \\ \cdot & \cdot & \cdot & \dots & \cdot \\ 1 & x_{n1} & x_{n2} & \dots & x_{nk} \end{bmatrix}$$

$$\beta = \begin{bmatrix} \beta_0 \\ \beta_1 \\ \cdot \\ \cdot \\ \beta_k \end{bmatrix} \quad \text{and} \quad \varepsilon = \begin{bmatrix} \varepsilon_1 \\ \varepsilon_2 \\ \varepsilon_3 \\ \varepsilon_4 \\ \varepsilon_5 \end{bmatrix}$$

In general,  $y$  is an  $(n \times 1)$  vector of the observations,  $X$  is an  $(n \times p)$  matrix of the levels of the independent variables,  $\beta$  is  $(p \times 1)$  vector of the regression coefficients, and  $\varepsilon$  is an  $(n \times 1)$  vector of the random errors [22].

In order to find the vector of least squares estimators,  $\hat{\beta}$ , that minimizes

$$L = \sum_{j=1}^n \varepsilon_j^2 = \varepsilon' \varepsilon = (y - X\beta)'(y - X\beta) \quad (3.31)$$

$L$  may be expressed as

$$\begin{aligned} L &= y' y - \beta' X' y - y' X \beta + \beta' X' X \beta \\ &= y' y - 2\beta' X' y + \beta' X' X \beta \end{aligned} \quad (3.32)$$

Because  $\beta' X' y$  is a  $(1 \times 1)$  matrix, or a scalar, and its transpose  $(\beta' X' y)' = y' X \beta$  is the same scalar. The least squares estimators must satisfy[22]

$$\left. \frac{\partial L}{\partial \beta} \right|_{\beta} = -2X' y + 2X' X \hat{\beta} = 0 \quad (3.33)$$

which simplifies to

$$X' X \hat{\beta} = X' y \quad (3.34)$$

Equation 3.30 is the matrix form of the least squares normal equations. It is identical to Equation 3.34. The both sides of the Equation 3.34 is multiplied by the inverse of the  $X' X$  so the normal equations may be solved. Therefore, the least squares estimator of  $\beta$  is [22].

$$\hat{\beta} = (X' X)^{-1} X' y \quad (3.35)$$

## **CHAPTER 4**

### **MILLING PARAMETERS IN MANUFACTURING**

Milling parameters are very important because they affect the surface quality obtained at the end of the milling process. Therefore, appropriate milling parameters must be determined before starting a milling process to obtain desired surface quality.

#### **4.1 Determining the Test Specimen**

Nowadays, Forging dies are generally manufactured by using CNC milling machines. The surface quality is important in forging dies. By milling process, obtaining desired surface quality on the curved geometries of die cavities is critical. So choosing the right cutting parameters is essential while the correct cutting strategies are used during the milling of die cavities.

Several close dies used for forging have been examined in Aksan Steel Forging Company located in Ankara. The die used for manufacturing of M24 eyebolt (Figure 4.1) has been considered as a case study. This die imparts three curved section as indicated on Figure 4.2. In this study, machining of the curved section-1 which forms the shank part of the eye bolt will be examined. For the die of M24 eye bolt, the curved section-1 is a half cylindrical cavity which has a 13.6 mm radius.

The half of the curved section-1 given in Figure 4.3 will be sufficient as a test specimen section because of the symmetry. The particular cavity is separated into the divisions, each having 10 mm width. Each division is machined by using different cutting parameters combinations which will be discussed in the Chapter 5 and Chapter 6.



**Figure 4.1 CAD model of M24 forged eye bolt**

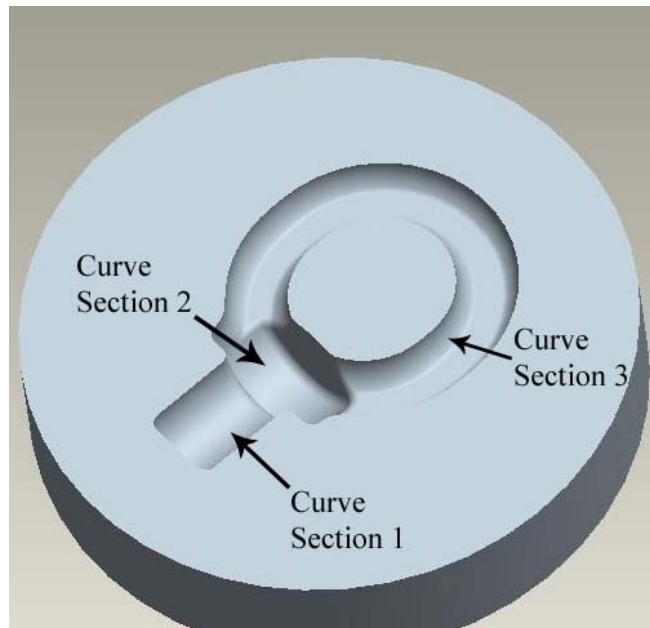


**Figure 4.2 Die of the eye bolt**

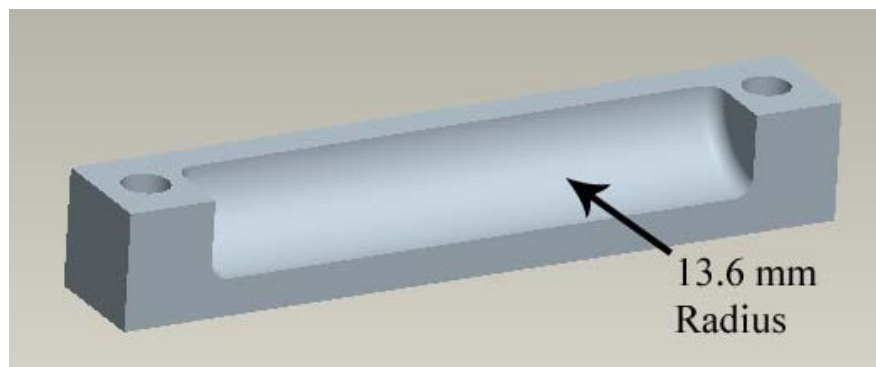


**Figure 4.3 Designed model of the test specimen**

## 4.2 Milling Tool Selection

Milling tools are chosen according to the geometry and dimensions of the die cavities that will be machined. The edge fillets on the die cavities are one of the limiting features for selection of tools. Generally, using a single milling tool and avoiding the changing the tool during rough cut of the entire die cavity may be considered as another criteria. The shank section of die of M24 eye bolt has 3.4 mm edge fillet as shown in Figure 4.4. For rough cut, the endmill with the diameter of 6 mm is adequate to machine the shank section together with the other sections by using single milling tool, due to the limiting dimension of the edge fillet. With a similar consideration of using a single milling tool for finish cut, the ball endmill with a diameter of 6 mm is selected to machine the entire cavity including machining the edge fillets as well.

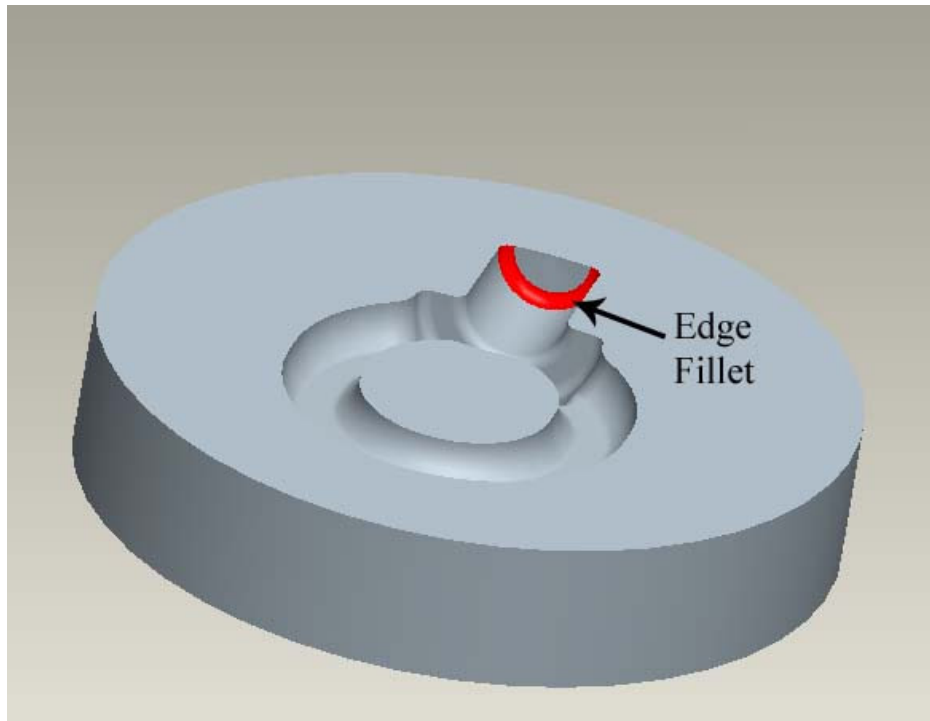


**Figure 4.4 Edge fillet of the shank section of die of eye bolt**

The endmill with 4 flutes and 30° helix angle is chosen for rough cut. The dimensions of endmill are  $D = 6$  mm,  $d = 6$  mm,  $A_p = 13$  mm and  $L = 50$  mm in Figure 4.5.

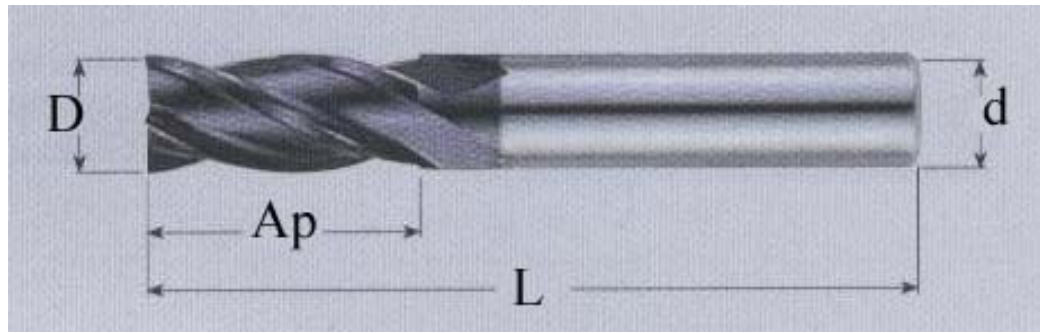


**Figure 4.5 Endmill [25]**

For the finish cut, the ball endmill with 2 flutes and  $30^\circ$  helix angle is chosen and the dimensions of ball endmill are  $D = 6$  mm,  $d = 6$  mm,  $R = 3$  mm,  $A_p = 6$  mm,  $L = 90$  mm,  $d_1 = 5.9$  mm,  $H = 12$  mm in Figure 4.6.

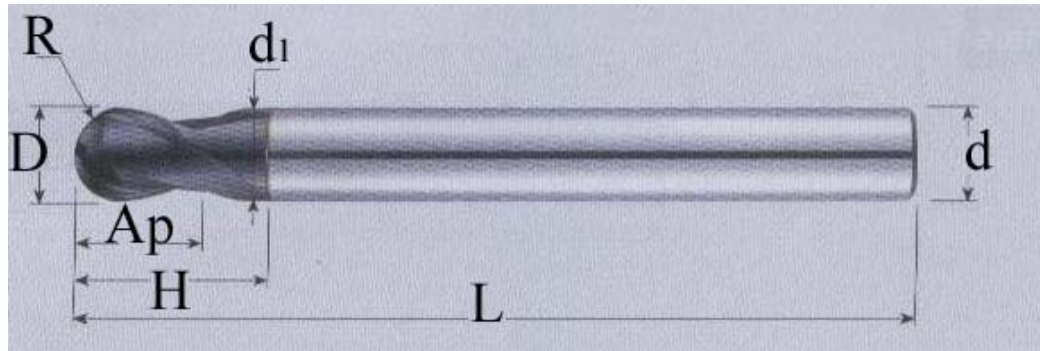


**Figure 4.6 Ball endmill [25]**

### 4.3 Three and Five Axes CNC Milling

Three axes milling machines are very common in the industry due to easier programming and lower price compared to the five axes CNC milling machines. However, one of the main disadvantages of machining on three axes CNC milling machine is the variation of distance between the cutting points of the milling tool and the tool axis during the milling process of a curved surface as shown in Figure 4.7. This variation causes different cutting speeds during the milling process of the same curved surface [26].

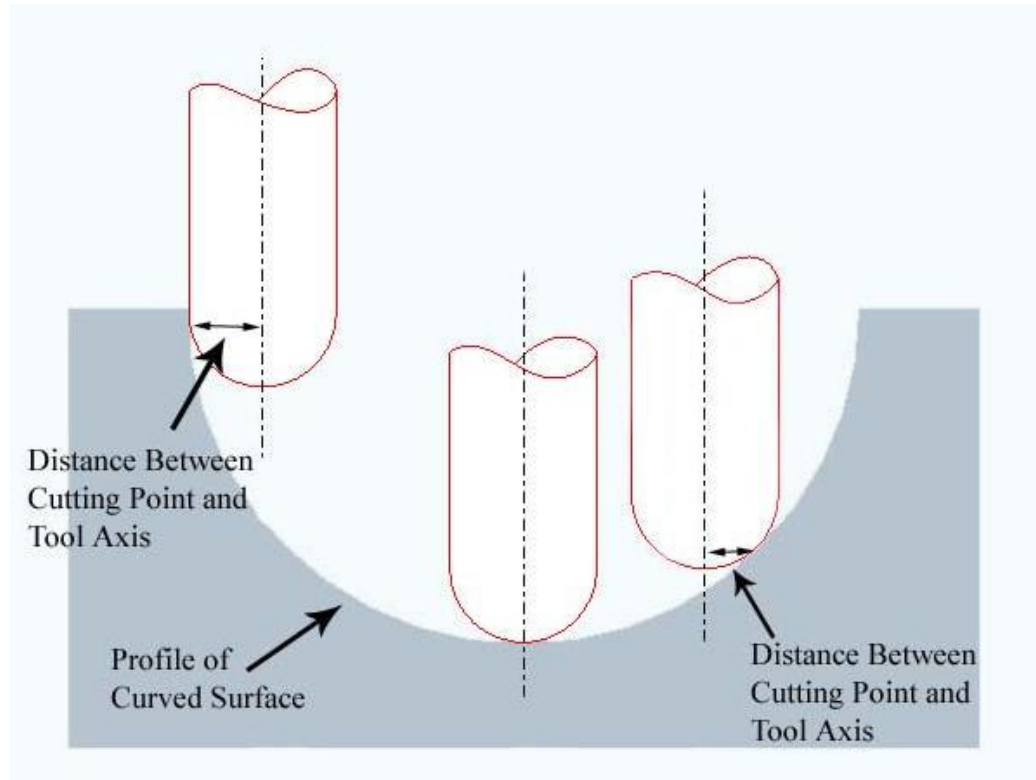


**Figure 4.7 3-axes milling**

In five axes CNC milling, preparation of the NC codes is more complex. However, in 5-axes milling, the distance between the tool axis and the cutting point can be kept constant, which will provide the same cutting speed during the whole machining process. For a standard 5-axes milling, the cutting tool is always oriented normal to the surface [12]. As a result, the cutting points which are in contact with the die cavity during milling are always at the tool tip as illustrated in Figure 4.8. The cutting speed goes to zero as the distance between the cutting points and axis of the tool approaches to zero. In order to avoid this situation, an inclination angle can be applied as shown in Figure 4.9. As a result, the tool may be oriented such that the same distance between the cutting points of the tool and the tool axis can be obtained during the milling process. Consequently, constant cutting speed can be achieved. An inclination angle of 15 degree is recommended in literature [12] [13].



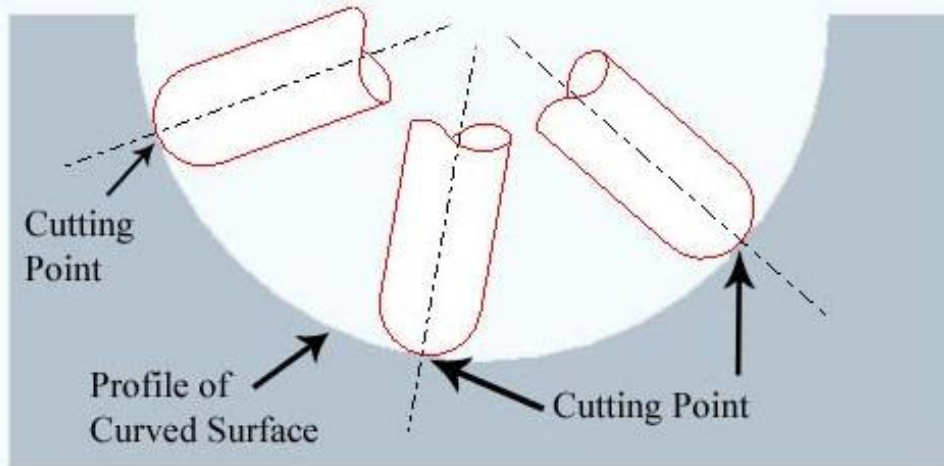


**Figure 4.8 Cutting Points in 5-axes milling**

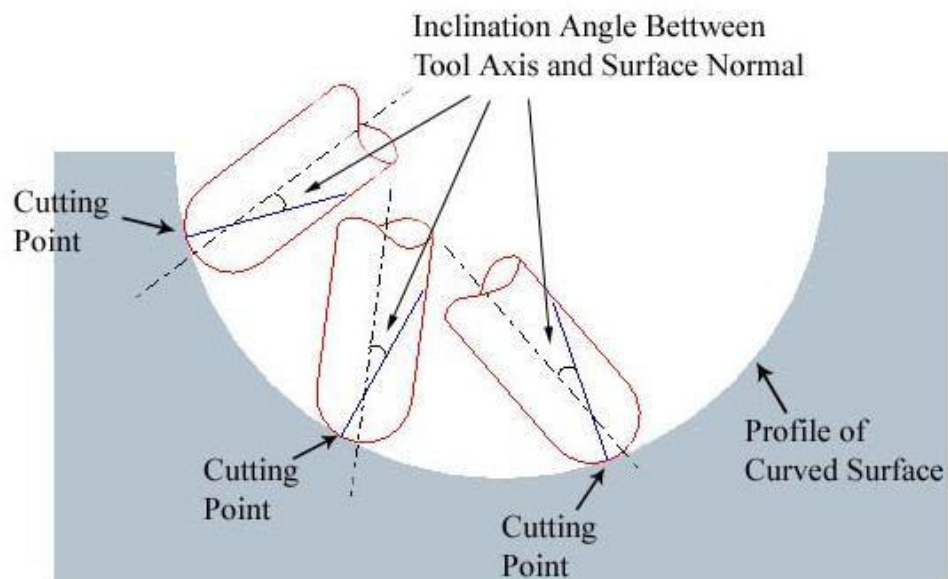


**Figure 4.9 5-axes milling with an inclination angle**

The inclination angle takes the names “tilt” or “lead” according to its position with respect to the feed direction. The inclination angle, which is

between the tool axis and the surface normal in the direction of tool travel, is called lead angle as demonstrated in x-z plane, in Figure 4.10. On the other hand, Tilt angle is the inclination angle between the surface normal and the tool axis which is perpendicular to the direction of tool travel. The tilt angle is shown in y-z plane, in Figure 4.11.

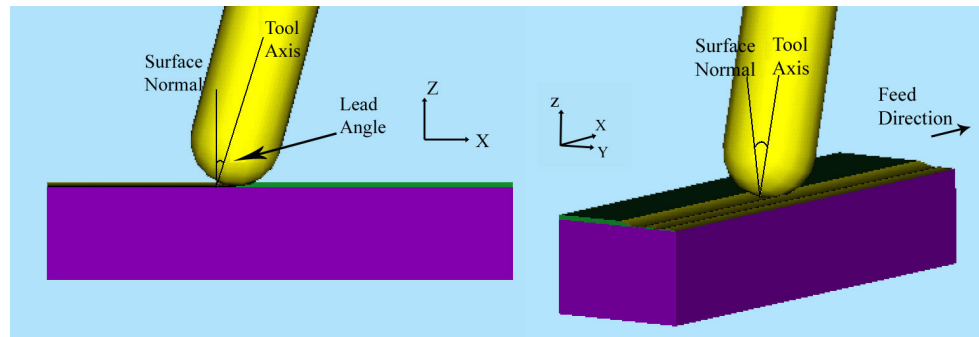


**Figure 4.10 Lead angle**

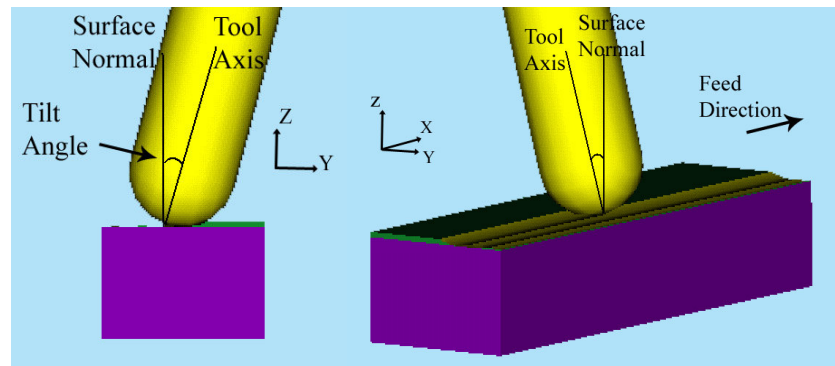


**Figure 4.11 Tilt angle**

An experimental study will be described in Chapter 5 to demonstrate the effects of three axes milling and five axes milling on the surface quality.

#### **4.4 Determination of the Value of Depth of Cut in Rough Cutting**

In rough cut, generally endmills are used. The parameters, which are used in rough cut, are defined according to the milling tool properties and required depth of cut value at finish cut ( $d_f$ ). The  $d_f$  should be within the maximum allowable

( $d_{af-max}$ ) and minimum allowable ( $d_{af-min}$ ) depth of cut values for finish cut which are predefined by tool manufacturer according to chosen milling tool. Rough cut must be performed by taking this range into consideration. After rough cut, a surface with a staircase shape is formed over the radius as shown in Figure 4.12. Because of this staircase shaped surface, the material thickness left over the surface which will be machined at the finish cut, is not constant. The thickness of minimum material left on the surface ( $t_m$ ), which is defined in rough cut as “finish allowance”, is always same over the surface. Because of the height of the stairs, a thickness of material ( $t_s$ ) is formed over the minimum material left boundary which is a variable. The material thickness to be machined during the finish cut (i.e. depth of cut in finish cut) is determined using these two thicknesses  $t_m$  and  $t_s$  as follows;

$$t_m \leq d_f \leq t_m + t_s \quad (4.1)$$

The heights of the stairs are equal to the value of depth of cut during rough cut ( $d_r$ ) as demonstrated in Figure 4.12. Therefore, if the value of  $d_r$  increases,  $t_s$  value will also increase. As a result, the value of the depth of cut in rough cut must be chosen carefully to keep the material thickness that will be machined during the finish cut ( $d_f$ ) in the range of recommended values.

As the  $d_f$  value must be within recommended  $d_{af-min}$  and  $d_{af-max}$  values, they may be used as limit of thickness values which are given in Equation 4.1.

$$t_m + t_s \leq d_{af-max} \quad (4.2)$$

$$d_{af-min} \leq t_m \quad (4.3)$$

In 5-axes milling with an inclination angle “ $\alpha$ ”, the material thickness that is cut by the milling tool is the division of  $t_m + t_s$  by  $\cos\alpha$  as indicated in Figure 4.13. As a result of this situation the Equation 4.2 is written as;

$$\begin{aligned} \frac{(t_m + t_s)}{\cos \alpha} &\leq d_{af-max} \\ t_m + t_s &\leq d_{af-max} \times \cos \alpha \end{aligned} \quad (4.4)$$

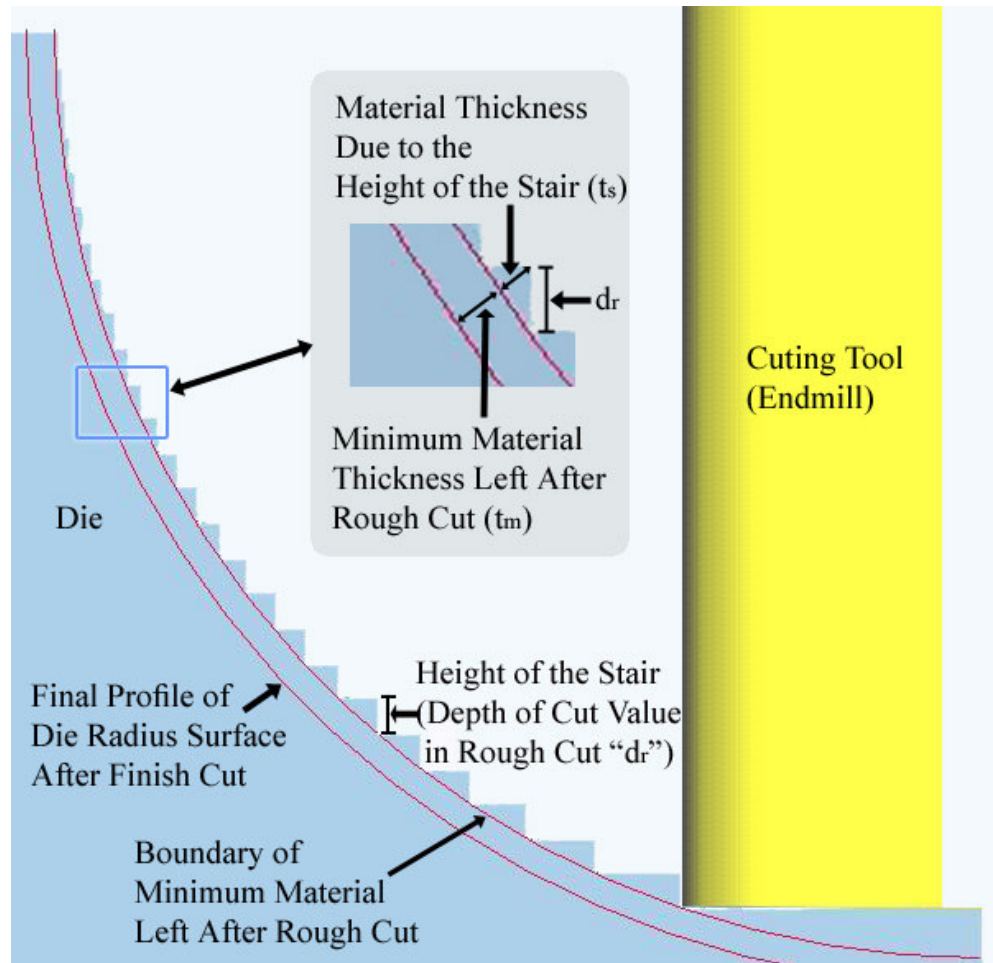


Figure 4.12 Die surface geometry after rough cut

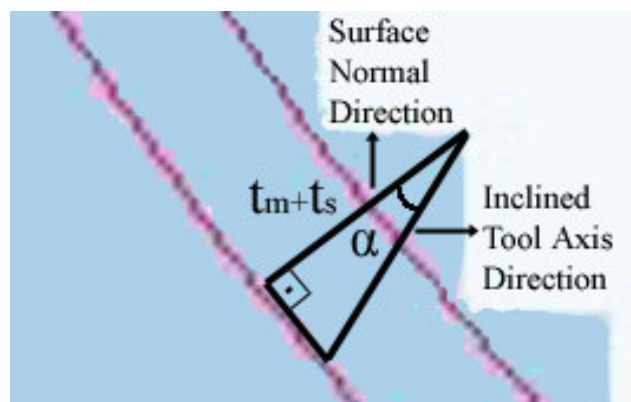


Figure 4.13 Material thickness that is left after rough cut

The  $t_s$  is a variable and maximum possible value of  $t_s$  is equal to the  $d_r$  value. As  $t_m$  is a constant value, for the maximum value of  $t_s$ , the Equation 4.4 may be written as;

$$\begin{aligned} t_m + t_{s-\max} &= d_{af-\max} \times \cos \alpha \\ t_m + d_r &= d_{af-\max} \times \cos \alpha \\ d_r &= d_{af-\max} \times \cos \alpha - t_m \end{aligned} \quad (4.5)$$

By minimizing the  $t_m$  value, the highest possible  $d_r$  value may be calculated. Minimum possible  $t_m$  value is equal to  $d_{af-\min}$  (Equation 4.3). As a result  $d_r$  is found as follows;

$$\begin{aligned} d_r &= d_{af-\max} \times \cos \alpha - t_m \\ d_r &= d_{af-\max} \times \cos \alpha - d_{af-\min} \end{aligned} \quad (4.6)$$

The boundary of the minimum material left is the curve which passes over the bottom points of the stairs. Therefore, the uncut boundary formed after rough cut may be used to calculate the thickness of material between the stair tips and the die surface, which is equal to  $t_m + t_s$ . Then, according to the results of the calculations, it is possible to see the material thickness variation over the radial die cavity.

The formula of circle which is used to define the boundary of minimum material left in the cartesian coordinate system is given as follows:

$$r^2 = (x-a)^2 + (y-b)^2 \quad \text{for} \quad \begin{cases} t_m \leq x \leq r \\ t_m \leq y \leq r \end{cases} \quad (4.7)$$

Where,

“r” is the radius of the circle

“a” is the coordinate of the center of the circle on the x axis

“b” is the coordinate of the center of the circle on the y axis

The material thickness between the stair tips and the die surface ( $t_m + t_s$ ) is the difference of the distance of the staircase tips to the die radius center ( $r^{\circ}$ ) and die radius ( $r = r^{\circ} + t_m + t_s$ ) as seen in Figure 4.14. As a result, firstly  $r^{\circ}$  can be calculated as follows;

$$r^{\circ} = \sqrt{X_1^2 + Y_1^2} \quad (4.8)$$

Where

$X_1$  is the distance between the stair tip and the x-coordinate of the die radius center.

$Y_1$  is the distance between the stair tip and the y-coordinate of the die radius center.

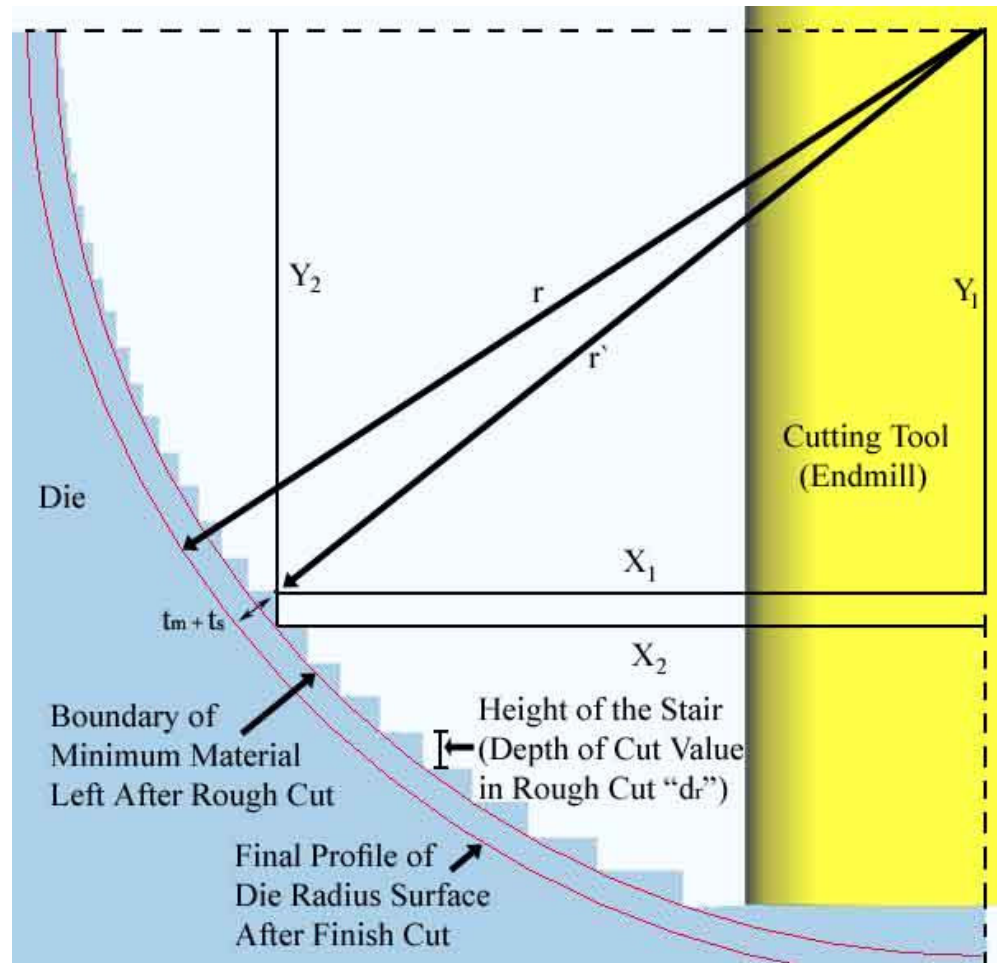


**Figure 4.14 The position of the stair tips with respect to the radius center**

$X_2$  and  $Y_2$  are the distances between the bottom point of stairs and center of die radius. The stairs are formed during each step of the depth of rough cut. Therefore,  $Y_2$  value of the stair is the product of  $d_r$  with the number of step of depth of the rough cut.  $Y_1$  values of every stair tips are equal to the difference of the depth of cut value in the rough cut and  $Y_2$  value. As a result of this evaluation,

$Y_1$  value can be computed.  $X_2$  values can be calculated by substituting  $Y_2$  into the boundary formula of minimum material left (Equation 4.7). On the other hand,  $X_1$  is equal to  $X_2$ . Hence by using the  $X_2$  value,  $X_1$  may be also found.

Using  $X_1$  and  $Y_1$  values,  $r^*$  is calculated and the difference of  $r^*$  and the die radius ( $r$ ) gives the thickness of the material which is left at the tip of stairs in the surface normal direction. If the tool cuts with an inclination angle ( $\alpha$ ) with respect to the surface normal, the material thickness in the surface normal direction is divided by  $\cos\alpha$  to find the thickness of material which the tool cuts at the stair tips.

In this study, the recommended value of depth of cut at the finish cut for  $d_{af-min}$  is 0.15 mm and for  $d_{af-max}$  is 0.30 mm for the chosen milling tool [27]. Therefore, for 5-axes milling with a  $15^\circ$  inclination angle, the  $d_r$  value is calculated by considering the Equation 4.6 as;

$$d_r = 0.30 \times \cos 15 - 0.15 = 0.14 \text{ mm} \quad (4.9)$$

When the value of depth of cut is taken as 0.14 mm in the rough cut and calculated as described, it is observed that the thicknesses of the material left for finish cut change between 0.156 mm and 0.300 mm at the stair tip positions as given in Appendix A. These values are within the limits of recommended range of depth of cut values for the finish cut. Therefore, for this study 0.14 mm was used as the depth of cut value in the rough cut. After the finish cut the die surface is obtained as in the Figure 4.15.

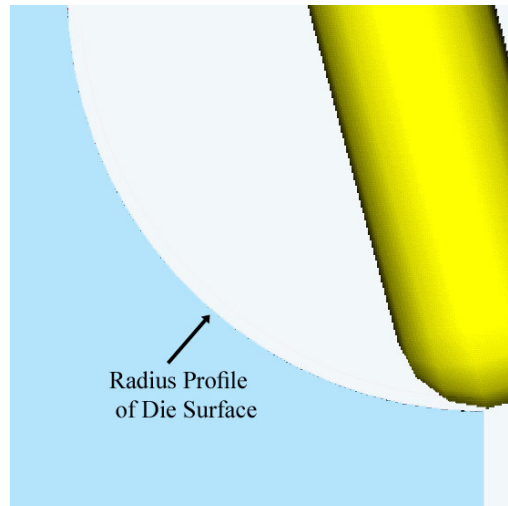


**Figure 4.15 Radius profile after the finish cut**

## 4.5 Cutting Path

In the study, two different cutting paths were used on the test specimen. First one was a circular path like in Figure 4.16. The other one was a linear path as shown in Figure 4.17. The lines in the figures show the tool movements.

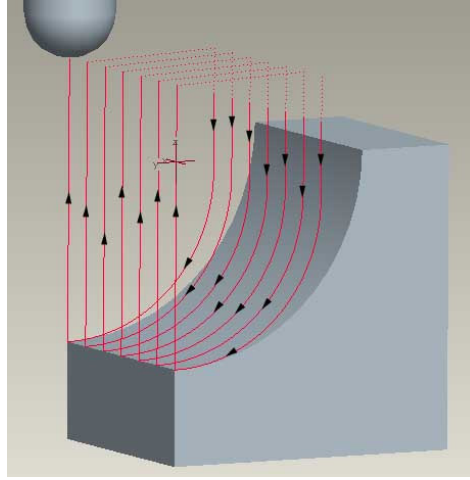


**Figure 4.16 Circular tool path**

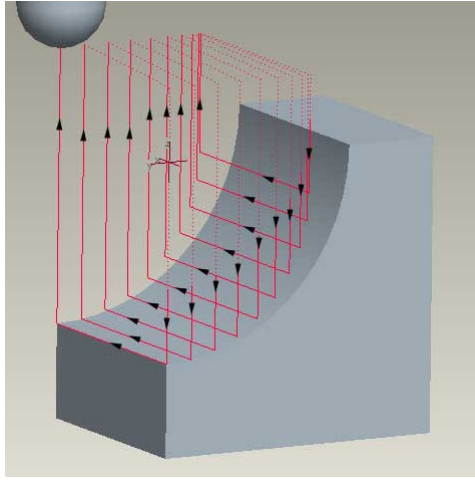


**Figure 4.17 Linear tool path**

For the comparison of the two different cutting paths, a machining analysis program Vericut was used [28]. A stepover value, which will be described in section 4.7, of 0.25 mm was used in the milling simulations. Firstly, The CAD model of die surface with a radius of 13.6 mm was obtained using Pro-Engineer as illustrated in Figure 4.18. Using NC program, the cutting paths with the determined stepover value were created as shown in Figure 4.19. Then the cutting paths were converted into NC codes for the CNC milling machine by using MANUS post processor program developed by METU BILTIR CENTER [10] (Figure 4.20). The milling simulations were conducted in Vericut by using the NC codes obtained from MANUS post processor program on a CAD model of a workpiece which was created in Vericut. The surface of the CAD model, which was machined in the milling simulation program, was compared with the surface of the designed CAD model exported from the Pro-Engineer, by using AUTO-DIFF module of Vericut.



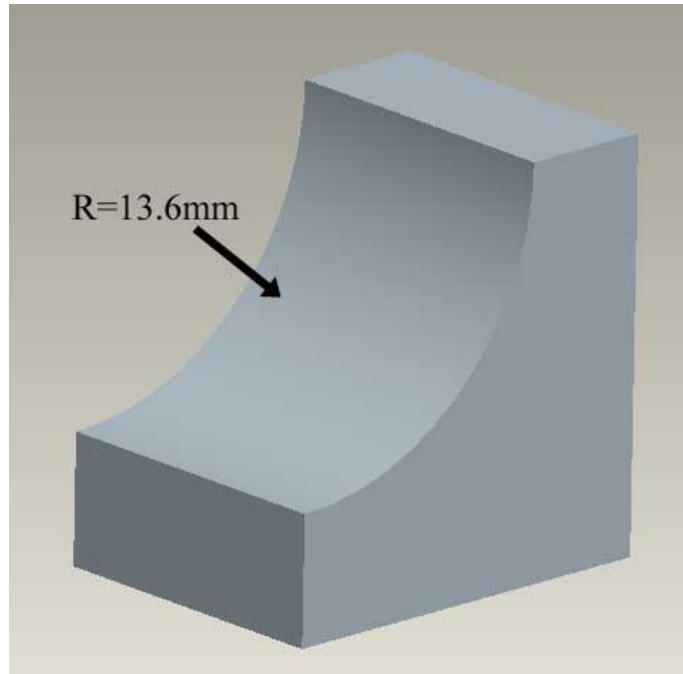


**Figure 4.18 The CAD model of die surface**

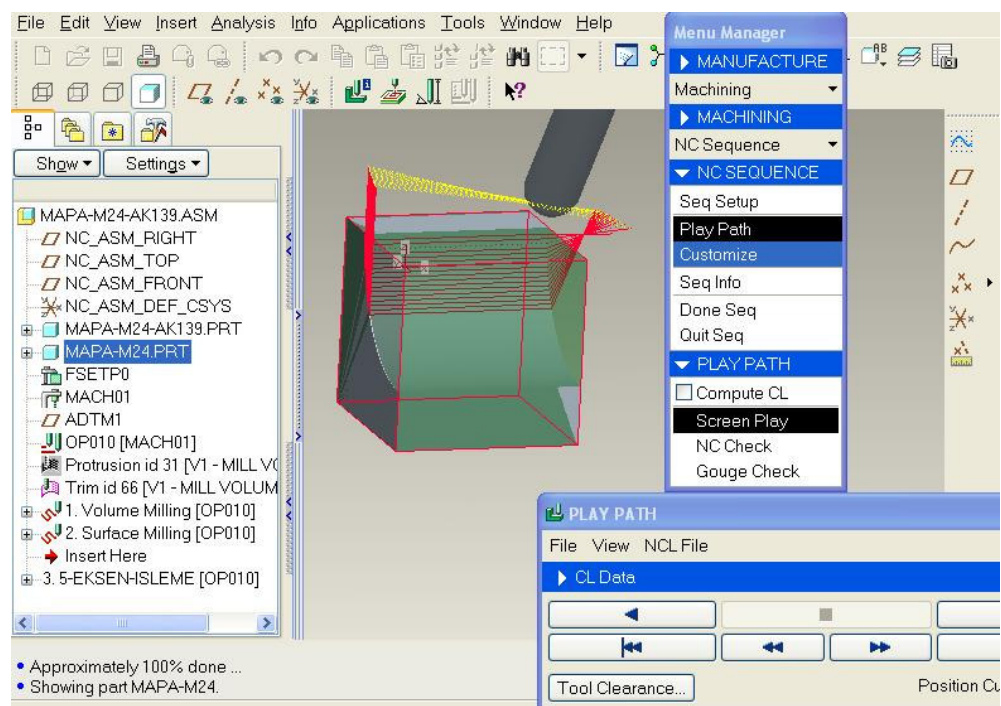


**Figure 4.19 NC programming**

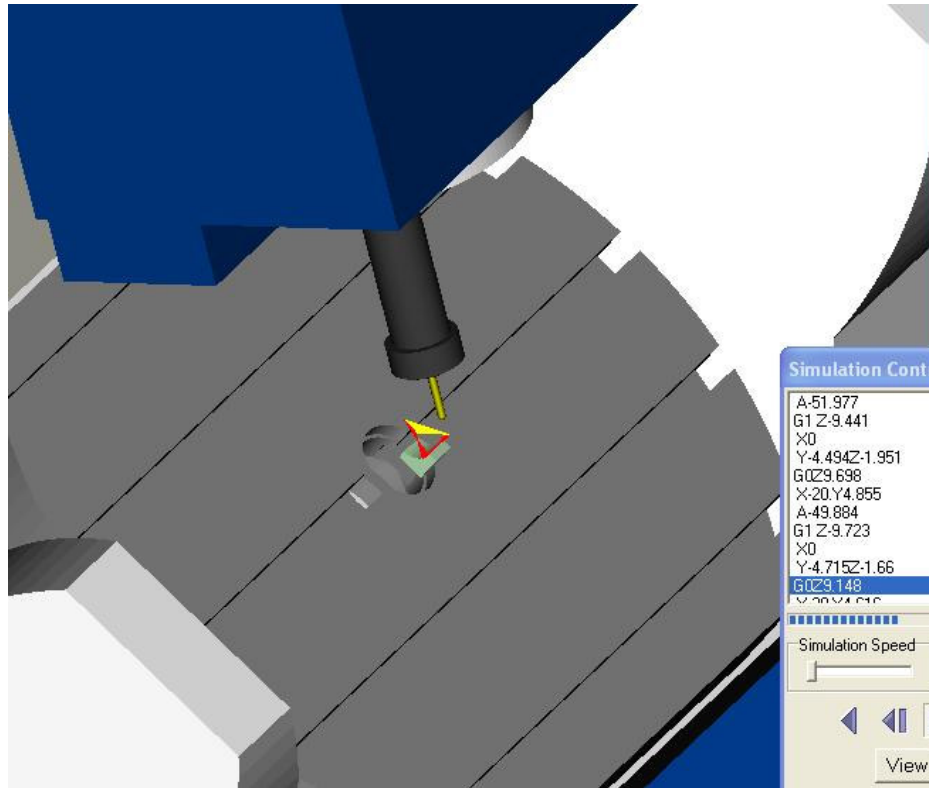


**Figure 4.20 Simulation of MANUS post processor program**

The result of the Vericut simulation program for the finish cut which was carried out using circular cutting paths is shown in Figure 4.21. Different colors on the die radius represent the excess material and gouge amounts in the range which was defined in the AUTO-DIFF window in Vericut. The result of the Vericut simulation program for the milling process using linear cutting paths is demonstrated in Figure 4.22. The simulation indicates that the surface was obtained without any excess material and gouges on it.

Furthermore, the Vericut program reports numerical results of the excess material and gouge amounts with their positions for the milling given in Appendix B. When these two different milling paths are compared, it was seen that cutting using linear paths provides better results contrary to cutting using circular paths.

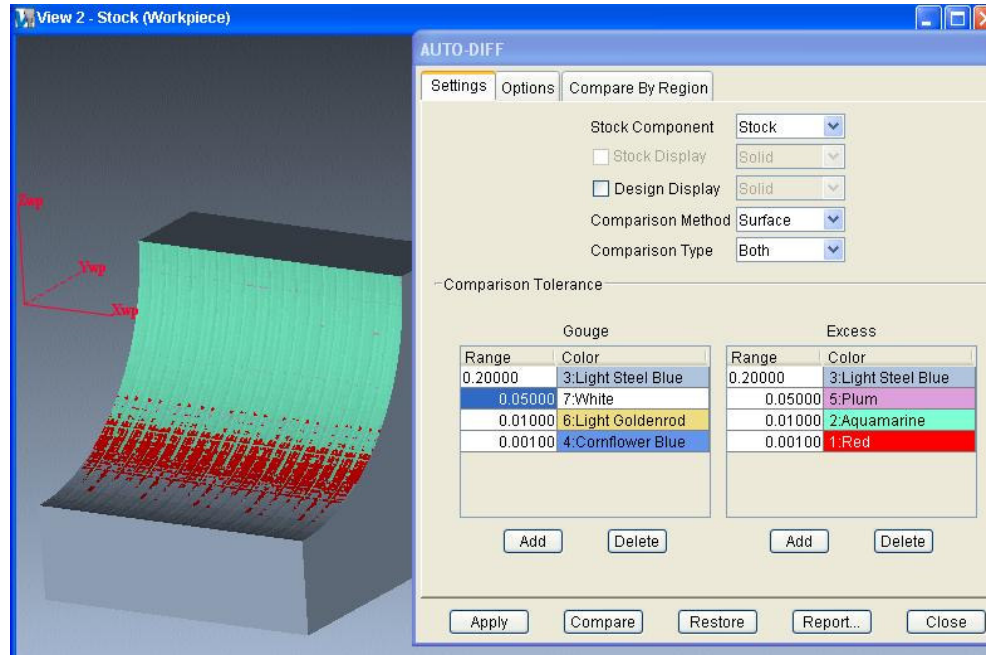


Figure 4.21 Simulation result of Vericut when circular tool paths were used

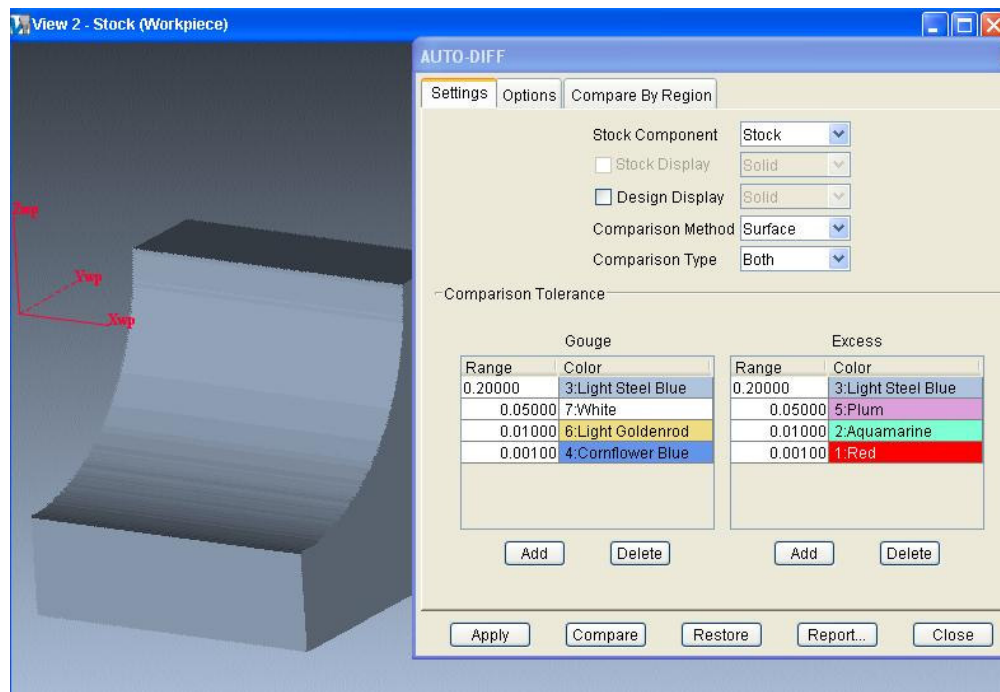
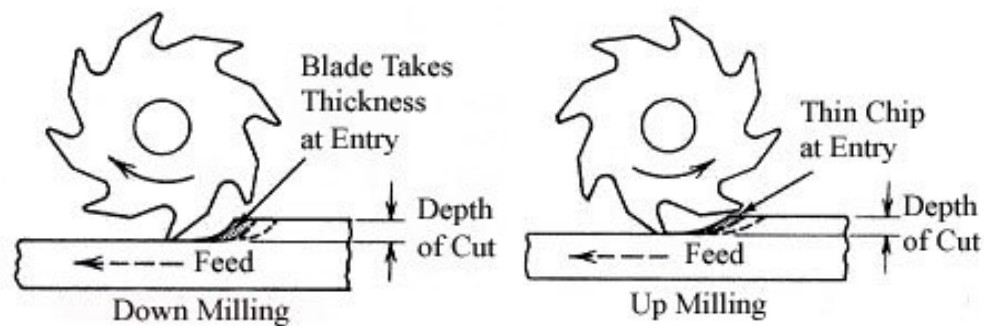


Figure 4.22 Simulation result of Vericut when linear tool paths were used

The simulation program Vericut does not consider most of the cutting effects like feed, cutting speed, vibration, material of tool and stock, amount of material that is left in previous cut and etc. The program only removes the material where the tool passes according to NC codes. Consequently, the results of the program are just an approximation. However, the relative differences in the results with respect to each other provide an approach to compare the cutting paths. In Chapter 5, effect of cutting paths will be analyzed by using experimental results to test the comparison of the Vericut machining simulation program.

#### 4.6 Down (Climb) and Up (Conventional) milling

There are two different ways in cutting processes, according to the relative movement of tool on the stock material [29]. In up milling the cutter rotates against the direction of feed of the workpiece and in down milling the rotation is at the same direction as the feed as demonstrated in Figure 4.23 [9].



**Figure 4.23 Down milling and up milling [9]**

In down milling the cutting edge is mainly exposed to compressive stresses, which are much more favorable for the properties of carbide tool compared with the tensile stresses developed in up milling. It assures low milling tool wear although cutting process is more affected because of greater cutting forces. Modern machine tools are more rigid, that is why allowing use of down milling [30]. In order to see the effect of these cutting ways on surface quality an experimental study is done and the results are shown in Chapter 5 for comparison.

#### 4.7 Cutting Parameters in CNC Milling

a) Cutting speed: It is the speed at which the cutting tooth of the tool moves with respect to the work. It depends on the tool diameter (D) and spindle speed (N) and calculated according to following equation.

$$V_c = \frac{\pi \times D \times N}{1000} \quad (4.10)$$

For the cutting speed (V<sub>c</sub>), a range of 60-80 m/min for rough cut and 100-130 m/min for finish cut is recommended [27] when the chosen tools are used on DIN 2344 die material.

b) Feed per tooth: For the study, the values between 0.050 and 0.132mm/tooth for rough cutting and the values between 0.066 mm/tooth and 0.034 mm/tooth for finish cutting, are recommended as a feed per tooth value (f<sub>z</sub>) [25]. It depends on the spindle speed (N), number of flutes (z) and table feed (V<sub>f</sub>) and the formula is;

$$f_z = \frac{V_f}{N \times z} \quad (4.11)$$

c) Stepover: Radial engagement of tool with the workpiece is called stepover as shown in Figure 4.24. During rough cutting, it is important to cut in higher volumetric rates to minimize the cutting time. To achieve this, about 100% radial engagement seems more logical. However, choosing that much of step over values may decrease the tool life. It is better for longer tool life with 66% radial engagement because of the entry angle of the cutting edge of the tool with the workpiece [31]. As a result, the stepover is chosen as 4mm in rough cutting process, which is 66.7% of 6mm.

In finish operation, the recommended range of stepover is 0.15 mm-0.25 mm for the chosen ball endmill [27]. It is an important parameter in determination of the surface quality in finish cut.

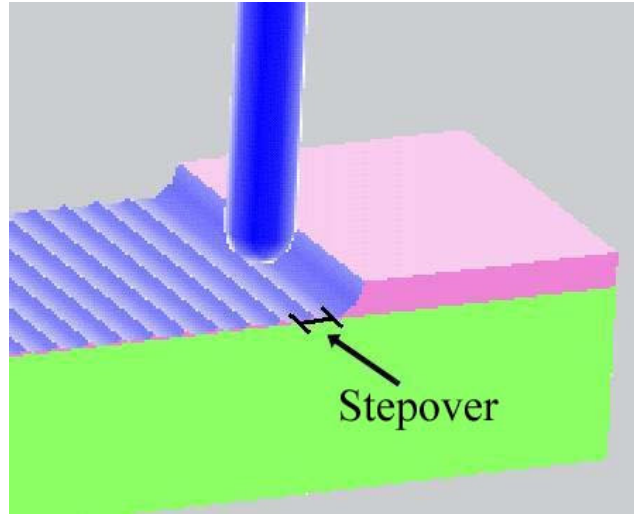


**Figure 4.24 Stepover**

#### **4.8 Other Parameters**

This study has been done by using CNC vertical machining center, Mazak VARIAXIS 630-5X, which is in use in METU BILTIR Center, shown in Appendix C. For the study, the steel DIN 2344 is chosen as the test material, as it is commonly used for forging dies in industry. The properties and composition of the test material is given in Appendix D. For cutting process, especially for finish cutting process using high precise collet is essential to minimize the vibration on the cutting tool. So an AA class collet [25] will be used to connect tools to the holders. Moreover cooling is important and air cooling will be used according to the advice of tool manufacturer [27].

## CHAPTER 5

### MACHINING EXPERIMENTS ON CNC MILLING MACHINE

#### 5.1 Test Specimen and Cutting Parameters

Initial geometry of the test specimen is shown in Figure 5.1, which was used to compare the milling methods discussed in Chapter 4. The specimen was machined from cylindrical block of DIN 2344 steel by using the Wire Electrical Discharge Machine in METU-BİLTİR Center.

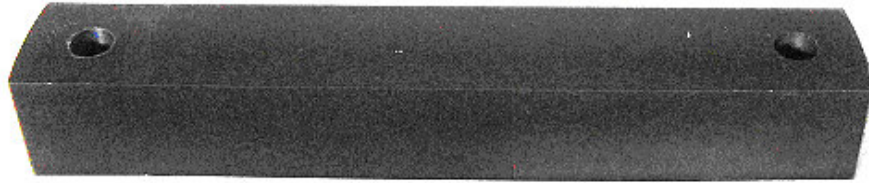


**Figure 5.1 The test specimen**

The specimen was fixed on the table of the CNC milling machine by using the holes that were drilled near the edges. Then, rough cut was performed on the region of the middle as shown in Figure 5.2. During the rough cut, the cutting parameters; finish allowance of 0.15 mm, depth of cut of 0.14 mm, step over of 4 mm, the average recommended cutting speed of 60 m/min and feed per tooth value of 0.091mm/tooth have been used. After rough cut, for the comparison, finish cuts were performed by using different cutting methods on each segments width of 10 mm on the specimen as demonstrated in Figure 5.3. As a result, for each 10 mm length of the specimen, different surface qualities were obtained.



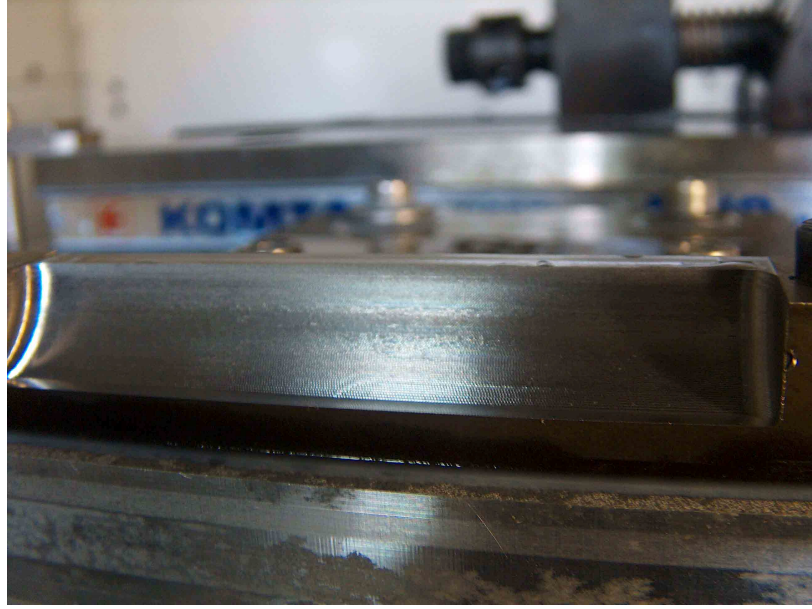


**Figure 5.2 Test specimen after rough cut**

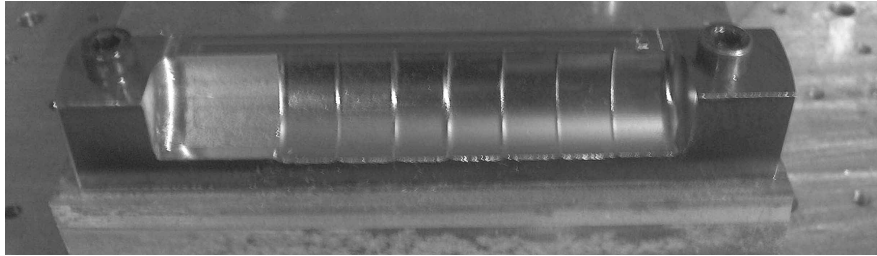


**Figure 5.3 Test specimen during finish cut**

In order to compare the quality of the die surfaces obtained on the specimen after finish cut, the Ra values of the divisions were measured as Ra is the most commonly used factor to identify the surface quality. The Ra values were measured by using Taylor Hobson's Talysurf PGI stylus type surface roughness measuring machine in ASELSAN, Ankara. The stylus tip of the measuring machine, illustrated in Figure 5.4, has 2  $\mu\text{m}$  curvature with 90° angle which provides precise measurement. The surface texture parameter uncertainty of the measurement machine is 2 % + 4nm [32]. According to the recommendation of ORTADOĞU RULMAN SANAYİ Quality Department, 2.5 mm cut off length and Gaussian digital filter was chosen for the measurements [33].





**Figure 5.4 Taylor Hobson's Talysurf PGI stylus type surface roughness measuring machine**

## **5.2 The Milling Experiments for Comparison**

In the first set of experiments a comparison study is done. The comparisons were done in three different methods. First of all, three and five axes milling, secondly; down and up milling and lastly two different cutting paths were compared to each other based on surface quality. The cutting parameters, which were used during finish cut for all experiments, were same and given in Table 5.1. These values are the average of the recommended limits which were discussed in Chapter 4. For each experiment, three Ra measurements were taken and average of these three measurements was used in the comparison study. The parameters used in the experiments and the measurement results are given in detail in Table 5.2 and Table 5.3. The photographs of the surfaces are demonstrated in Figure 5.5.

**Table 5.1 Cutting parameters used in the first set of experiments**

Cutting Speed	Feed per tooth	Step over
115 mm/min	0.050 mm/tooth	0.2 mm

**Table 5.2 The methods used during the first set of experiments**

Experiment Number	Methods Used During the Experiments		
	3-axes & 5-axes Milling	Down & Up Milling	Linear & Circular Paths
1-1	3-axes milling	Down milling	Linear path
1-2	3-axes milling	Down + Up milling	Linear path
1-3	5-axes milling with 15° inclination angle	Down milling	Linear path
1-4	5-axes milling with 15° inclination angle	Up milling	Linear path
1-5	5-axes milling with 15° inclination angle	Down + Up milling	Linear path
1-6	5-axes milling with 15° inclination angle	Down milling	Circular path
1-7	5-axes milling with 15° inclination angle	Down + Up milling	Circular path
1-8	5-axes milling normal to the surface	Down milling	Linear path
1-9	3-axes milling	Down milling	Circular path

**Table 5.3 The Ra measurement results of the first set of experiments**

Experiment Number	Measurement 1 Ra ( $\mu\text{m}$ )	Measurement 2 Ra ( $\mu\text{m}$ )	Measurement 3 Ra ( $\mu\text{m}$ )	Average Ra ( $\mu\text{m}$ )
1-1	0.679	0.653	0.677	0.670
1-2	0.772	0.752	0.776	0.767
1-3	0.950	0.958	0.944	0.951
1-4	0.989	0.978	0.984	0.984
1-5	1.171	1.175	1.169	1.171
1-6	1.102	1.076	1.129	1.103
1-7	1.344	1.298	1.317	1.320
1-8	1.558	1.581	1.594	1.578
1-9	1.555	1.577	1.609	1.580

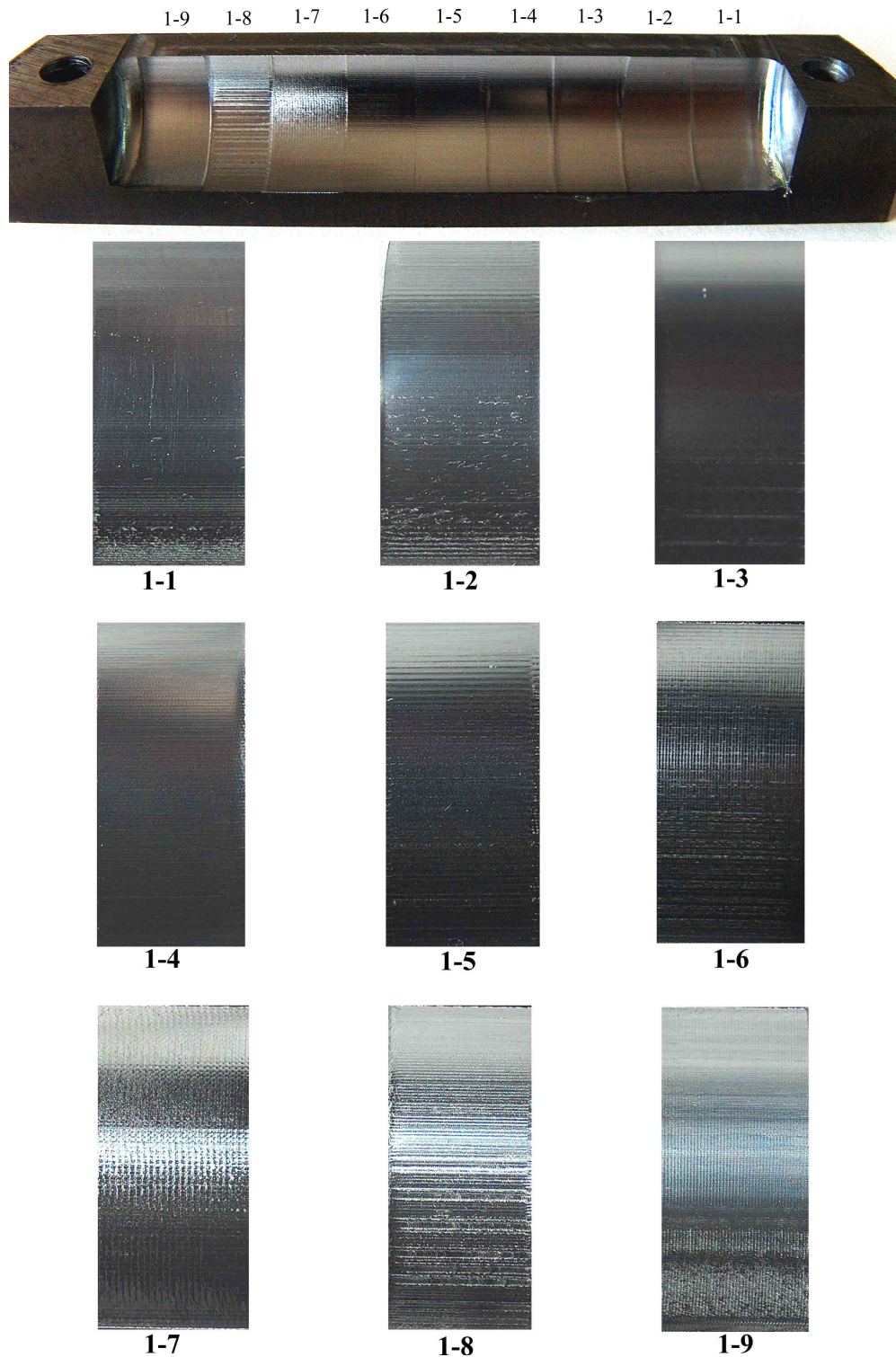


**Figure 5.5 The photographs of test specimen surfaces of first set of experiments used for comparison study**

### 5.3 Comparison of 3-Axes and 5-Axes Milling

In the first group of first set of experiments, 3-axes and 5-axes milling were compared. Three different cutting methods are used to see if these methods make any difference in the comparison of 3-axes and 5-axes milling. The chosen methods are down milling along linear path, down and up milling used together along linear path and down milling along circular path.

#### 5.3.1 3-Axes Milling

When the die surfaces which are machined by using three axes milling were analyzed, it was observed that the imperfections were more obvious at the bottom region of the curved die cavity profile as shown in Figure 5.6. This is an expected result as the cutting points of the tool which are in contact with the material of the radial die cavity, are getting closer to the tool tip where the cutting speed approaches to zero. However, this is a small part of the radial die cavity and the surface quality in the remaining part of the radial die cavity is comparatively better. The average Ra values measured over the surface machined using different parameters by 3-axes milling over the first specimen is given in Table 5.4.

**Table 5.4 The Ra values of the 3 axes milling experiments**

Experiment Number	The methods used during the experiment		Average Ra Values ( $\mu\text{m}$ )
	Down & Up Milling	Linear & Circular Paths	
1-1	Down milling	Linear path	0.670
1-2	Down + Up milling	Linear path	0.767
1-9	Down milling	Circular path	1.580

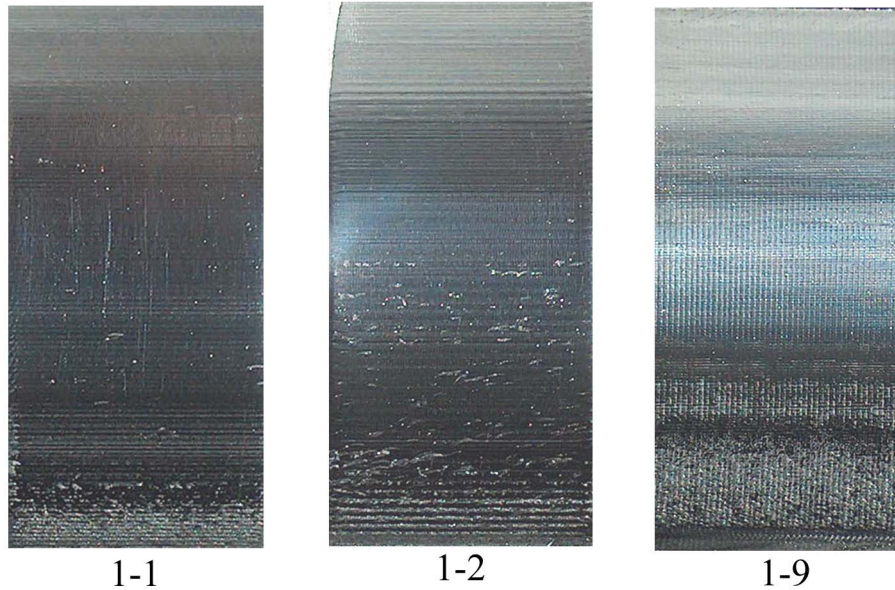
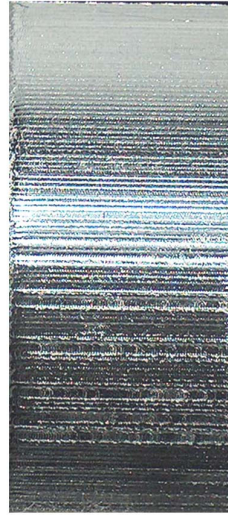


**Figure 5.6 The Photographs of the surfaces that are machined by using 3-axes CNC milling**

### **5.3.2 5-Axes Milling**

In 5-axes milling, it is possible to achieve the same cutting speed at every part of the radial die cavity which results in a similar surface texture for all portions of the surface. During 5 axes milling if an inclination angle is not used, the milling tool is always positioned normal to the machined surface and cutting is performed by the tip of the tool, where the cutting speed is nearly zero. The surface with the experiment number “1-8” was machined by this method and, it was observed that the lay profile formed after the finish cut was clear because of the low cutting speed. On the other hand, the surface texture is similar on the entire profile as demonstrated in Figure 5.7.

It is possible to improve the surface quality in 5-axes milling by using an inclination angle as described in Chapter 4. While preparing the NC codes, the tool orientation which is normal to the surface by default may be altered and an inclination angle can be set in NC program so the tool may be oriented like in Figure 5.8. As a result, a constant cutting speed with higher speed values is obtained.



1-8

**Figure 5.7 The photograph of the surface that is machined by using 5-axes milling normal to surface**

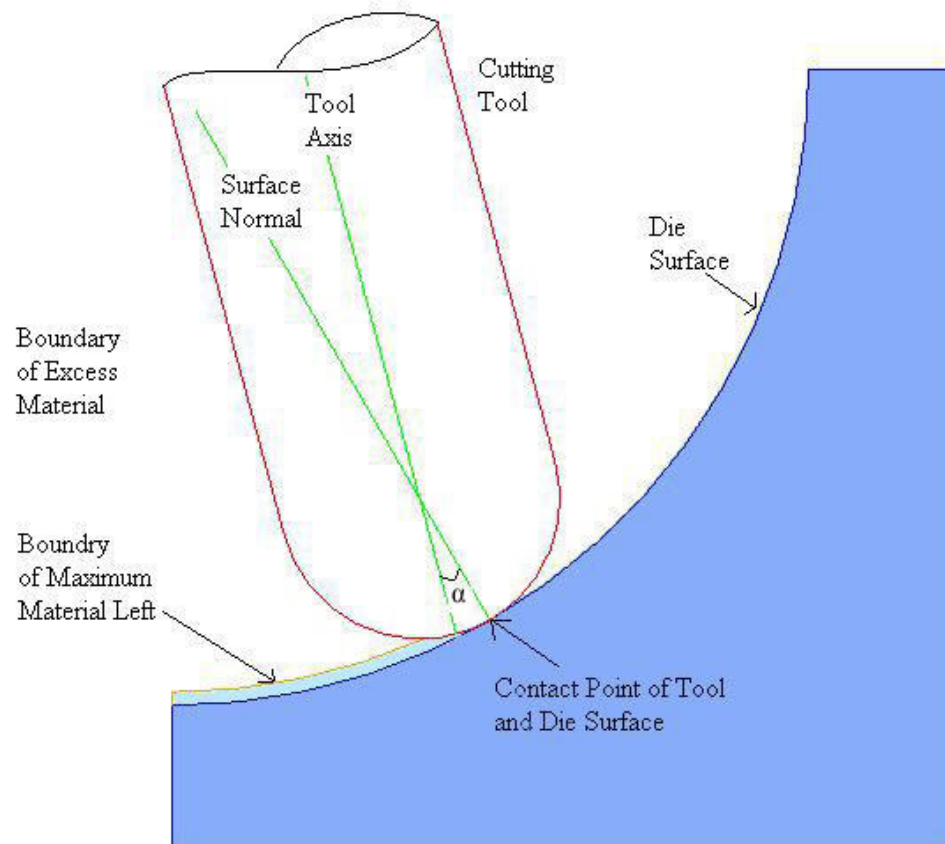


**Figure 5.8 5-axes machining of the radial die cavity with an inclination angle**

The distance of the cutting point ( $d_{cp}$ ) to the tool axis for an inclined milling tool with an angle  $\alpha$  is as follows (Figure 5.9);

$$d_{cp} = \frac{D}{2} \times \sin \alpha \quad (5.1)$$

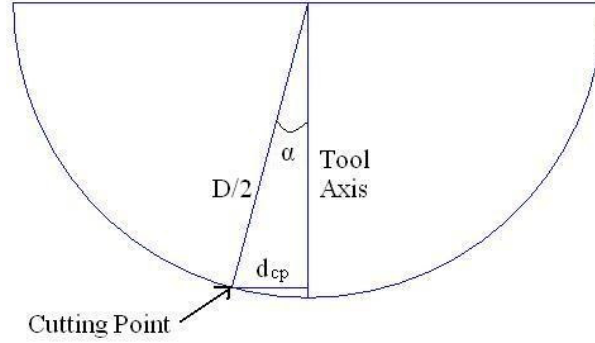


**Figure 5.9 Tool tip of a ball endmill**

For the chosen ball endmill with diameter of 6 mm, 15° inclination angle is used in the study and the distance of cutting point is calculated as;

$$\begin{aligned} d_{cp} &= \frac{D}{2} \times \sin 15 \\ d_{cp} &= 3 \times 0.26 = 0.78 \text{ mm} \end{aligned} \quad (5.2)$$

As the distance between the cutting point of the milling tool and the tool axis is 26% of tool diameter, the cutting speed at the cutting points of the milling tool is also 26% of the cutting speed which remains constant in milling process.

The results of the Ra measurements of the surfaces machined by determined methods using 5-axes milling with inclination angle of 15° were given in Table 5.5 and the surfaces are demonstrated in Figure 5.10.

**Table 5.5 The Ra results of 5-axes milling with 15 degree inclination angle**

Experiment Number	The methods used during the experiment		Average Ra Values ( $\mu\text{m}$ )
	Down & Up Milling	Linear & Circular Paths	
1-3	Down milling	Linear path	0.951
1-5	Down + Up milling	Linear path	1.171
1-6	Down milling	Circular path	1.103



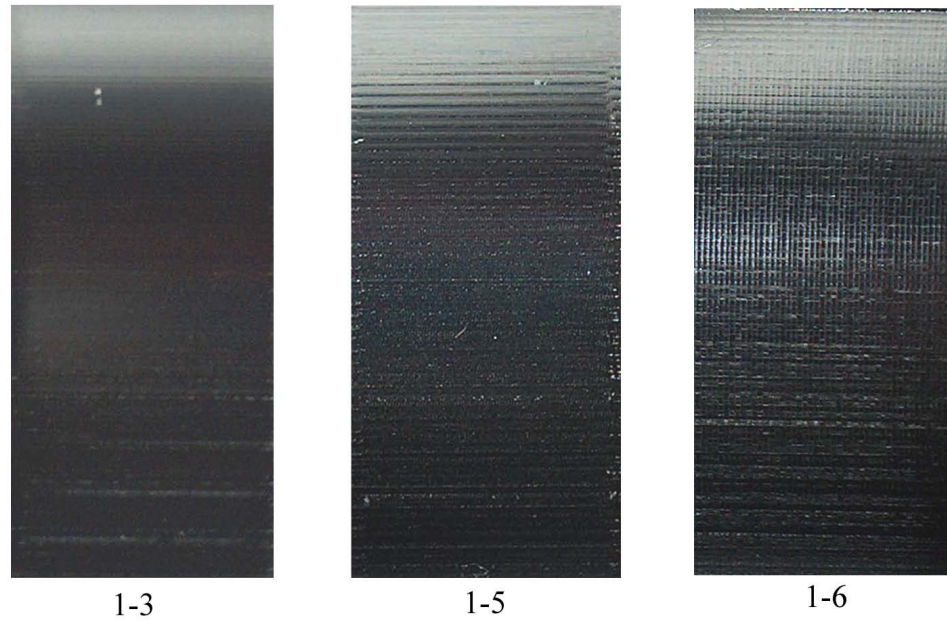


**Figure 5.10 Photographs of Surfaces that are machined using 5-axes milling**

### **5.3.3 Discussion of Results**

The Ra values of the surfaces, which are machined using 3-axes and 5-axes milling, are given in Table 5.6 for comparison. It is observed that the average Ra values measured over the surfaces which were machined using 3-axes milling along linear path were better than the results obtained over the surfaces machined by 5-axes milling. However, the case was quite different if the similarity of the surface quality over the radial die cavity is compared. 5-axes milling provided similar surface quality all over the die cavity. On the other hand, the bottom region of die cavity obtained by 3-axes milling is poor in surface quality which is also seen in Figure 5.6. Although the bottom portion of the radial die cavity is a small part of the surface, which is machined by using 3-axes milling, it is better to obtain a surface with similar surface quality in all parts. Because, these imperfections condensed at the bottom portion may lead micro cracks and also cause higher friction rates with respect to other regions during forging process which is undesirable. Thus, 5-axes milling with an inclination angle as illustrated in Figure 5.11 is more favorable than 3-axes milling.



**Table 5.6 Ra Comparison of manufacturing by 3-axes and 5-axes milling**

Used Method		Average Ra Values ( $\mu\text{m}$ )	
		3-Axes	5-Axes
Down milling	Linear path	0.670	0.951
Down + up milling	Linear path	0.767	1.171
Down milling	Circular path	1.580	1.103

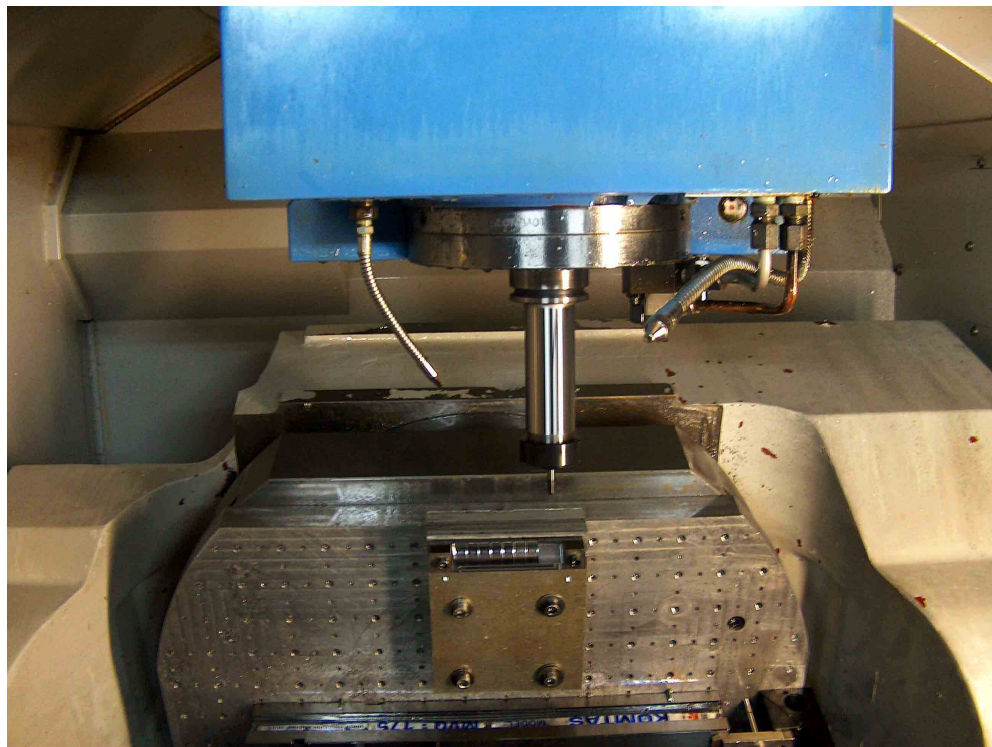


**Figure 5.11 5-axes machining with an inclination angle**

#### **5.4 Comparison of Down and Up Milling**

In the second group of first set of experiments, up and down milling approaches were compared. This comparison was done by using 5-axes milling with an inclination angle of  $15^\circ$ , since it provides better and similar surface quality over the machined surface. The results of the experiments are

demonstrated in Table 5.7. The surfaces, which are obtained after these, experimental machining, are shown in Figure 5.12.

**Table 5.7 Results of manufacturing by down and up milling**

Experiment Number	Compared Methods	Cutting Time	Average Ra Values ( $\mu\text{m}$ )
1-3	Down milling	8.39	0.951
1-4	Up milling	8.39	0.984
1-5	Down + Up milling	2.27	1.171

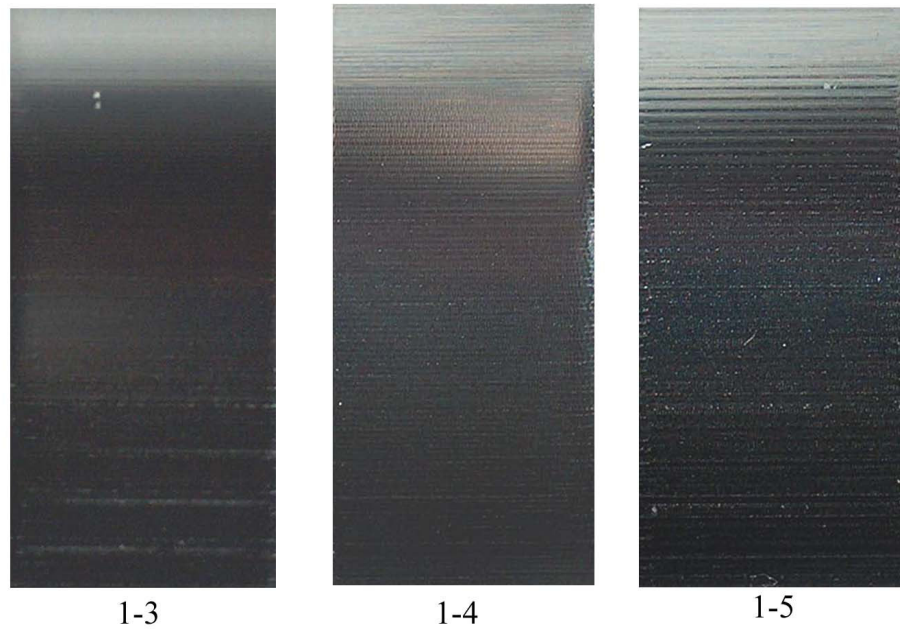


**Figure 5.12 The photographs of the surfaces that are machined for the comparison of down and up milling**

In accordance with the results of Ra measurements, it is seen that the down milling and up milling methods give very close results. The Ra result for down milling is slightly better than up milling and the cutting times for the experiments “1-3” and “1-4” is the same. In order to use down milling or up milling over the entire surface of the selected geometry, it will be necessary to do

a retract movement and move back to the starting side in every stepover stage as illustrated in Figure 5.13 and it will unavoidably increase the cutting time. However, when down and up milling are used together, the tool will be not retracted for the entire cutting process as demonstrated in Figure 5.14. For the experiment “1-5”, the cutting time is 2.27 minutes if down and up milling used together. However, the cutting time increases to 8.39 minutes if only down milling or only up milling is used which is shown in Table 5.7. This is an important difference. Also the average Ra value did not change much if up and down milling used together with respect to the use of down milling. So, it is possible to propose that using down and up milling together is more appropriate for milling operations of such geometries for the defined milling conditions as the cutting time is critical.

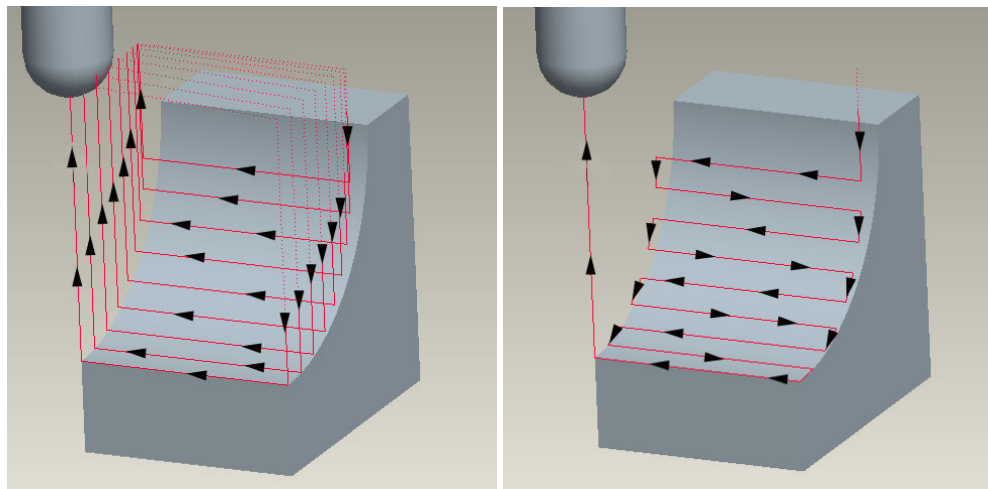


**Figure 5.13 Simulation of down milling    Figure 5.14 Simulation of down and up milling used together**

## 5.5 Comparison of Cutting Paths

In the last group of first set of cutting experiments, linear cutting paths and circular cutting paths are analyzed which are discussed in Chapter 4 and demonstrated in Figure 4.16 and Figure 4.17. Firstly, down milling was used and

secondly, down and up milling were used together for the comparison of linear and circular tool paths. The measurement results are given in Table 5.8 and Table 5.9. The surfaces which are the results of these experiments are demonstrated in Figure 5.15 and Figure 5.16. In Chapter 4, the Vericut analysis program was used for comparison and cutting in linear paths appeared to be better in surface analysis results. Like the results of the Vericut analysis program [28], when the Ra results of the experiments are compared, it is seen that cutting along linear paths provided better surface quality than cutting along circular path for the particular curved surface that is selected.

**Table 5.8 Ra values for linear and circular cutting paths when down milling was used**

Experiment Number	Compared Strategies	Average Ra Values ( $\mu\text{m}$ )
1-3	Linear path	0.951
1-6	Circular path	1.103

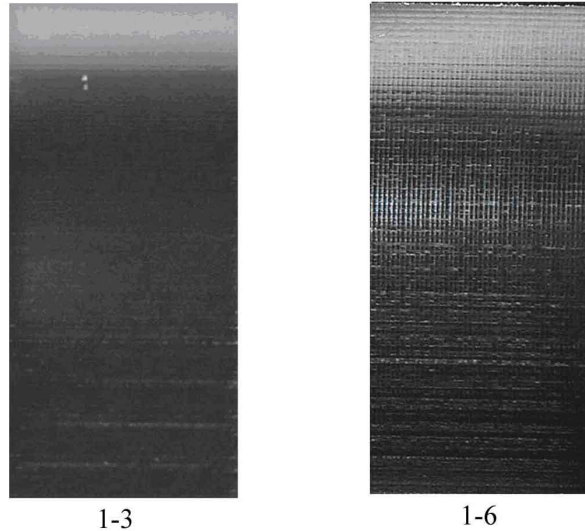


**Figure 5.15 Photographs of the surfaces, machined for the comparison of tool path strategies when down milling was used**

**Table 5.9 Ra values for linear and circular cutting paths when down and up milling were used together**

Experiment Number	Compared Strategies	Average Ra Values ( $\mu\text{m}$ )
1-5	Linear path	1.171
1-7	Circular path	1.320

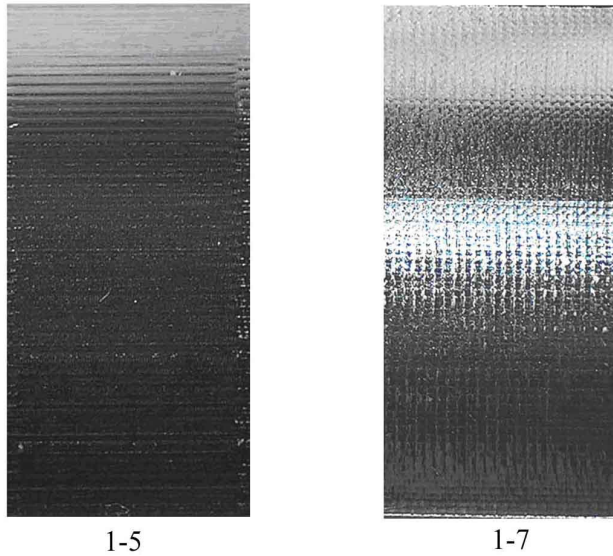


**Figure 5.16 Photographs of the surfaces, machined for the comparison of tool path strategies when down and up milling were used together**

### **5.6 General Discussion of the First Set of Experiments**

In summary, based on these three groups of cutting experiments, it is possible to conclude that when Ra value is important, 5-axes milling with an inclination angle in linear paths and using down milling or up milling is the most appropriate combination for the milling operations for the chosen particular curved surface.

However, besides roughness if cutting time is also taken into consideration; it will be better to use down and up milling together in addition to cutting by 5-axes milling with an inclination angle in linear path for the chosen particular curved surface.

## CHAPTER 6

### ANALYSIS OF THE EXPERIMENTS AND DERIVATION OF Ra PREDICTION FORMULAS

In this experimental study, feed per tooth, cutting speed and step over (radial depth of cut) have been chosen as process variables and their effects on average surface roughness have been examined by considering “Design of Experiment” approach as described in Chapter 3. The  $2^3$  Factorial design has been used to include the interaction effects of the parameters on the surface roughness.

In the first set of experiments, which was discussed in Chapter 5, a comparison study is performed and according to the results of these experiments, two different cutting methods were determined for the subsequent milling experiments. In the second set of experiments, down milling was used and in the third set of experiments, down milling and up milling were used together. The mathematical prediction formula of Ra value, for each of these cutting methods will be presented in this chapter. In order to test the accuracy of prediction formula, the forth set of experiments were conducted. In the second and third set of experiments, same limits of milling parameters were used, which were given in Table 6.1 and decided as discussed in Chapter 4.

**Table 6.1 Limits of milling parameters for Ra prediction experiments**

<b>Milling Parameters</b>	<b>Minimum</b>	<b>Maximum</b>
<b>Spindle speed</b>	100 mm/min	130mm/min
<b>Feed per tooth</b>	0.034mm/tooth	0.066mm/tooth
<b>Step over</b>	0.15 mm	0.25 mm

6.1 Ra Analysis for Down Milling

In the second set of experiments, the 5-axes milling with 15° inclination angle in linear paths using down milling was used. As the 2<sup>3</sup> factorial design was chosen, eight experiments were performed. Three Ra measurements were taken over the surfaces and the average of the results were used to analyze the change in surface quality when different cutting parameters were used. The Geometric View of the 2<sup>3</sup> factorial design for Ra prediction experiments are shown in Figure 6.1 and their measurement results are given in the Table 6.2. Moreover, the photograph of the test specimen which has been obtained during these experiments is demonstrated in Figure 6.2.

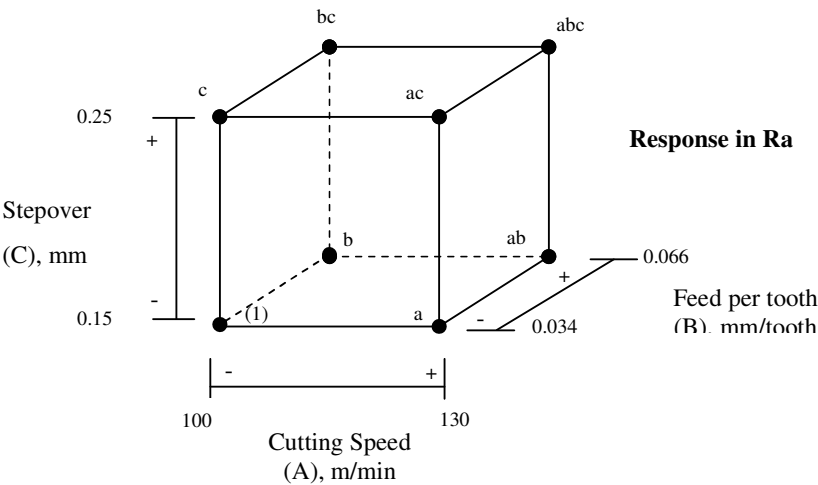


Figure 6.1 The Geometric View of the 2<sup>3</sup> factorial design for Ra prediction experiments

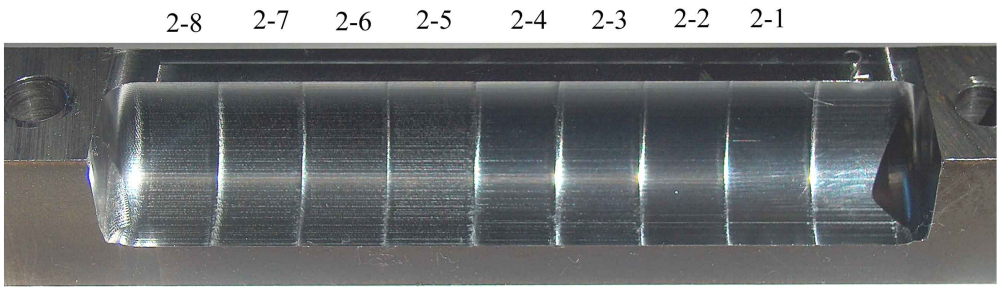


Figure 6.2 The photograph of the test specimen of the second set of experiments manufactured by down milling



**Table 6.2 The results of second set of experiments for Ra prediction**

		Input Parameter Values			Response of the experiments			
Experiment Number	Process Design	A (cutting Speed)	B (feed/ tooth)	C (step over)	Ra 1 ( $\mu\text{m}$ )	Ra 2 ( $\mu\text{m}$ )	Ra 3 ( $\mu\text{m}$ )	Average Ra ( $\mu\text{m}$ )
2-1	1	100	0.034	0.15	0.945	0.942	0.935	0.941
2-2	a	130	0.034	0.15	0.885	0.891	0.904	0.893
2-3	b	100	0.066	0.15	0.887	0.879	0.904	0.890
2-4	ab	130	0.066	0.15	0.877	0.898	0.882	0.885
2-5	c	100	0.034	0.25	1.006	1.037	1.015	1.019
2-6	ac	130	0.034	0.25	1.049	1.036	1.071	1.052
2-7	bc	100	0.066	0.25	1.073	1.100	1.076	1.083
2-8	abc	130	0.066	0.25	1.015	1.050	1.024	1.029

### 6.1.1 Effect Estimation

Using the Equations defined in Chapter 3, the main and interaction effects of the selected parameters are calculated:

By using Equation 3.10,

$$A = \frac{1}{4}[-0.941 + 0.893 - 0.890 + 0.885 - 1.019 + 1.052 - 1.083 + 1.029] \quad (6.1)$$

$$A = \frac{1}{4}[-0.073] = -0.018$$

By using Equation 3.11,

$$B = \frac{1}{4}[-0.941 - 0.893 + 0.890 + 0.885 - 1.019 - 1.052 + 1.083 + 1.029] \quad (6.2)$$

$$B = \frac{1}{4}[-0.018] = -0.004$$

By using Equation 3.12,

$$C = \frac{1}{4}[-0.941 - 0.893 - 0.890 - 0.885 + 1.019 + 1.052 + 1.083 + 1.029] \quad (6.3)$$

$$C = \frac{1}{4}[0.575] = 0.144$$



By using Equation 3.16,

$$AB = \frac{1}{4}[0.941 - 0.893 - 0.890 + 0.885 + 1.019 - 1.052 - 1.083 + 1.029] \quad (6.4)$$

$$AB = \frac{1}{4}[-0.043] = -0.011$$

By using Equation 3.17,

$$AC = \frac{1}{4}[0.941 - 0.893 + 0.890 - 0.885 - 1.019 + 1.052 - 1.083 + 1.029] \quad (6.5)$$

$$AC = \frac{1}{4}[0.031] = 0.008$$

By using Equation 3.18,

$$BC = \frac{1}{4}[0.941 + 0.893 - 0.890 - 0.885 - 1.019 - 1.052 + 1.083 + 1.029] \quad (6.6)$$

$$BC = \frac{1}{4}[0.100] = 0.025$$

By using Equation 3.19,

$$ABC = \frac{1}{4}[-0.941 + 0.893 + 0.890 - 0.885 + 1.019 - 1.052 - 1.083 + 1.029] \quad (6.7)$$

$$ABC = \frac{1}{4}[-0.129] = -0.032$$

The main and interaction effects are summarized in Table 6.3. When their absolute values are compared, the stepover value (C) has the biggest effect. The main effects of the other parameters and their interactions effects are small compared to the effect of step over.

According to the results of effect calculations, it is understood that a change in step over from 0,15 mm up to 0,25 mm increases the Ra value 0.144  $\mu\text{m}$  which decreases the quality of the surface. This effect is the largest effect and if the Ra value is important, even though it increases the time of machining, taking the minimum value of step over will be better. However, this is the result of main effect of stepover. The interaction effect of feed per tooth and step over (BC) is 0.025  $\mu\text{m}$ . At their maximum values their interaction effect causes an increase of 0.025  $\mu\text{m}$  in the Ra value, which must be also considered besides the main effect of stepover. Second important effect is the interaction effect of cutting speed, feed per tooth and stepover (ABC) which is -0.032  $\mu\text{m}$ . This interaction effect decreases the Ra value at the maximum level of parameters and improves the surface quality. The main effect of cutting speed (A), feed per

tooth (B), interaction effect of cutting speed and feed per tooth (AB) and interaction effect of cutting speed and stepover (AC) have small effects on Ra value which is shown in Table 6.3.

**Table 6.3 Main and Interaction Effects on Ra ( $\mu\text{m}$ ) value when down milling is used**

A	-0.018
B	-0.004
C	0.144
AB	-0.011
AC	0.008
BC	0.025
ABC	-0.032

The main effect and the interaction effects are plotted in Figure 6.3 and Figure 6.4 to show the influence of the parameters and their interaction effect on Ra value. In the Figures 6.3, it is also seen that the main effect of step over is the most important one which influences the Ra.

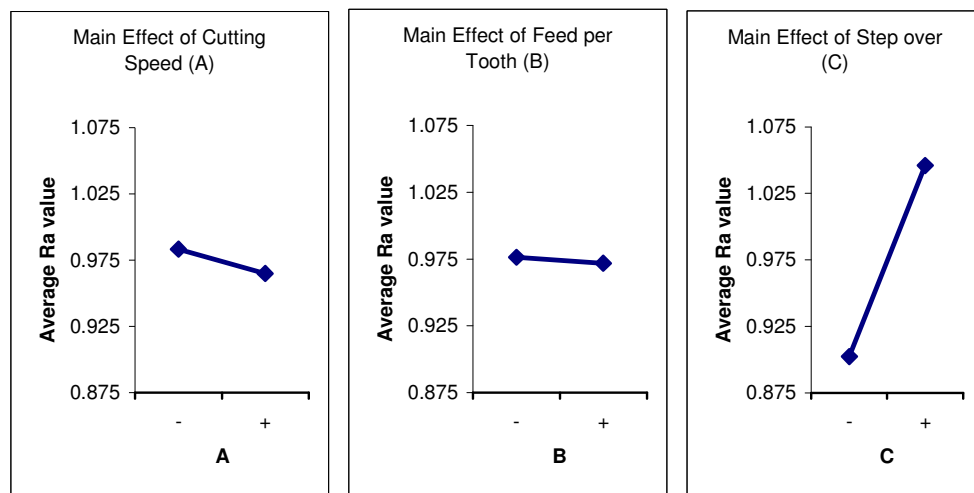


**Figure 6.3 Main effects plots on Ra value when down milling is used**

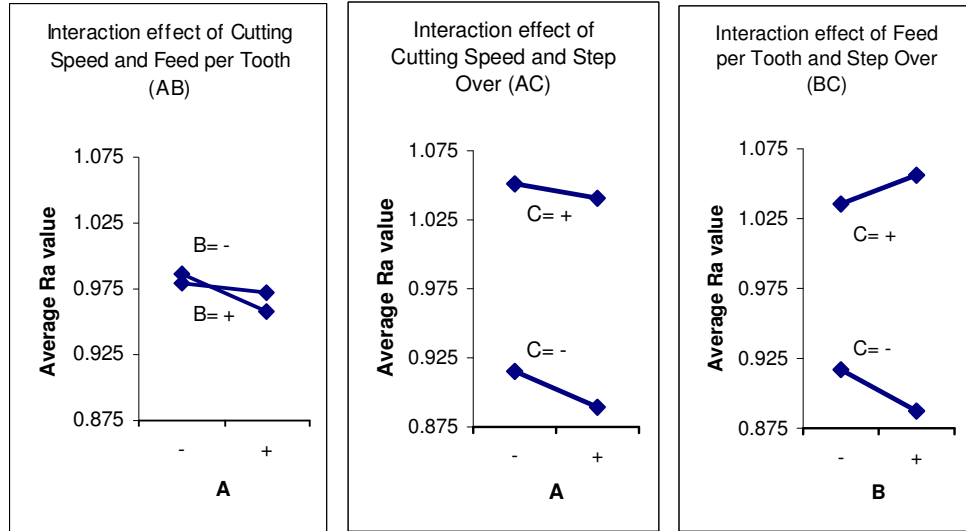


**Figure 6.4 Interaction effects plots on Ra value when down milling is used**

### 6.1.2 Ra Prediction Formula

In order to derive Ra prediction formula, the values of the variable coefficients ( $\beta$ ) of multiple linear regression model, which is discussed in Chapter 3, have to be calculated. Least square method is used to compute the  $\beta$  values.

The least square estimate of  $\beta$  is as follows [22].

$$\beta = (X'X)^{-1} X'y \quad (6.8)$$

Where X is the matrix obtained from input parameters used in the experiments and y is the vector of results of the experiments (Ra values). The input parameters of the experiments and the results of the experiments can be seen in Table 6.4.

The variable coefficients are calculated in Appendix E by applying the least square method to the experimental data obtained from the  $2^3$  factorial design experiments, shown in Table 6.4, and the mathematical model was found as,

$$\begin{aligned} Ra = & 2.47 - 0.0141x_1 - 31.8x_2 - 7.75x_3 \\ & + 0.248x_4 + 0.073x_5 + 171x_6 - 1.35x_7 \end{aligned} \quad (6.9)$$

**Table 6.4 Measurement results of Ra values for second set of experiments**

	Input Parameter Values			Measurement Results
	A (cutting Speed)	B (feed/tooth)	C ( step over)	Response of experiment (Average Ra value)
2-1	100	0.034	0.15	0.941
2-2	130	0.034	0.15	0.893
2-3	100	0.066	0.15	0.890
2-4	130	0.066	0.15	0.885
2-5	100	0.034	0.25	1.019
2-6	130	0.034	0.25	1.052
2-7	100	0.066	0.25	1.083
2-8	130	0.066	0.25	1.029

After the main effect and interaction effect terms are substituted into the Equation 6.9 such as,  $x_1=Vc$ ,  $x_2=fz$ ,  $x_3=ae$ ,  $x_4=Vc.fz$ ,  $x_5= Vc.ae$ ,  $x_6= fz.ae$ ,  $x_7= Vc.fz.ae$  the Ra prediction formula is obtained.

$$Ra = 2.47 - 0.0141 \cdot Vc - 31.8 \cdot fz - 7.75 \cdot ae + 0.248 \cdot Vc \cdot fz + 0.073 \cdot Vc \cdot fz + 171 \cdot fz \cdot ae - 1.35 \cdot Vc \cdot fz \cdot ae \quad (6.10)$$

The difference between the observed value and the predicted value which is found using the Equation 6.10 gives the error of Ra prediction (Equation 6.11). Moreover, the percentage of the error can be calculated by Equation 6.12.

The error (e) is,

$$e = \left| y' - y \right| \quad (6.11)$$

Where

$y'$  is the observed Ra value

$y$  is the predicted Ra value

The percentage of the error ( $e_p$ ) is,

$$e_p = \left| \frac{y' - y}{y} \right| \times 100 \quad (6.12)$$

The eight experimental points are substitute into the Equation 6.10 to calculate the error (Table 6.5). The estimated error percentages are very small. They are changing between 0.36 % and 0.25 % of the real values. This was an expected result because the formula is derived using these eight points and the error results shows that the formula fits to these eight points.

**Table 6.5 Calculated error and error percentage values for second set of experiment of Ra prediction**

Experiment Number	Predicted Ra value	Observed Average Ra value	Error	Error Percentage
2-1	0.938	0.941	0.002	0.25
2-2	0.890	0.893	0.003	0.36
2-3	0.887	0.890	0.003	0.28
2-4	0.882	0.885	0.003	0.32
2-5	1.016	1.019	0.003	0.34
2-6	1.049	1.052	0.003	0.31
2-7	1.080	1.083	0.003	0.30
2-8	1.027	1.029	0.003	0.25

This formula is an approximation for the Ra value and the results of these eight points do not show the accuracy of this formula. Some additional experiments with different cutting parameters were performed in forth set of experiments and Ra values of the surfaces were measured (Table 6.6) to test the correctness of this Ra prediction formula.

**Table 6.6 The observed Ra values used to test the accuracy of Ra prediction formula**

Experiment Number	Cutting Speed (m/min)	Feed Per Tooth (mm/tooth)	Step Over (mm)	Ra 1 (µm)	Ra 2 (µm)	Ra 3 (µm)	Average Ra (µm)
1-3	115	0.050	0.200	0.950	0.958	0.944	0.951
4-1	110	0.050	0.150	0.937	0.948	0.908	0.931
4-3	122.5	0.058	0.225	1.032	1.007	1.037	1.026
4-4	107.5	0.042	0.175	0.952	0.944	0.941	0.946

The parameters used in these additional experiments are substituted into the Equation 6.10 and the error calculation results are shown in Table 6.7. The maximum error percentage value is 2.94%. This is acceptable and confirms that this formula is suitable in the defined limits for Ra value prediction when down milling is used.

**Table 6.7 Calculated error and error percentage values for test experiments**

Experiment Number	Observed Average Ra value	Predicted Ra value	The error	The error percentage
1-3	0.951	0.971	0.020	2.09
4-1	0.931	0.904	0.027	2.94
4-3	1.026	1.002	0.023	2.28
4-4	0.946	0.946	0.000	0

## 6.2 Ra Analysis When Down and Up Milling is Used Together

Another Ra formula was derived for the cutting type in which down and up milling were used together as the cutting time was shorter in this method for the selected geometry.

By using the same parameters defined before, eight experiments were conducted as a third set of experiments and their Ra values were measured as shown in Table 6.8 to derive a Ra prediction formula when both of down and up milling was used together. The test specimen, which was machined to drive the formula, is shown in Figure 6.5.

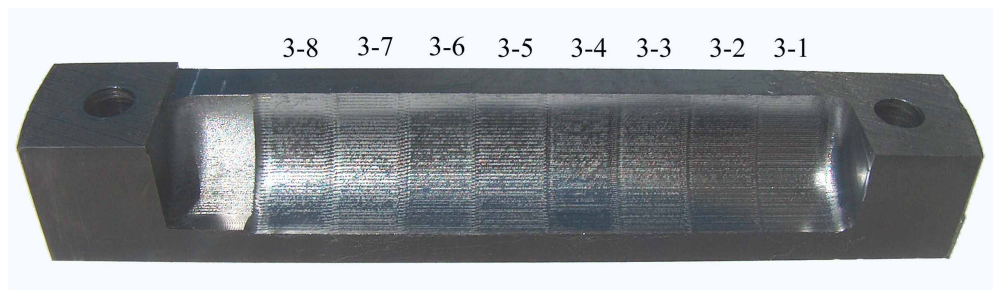


**Figure 6.5 The photograph of the test specimen of the third set of experiments manufactured by using down and up milling together**

**Table 6.8 The result of the third set of Ra prediction experiments**

		Input Parameter Values			Response of the experiments			
Experiment Number	Process Design	A (cutting Speed)	B (feed/ tooth)	C (step over)	Ra 1 ( $\mu\text{m}$ )	Ra 2 ( $\mu\text{m}$ )	Ra 3 ( $\mu\text{m}$ )	Average Ra ( $\mu\text{m}$ )
3-1	1	100	0.034	0.15	1.101	1.130	1.131	1.121
3-2	a	130	0.034	0.15	1.122	1.155	1.133	1.137
3-3	b	100	0.066	0.15	1.250	1.232	1.212	1.231
3-4	ab	130	0.066	0.15	1.157	1.144	1.131	1.144
3-5	c	100	0.034	0.25	1.226	1.184	1.239	1.217
3-6	ac	130	0.034	0.25	1.234	1.217	1.197	1.216
3-7	bc	100	0.066	0.25	1.259	1.268	1.261	1.262
3-8	abc	130	0.066	0.25	1.343	1.301	1.295	1.313

### 6.2.1 Effect Estimation

The main and interaction effects are calculated like in the previous study.

By using Equation 3.10,

$$A = \frac{1}{4}[-1.121 + 1.137 - 1.231 + 1.144 - 1.217 + 1.216 - 1.262 + 1.313] \quad (6.13)$$

$$A = \frac{1}{4}[-0.022] = -0.005$$

By using Equation 3.11,

$$B = \frac{1}{4}[-1.121 - 1.137 + 1.231 + 1.144 - 1.217 - 1.216 + 1.262 + 1.313] \quad (6.14)$$

$$B = \frac{1}{4}[0.260] = 0.065$$

By using Equation 3.12,

$$C = \frac{1}{4}[-1.121 - 1.137 - 1.231 - 1.144 + 1.217 + 1.216 + 1.262 + 1.313] \quad (6.15)$$

$$C = \frac{1}{4}[0.376] = 0.094$$

By using Equation 3.16,

$$AB = \frac{1}{4}[1.121 - 1.137 - 1.231 + 1.144 + 1.217 - 1.216 - 1.262 + 1.313] \quad (6.16)$$

$$AB = \frac{1}{4}[-0.053] = -0.013$$

By using Equation 3.17,

$$AC = \frac{1}{4}[1.121 - 1.137 + 1.231 - 1.144 - 1.217 + 1.216 - 1.262 + 1.313] \quad (6.17)$$

$$AC = \frac{1}{4}[0.122] = 0.030$$

By using Equation 3.18,

$$BC = \frac{1}{4}[1.121 + 1.137 - 1.231 - 1.144 - 1.217 - 1.216 + 1.262 + 1.313] \quad (6.18)$$

$$BC = \frac{1}{4}[0.025] = -0.006$$

By using Equation 3.19,

$$ABC = \frac{1}{4}[-1.121 + 1.137 + 1.231 - 1.144 + 1.217 - 1.216 - 1.262 + 1.313] \quad (6.19)$$

$$ABC = \frac{1}{4}[0.154] = 0.039$$

According to the absolute values of main and interaction effect results, which are given in Table 6.9, the most important parameter is found as step over (C) value. When step over value is increased from 0.15 mm to 0.25 mm, the Ra value is also increase 0.094  $\mu\text{m}$  which decreases the surface quality. However, it should be pointed out that this is the main effect of stepover. In order to analyze the effect of stepover, its interaction effects also should be considered. For instance, the interaction effect of stepover with cutting speed (AC) on Ra value is 0.030  $\mu\text{m}$ , which must be also considered. The second important effect is the main effect of feed per tooth (B). It is 0.065  $\mu\text{m}$ , which means when B is maximized the Ra value increases 0.065  $\mu\text{m}$  with respect to minimum value of B. The interaction effect of cutting speed, feed per tooth and stepover (ABC) is the third important effect which is 0.039  $\mu\text{m}$ .

The main effect of cutting speed (A) and interaction effect of feed per tooth and stepover (BC) is very small. At their maximum value the Ra changes only 0.005  $\mu\text{m}$  and 0.006  $\mu\text{m}$ . Moreover the interaction effect of cutting speed and



feed per tooth (AB) is a small value. It only changes Ra -0.013  $\mu\text{m}$  between their maximum and minimum values.

**Table 6.9 Main and Interaction Effects on Ra ( $\mu\text{m}$ ) value when both of the down and up milling used together**

A	-0.005
B	0.065
C	0.094
AB	-0.013
AC	0.030
BC	0.006
ABC	0.039

The main and interaction effects are also plotted in Figure 6.6 and Figure 6.7 to show their influence on Ra value. From the plots it is also seen that the effect of C is the most important one.

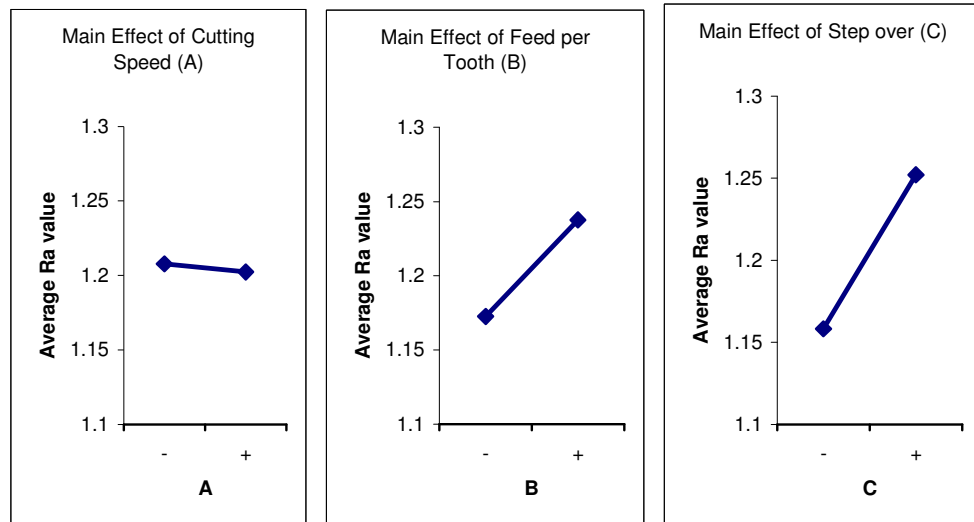


**Figure 6.6 Main effects plots when both of the down and up milling used together**

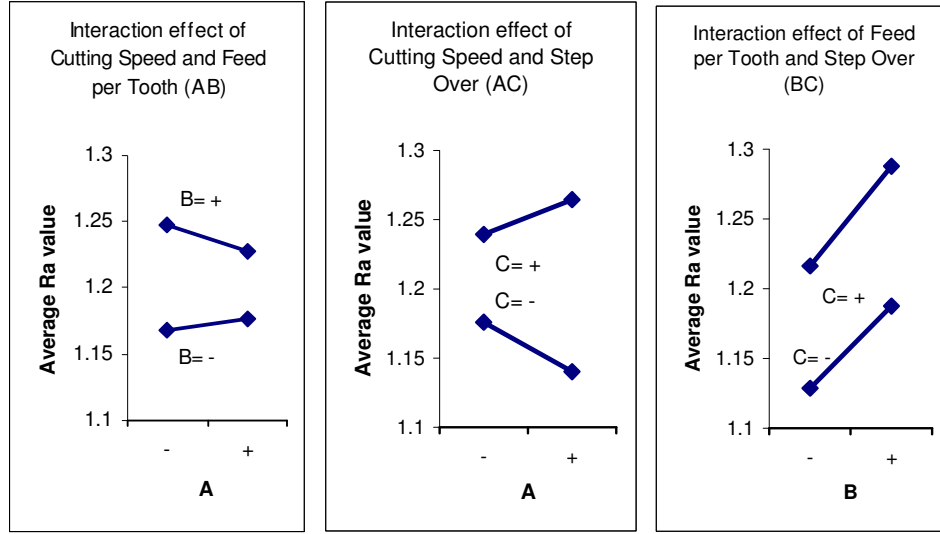


**Figure 6.7 Interaction effects plots when both of the down and up milling used together**

## 6.2.2 Ra Prediction Formula

Again the least square method is used to calculate variable coefficient ( $\beta$ ) values of the Ra prediction formula.

$$\beta = (X'X)^{-1} X'y \quad (6.20)$$

Using the input parameters and measurement results given in Table 6.10, the variable coefficients of Ra prediction formula for both down and up milling used together is calculated in Appendix E and the Ra prediction formula is derived as,

$$\begin{aligned} Ra = & -0.57 + 0.0133 \cdot Vc + 41.4 \cdot fz + 7.71 \cdot ae - 0.349 \cdot Vc \cdot fz \\ & - 0.0606 \cdot Vc \cdot ae - 182 \cdot fz \cdot ae + 1.615 \cdot Vc \cdot fz \cdot ae \end{aligned} \quad (6.21)$$

The error evaluation study is done for these eight points which are used to drive the formula to see if the formula fits to these points. The results of this study are given in Table 6.11.

The error percentage in Table 6.11 is changing between 0.35% and 0.06%. Small error values are as expected like the previous study, as they are used to derive the formula. However the results of these points can not analyze the

accuracy of the formula as they are used to obtain the formula. In order to test the formula new experiments were conducted in forth set of experiments by using different parameters in between the chosen limits and given in Table 6.12.

**Table 6.10 Measurement results of average Ra values for third set of experiments when down and up milling used together**

Experiment Number	Input Parameter Values			Measurement Results
	A (cutting Speed)	B (feed/tooth)	C (step over)	Response of experiment (Average Ra value)
3-1	100	0.034	0.15	1.121
3-2	130	0.034	0.15	1.137
3-3	100	0.066	0.15	1.231
3-4	130	0.066	0.15	1.144
3-5	100	0.034	0.25	1.217
3-6	130	0.034	0.25	1.216
3-7	100	0.066	0.25	1.262
3-8	130	0.066	0.25	1.313

**Table 6.11 Calculated error and error percentage values for Ra prediction when down and up milling is used together**

Experiment Number	Predicted Ra value	Observed Average Ra value	Error	Error Percentage
3-1	1.124	1.121	0.003	0.28
3-2	1.141	1.137	0.004	0.35
3-3	1.234	1.231	0.002	0.19
3-4	1.148	1.144	0.004	0.34
3-5	1.219	1.217	0.003	0.24
3-6	1.220	1.216	0.004	0.28
3-7	1.263	1.262	0.001	0.06
3-8	1.316	1.313	0.003	0.25

**Table 6.12 The observed Ra values used to test the accuracy of Ra prediction formula**

Experiment Number	Cutting Speed (m/min)	Feed Per Tooth (mm/tooth)	Step Over (mm)	Ra 1 (μm)	Ra 2 (μm)	Ra 3 (μm)	Average Ra (μm)
1-5	115	0.050	0.200	1.171	1.175	1.169	1.171
4-2	110	0.050	0.150	1.118	1.164	1.152	1.145
4-5	122.5	0.058	0.225	1.271	1.263	1.253	1.262
4-6	107.5	0.042	0.175	1.191	1.186	1.172	1.183

Using these new test points an error analysis is done for the formula and the result of the analysis is given in Table 6.13. The error percentage values are 3.13%, 1.99%, 0.81% and 1.06% which are acceptable. These values show that this formulation can be used for this type of milling to predict the Ra values in the defined limits.

**Table 6.13 Calculated error and error percentage values for test experiments**

Experiment Number	Observed Average Ra value	Predicted Ra value	The error	The error percentage
1-5	1.171	1.208	0.037	3.13
4-2	1.145	1.167	0.023	1.99
4-5	1.262	1.252	0.010	0.81
4-6	1.183	1.170	0.013	1.06

## **CHAPTER 7**

### **CONCLUSIONS AND FUTURE WORK**

#### **7.1 Conclusions**

In this study, a methodology has been developed for prediction of surface roughness of curved cavities manufactured by 5-axes CNC milling. Initially, appropriate milling methods have been decided for machining of a particular curved cavity of a forging die, in Mazak 5-axes high speed CNC milling machine in METU BİLTİR Center then a mathematical model has been established about the relation of the average roughness ( $R_a$ ) values of the machined surface with the milling parameters, which are the cutting speed ( $V_c$ ), the feed per tooth ( $f_z$ ) and step over ( $a_e$ ).

The general conclusions of this study can be summarized as follows;

1) It was observed that, the surface texture was not uniform over the curved cavities of forging dies due to the different cutting speeds in 3-axes milling of curved cavities. However, uniform surface texture was obtained over the die cavity in 5-axes milling with an inclination angle. Therefore, 5-axes milling with an inclination angle is more favorable than 3-axes milling for machining of the selected curved surface of die cavity.

2) For the selected curved cavity of forging die surface, on which the experiments were performed, linear and circular cutting tool path strategies were compared and discussed in Chapter 5. It was seen that, cutting along linear path results with lower  $R_a$  values than cutting along circular paths.

3) According to the experimental results, using down and up milling together will decrease the cutting time significantly with respect to the down milling alone or up milling alone. Also the average  $R_a$  values used for the

comparison of these methods are close to each other. Therefore for the selected geometry, using down and up milling together is better.

4) According to the conclusions which are discussed in the above first three discussion items, it can be concluded that 5-axes milling with an inclination angle along linear tool path by using down and up milling together was found as the most proper approach to obtain better surface quality with lower cutting time, for the milling of the selected curved cavity of forging die.

5) In the second set of experiments, the average of measured Ra values are changing in between 0.885  $\mu\text{m}$  and 1.083  $\mu\text{m}$  and in the third set of experiments the average of measured Ra values are changing in between 1.144  $\mu\text{m}$  and 1.313  $\mu\text{m}$ , in the limits of selected cutting parameters. As the difference is small, cutting time may be more important in deciding the cutting parameters. As a result, in the defined limits of cutting parameters by using the selected cutting methods, choosing the highest cutting speed value, feed per tooth value and stepover value may be better as this will decrease the cutting time.

6) It has been also shown that the  $2^3$  factorial design of experiments combined with method of multiple linear regression may be applied to derive a mathematical model for the behavior of the surface roughness obtained in milling processes as a result of determined milling parameters (i.e. cutting speed, feed per tooth and step over). The advantage of this method is that the formula may be derived without performing a large number of experiments. Two set of experiments were performed and during each set, different milling methods were used. In the first case only down milling was used and in the second case both of the down and up milling was used together. A mathematical model is established for each set of experiment for prediction of average roughness (Ra). The resulting equations of the different milling conditions are derived in Chapter 6 and presented below.

Prediction formula for down milling is as seen in Equation 6.10;

$$\begin{aligned} Ra = & 2.47 - 0.0141 \cdot Vc - 31.8 \cdot fz - 7.75 \cdot ae + 0.248 \cdot Vc \cdot fz \\ & + 0.073 \cdot Vc \cdot fz + 171 \cdot fz \cdot ae - 1.35 \cdot Vc \cdot fz \cdot ae \end{aligned}$$

Prediction formula for down and up milling is as seen in Equation 6.21;

$$\begin{aligned} Ra = & -0.57 + 0.0133 \cdot Vc + 41.4 \cdot fz + 7.71 \cdot ae - 0.349 \cdot Vc \cdot fz \\ & - 0.0606 \cdot Vc \cdot ae - 182 \cdot fz \cdot ae + 1.615 \cdot Vc \cdot fz \cdot ae \end{aligned}$$

In Equations 6.10 and 6.21  $Ra$  is average surface roughness in  $\mu m$ , cutting speed ( $Vc$ ) is in m/min, the feed per tooth ( $fz$ ) is in mm/tooth, and the step over ( $ae$ ) in mm. Each formula which is derived in this study is suitable for the defined conditions and parameter limits used in this study. For different conditions and parameter limits, this methodology may be used to obtain prediction formulas which are proper for those situations.

7) The measured values of the average surface roughness, of the selected curved cavity of forging die surfaces, obtained by using down milling are compared with the predicted  $Ra$  values, calculated through Equation 6.10 and it was seen that the maximum error percentage is 2.94%. When the comparison is repeated for the  $Ra$  values predicted for a cutting process of down and up milling used together and calculated through Equation 6.21, the maximum error percentage is 3.13%. These results show that the mathematical model well predicts the  $Ra$  values for both of the set of experiments.

8) For both of the milling conditions that were analyzed, it was observed that the decrease of value of stepover is improves the surface roughness ( $Ra$ ) and the effect of the stepover on surface roughness is the most significant effect, among the main effects of the other milling parameters and effects of their interactions.

## 7.2 Future work

The proposals for the future work to this study may be listed as fallows:

1) If needed, the mathematical model obtained with this study can be further optimized with the statistical programs and the accuracy of the result may be compared with the results that are obtained from  $2^3$  Factorial design of experiments which is used in this study.

2) In the study, the most common used roughness parameter ( $Ra$ ) is analyzed and a mathematical model is derived for this parameter. Other roughness

parameters like Rz, Rmax or Rq can be measured on the machined surfaces and mathematical models may be derived for these parameters.

3) An experimental approach used in the study can be applied for other die materials, cutting tools and curved surfaces of die cavities.

4) The effects of milling parameters on tool life may be studied and ways to improve the tool life may be searched.

5) Precision forging may decrease the material cost and eliminate additional processes on the product. However, the geometric accuracies of forging die in the precision forging are very significant. Geometric accuracies of the curved surfaces of die cavities may be studied and effects of milling methods on the accuracy of die cavities may be analyzed.

6) Cutting forces, which occur during the machining of die cavities, may be analyzed in different milling methods.



## REFERENCES

- [1] Tunç Mehmet, "Computerized cost estimation for forging industry" M. S. Thesis, Middle East Technical University, Ankara, Turkey, 2003
- [2] Altan Taylan, Lilly Blaine, Yen Y.C., (2001) "Manufacturing of Dies and Molds", Ann. CIRP, 50/2, pp.405
- [3] Lou Mike S., Chen Joseph C., Li Caleb M. (1998) "Surface Roughness Prediction Technique For CNC End-Milling", Journal of Industrial Technology, Vol. 15
- [4] Boothroyd Geoffrey, Knight Winston A., (1989) "Fundamentals of machining and machine tools", second edition, New York : Marcel Dekker
- [5] Ghanem F., Braham C., Sidhom H., ( 2003) "Influence of steel type on electrical discharge machined surface integrity", Journal of Materials Processing Technology, Vol. 142, Issue 1 , pp. 163-173.
- [6] Cusanelli G. , Hessler-Wyser A., Bobard F. , Demellayer R. , Perez R. , Flükiger R., (2004) "Microstructure at submicron scale of the white layer produced by EDM technique", Journal of Materials Processing Technology, Vol. 149, pp. 289-295
- [7] Ngan Chiu-Chun, Tam Hon-Yuen, (2004) "A non-contact technique for the on-site inspection of molds and dies polishing", Journal of Materials Processing Technology Vol.155, pp. 1184–1188
- [8] Aksan Steel Forging Company, Ankara, Turkey

- [9] Degarmo E. Paul, Black J. Temple, Kohser Ronald A., (1984) “Materials and process in manufacturing”, sixth edition, New York : Macmillan
  
- [10] Cengiz Ender, “Development of postprocessor, simulation and verification software for a five-axis CNC milling machine” M. S. Thesis, Middle East Technical University, Ankara, Turkey, 2005
  
- [11] G-Post (ProEngineer NC Postprocessing module) manual
  
- [12] Baptista R., Antune Simoes J.F., (2000), “Three and five axes milling of sculptured surfaces”, Journal of Materials Processing Technology, Vol. 103, pp. 398-403
  
- [13] Ko T. J., Kim H. S. and Lee S. S. (2001) “Selection of the Machining Inclination Angle in High-Speed Ball End milling”, The International Journal of Advanced manufacturing Technology, Vol 17, pp 163–170
  
- [14] Bouzakis D., Efstathiou K., Aichouh P., (2003) “Determination of the chip geometry, cutting force and roughness in free form surfaces finishing milling, with ball end tools”, International Journal of Machine Tools and Manufacture, Vol. 43, Number 5, pp. 499-514
  
- [15] Vivancos J., Luis C.J., Costa L., Ortiz J.A., (2004) “Optimal machining parameters selection in high speed milling of hardened steels for injection moulds”, Journal of Materials Processing Technology, Vol. 155, pp. 1505–1512
  
- [16] Precision Devices, Inc., *web site*: “<http://www.predev.com>” *last accessed*: March 2007

- [17] Broadstone J. A., (1968) "Control of surface quality" ,Surface checking gage company, USA
  
- [18] Karabay Macit "Lecture Notes on Engineering Metrology and Quality Control", Middle East Technical University, Mechanical Engineering Department, Ankara, 2003, pp 61-73
  
- [19] Thomas T.R., (1982) "Rough surfaces", New York : Longman
  
- [20] Mahr Federal Inc., *web site* : "<http://www.mahr.com>" *last accessed:* March 2007
  
- [21] Taylor Hobson Ltd., *web site* : "<http://www.taylor-hobson.com>" *last accessed:* March 2007
  
- [22] Montgomery D.C., (2001), "Design and Analysis of Experiments", Fifth Edition, New York : Wiley
  
- [23] İlkün Özkan, "Effects of Production Parameters on Porosity and Hole Properties in Laser Sintering Rapid Prototyping Process", M. S. Thesis, Middle East Technical University, Ankara, Turkey, 2005
  
- [24] Myers Raymond H., Montgomery Douglas C., (1995) "Response Surface Methodology, process and product optimization using designed experiments" New York : Wiley
  
- [25] Iscar The Concise Catalog of Metal Working Tools (2004)"Complete Machining Solutions"

- [26] Krajnik P., Kopa J., (2004) “Modern machining of die and mold tools”, Journal of Materials Processing Technology, 157-158, pp. 543–552
- [27] Personal Communication with Mr. Ali Murat Sağlam from ISCAR Kesici Takım Tic. ve İml. Ltd. Şti.
- [28] Vericut Software, *web site*: <http://www.cgtech.com>, *last accessed*: February 2007
- [29] Cakir M. Cemal, Irfan Ozgur, Cavdar Kadir, (2005) “An expert system approach for die and mold making operations”, Robotics and Computer-Integrated Manufacturing, Vol. 21, Pp. 175–183.
- [30] Kecelj B., Kopac J., Kampus Z., Kuzman K., (2004) “Speciality of HSC in manufacturing of forging dies”, Journal of Materials Processing Technology, 157-158, pp. 536–542
- [31] Fitzpatric Michael, (2005) “Machining and CNC technology”, MC Graw Hill
- [32] Operating Manual of “Taylor Hobson’s Talysurf PGI” stylus type surface roughness measuring machine
- [33] Personal Communication with Mr. Selahattin Çetin from ORS Quality Department
- [34] Operating Manual of “Mazak Variaxis 630-5X” CNC milling machine
- [35] Engineering Fundamentals, *web site* : “<http://www.efunda.com/materials>”, *last accessed*: April 2007

## APPENDIX A

### MATERIAL LEFT THICKNESSES AT THE STAIRCASE TIPS

For the die geometry which is described in Figure 4.12, the thickness of materials left after the rough cut between the staircase tips and die surface are given in Table A.1.

**Table A.1 Material left thicknesses at the staircase tips when the tool is cutting with 15° inclination angle**

Number of Stair Tip	Material left Thickness (mm)	Number of Stair Tip	Material left Thickness (mm)	Number of Stair Tip	Material left Thickness (mm)
1	0.156	33	0.204	65	0.253
2	0.158	34	0.206	66	0.254
3	0.159	35	0.207	67	0.256
4	0.161	36	0.209	68	0.258
5	0.162	37	0.210	69	0.259
6	0.164	38	0.212	70	0.261
7	0.165	39	0.213	71	0.262
8	0.167	40	0.215	72	0.264
9	0.168	41	0.217	73	0.265
10	0.170	42	0.218	74	0.267
11	0.171	43	0.220	75	0.268
12	0.173	44	0.221	76	0.270
13	0.174	45	0.223	77	0.271
14	0.176	46	0.224	78	0.273
15	0.177	47	0.226	79	0.274
16	0.179	48	0.227	80	0.276
17	0.180	49	0.229	81	0.277
18	0.182	50	0.230	82	0.279
19	0.183	51	0.232	83	0.280
20	0.185	52	0.233	84	0.282
21	0.186	53	0.235	85	0.283
22	0.188	54	0.236	86	0.285
23	0.189	55	0.238	87	0.286
24	0.191	56	0.239	88	0.288
25	0.192	57	0.241	89	0.289
26	0.194	58	0.242	90	0.291
27	0.195	59	0.244	91	0.293
28	0.197	60	0.245	92	0.294
29	0.198	61	0.247	93	0.296
30	0.200	62	0.248	94	0.297
31	0.201	63	0.250	95	0.299
32	0.203	64	0.251	96	0.300

## APPENDIX B

### EXAMPLES OF MILLING REPORTS OF VERICUT

In the reports of Vericut analysis program the excess material and gauge amounts may be seen numerically with their positions. Example reports are as follows;

#### B.1 Cutting report of Vericut when linear path is used with 0.25 mm stepover

AUTO-DIFF Surface Report

Comparison Type: Gouge and Excess  
Gouge Tolerance: 0.001  
Excess Tolerance: 0.001  
Gouge Check Distance: 1  
Excess Check Distance: 1

DESIGN COMPONENT(S) :

Component Name: Design  
Component Type: Design  
Model Type: POLYGON (eye bolt-m24-ak139-5eksen-2.ply)

SUMMARY:  
No error records to report

Record Number	Deviation	Gouge Location	Toolpath
Record	Tool ID		

#### B.2 Cutting report of Vericut when circular path is used with 0.25 mm stepover

AUTO-DIFF Surface Report

Comparison Type: Gouge and Excess  
Gouge Tolerance: 0.001  
Excess Tolerance: 0.001  
Gouge Check Distance: 1  
Excess Check Distance: 1

DESIGN COMPONENT(S):

Component Name: Design  
Component Type: Design  
Model Type: POLYGON (eye bolt-m24-ak139-5eksen-2.ply)

SUMMARY:  
Maximum gouge of 0.005924 occurred at record 888  
Number of Gouges: 6  
Maximum excess of 0.103667 occurred at record 3495  
Number of Excesses: 3184

Record Number	Deviation	Gouge Location	Toolpath	Record	Tool ID
11	0.02073		manus-atez-5eksen-isY45.159Z22.584A-73.52		
13	0.01777		manus-atez-5eksen-isY44.409Z20.249A-70.72		
14	0.01777		manus-atez-5eksen-isY43.992Z19.096A-69.32		
15	0.02073		manus-atez-5eksen-isY43.546Z17.954A-67.92		
16	0.02073		manus-atez-5eksen-isY43.073Z16.823A-66.52		
17	0.01777		manus-atez-5eksen-isY42.572Z15.704A-65.12		

18	0.02073	manus-atez-5eksen-isY42.043Z14.598A-63.72
19	0.01777	manus-atez-5eksen-isY41.488Z13.505A-62.32
20	0.02073	manus-atez-5eksen-isY40.906Z12.426A-60.92
21	0.01777	manus-atez-5eksen-isY40.297Z11.362A-59.52
22	0.01777	manus-atez-5eksen-isY39.663Z10.312A-58.12
23	0.01777	manus-atez-5eksen-isY39.003Z9.279A-56.712
24	0.01777	manus-atez-5eksen-isY38.318Z8.262A-55.312
25	0.01777	manus-atez-5eksen-isY37.608Z7.263A-53.902
26	0.01777	manus-atez-5eksen-isY36.874Z6.281A-52.5 2
27	0.01777	manus-atez-5eksen-isY36.116Z5.317A-51.092
28	0.01777	manus-atez-5eksen-isY35.335Z4.372A-49.682
29	0.01777	manus-atez-5eksen-isY34.533Z3.447A-48.2812
30	0.01777	manus-atez-5eksen-isY33.703Z2.542A-46.872
31	0.01481	manus-atez-5eksen-isY32.854Z1.657A-45.462
32	0.01777	manus-atez-5eksen-isY31.984Z.794A-44.0632
33	0.01481	manus-atez-5eksen-isY31.093Z-.048A-42.652
34	0.01481	manus-atez-5eksen-isY30.181Z-.868A-41.252
35	0.01481	manus-atez-5eksen-isY29.252Z-1.665A-39.842
36	0.01481	manus-atez-5eksen-isY28.299Z-2.439A-38.42
37	0.01481	manus-atez-5eksen-isY27.332Z-3.19A-37.0312
38	0.01777	manus-atez-5eksen-isY26.342Z-3.917A-35.62
39	0.01185	manus-atez-5eksen-isY25.337Z-4.619A-34.22
.		
.		
.		
868	0.01777	manus-atez-5eksen-isY8.591Z-11.965A-13.12
869	0.01481	manus-atez-5eksen-isY7.393Z-12.229A-11.72
870	0.01481	manus-atez-5eksen-isY6.19Z-12.464A-10.312
871	0.01481	manus-atez-5eksen-isY4.981Z-12.668A-8.902
872	0.01481	manus-atez-5eksen-isY3.768Z-12.844A-7.5 2
873	0.02962	manus-atez-5eksen-isY2.55Z-12.989A-6.0942
874	0.01185	manus-atez-5eksen-isY1.33Z-13.105A-4.6882
875	0.01481	manus-atez-5eksen-isY.107Z-13.19A-3.281 2
876	0.01185	manus-atez-5eksen-isY-1.118Z-13.245A-1.82
877	0.00889	manus-atez-5eksen-isY-2.344Z-13.271A-.462
878	0.00592	manus-atez-5eksen-isY-3.57Z-13.266A.938 2
888	-0.00592	manus-atez-5eksen-isY-15.682Z-11.574A15.2
973	0.02370	manus-atez-5eksen-isY45.159Z22.584A-73.52
974	0.02370	manus-atez-5eksen-isY44.798Z21.412A-72.12
975	0.02370	manus-atez-5eksen-isY44.409Z20.249A-70.72
976	0.02073	manus-atez-5eksen-isY43.992Z19.096A-69.32
977	0.02370	manus-atez-5eksen-isY43.546Z17.954A-67.92
978	0.02370	manus-atez-5eksen-isY43.073Z16.823A-66.52
979	0.04443	manus-atez-5eksen-isY42.572Z15.704A-65.12
.		
.		
.		
5889	0.01777	manus-atez-5eksen-isY21.154Z-7.174A-28.52
5890	0.01185	manus-atez-5eksen-isY20.07Z-7.748A-27.182
5891	0.01185	manus-atez-5eksen-isY18.973Z-8.295A-25.72
5892	0.01481	manus-atez-5eksen-isY17.863Z-8.815A-24.32
5893	0.01481	manus-atez-5eksen-isY16.74Z-9.307A-22.962
5894	0.01777	manus-atez-5eksen-isY15.606Z-9.772A-21.52
5895	0.01185	manus-atez-5eksen-isY14.46Z-10.209A-20.12
5896	0.01185	manus-atez-5eksen-isY13.304Z-10.618A-18.2
5897	0.00889	manus-atez-5eksen-isY12.138Z-10.998A-17.2
5898	0.01185	manus-atez-5eksen-isY10.964Z-11.349A-15.2
5899	0.00889	manus-atez-5eksen-isY9.781Z-11.672A-14.52
5900	0.01185	manus-atez-5eksen-isY8.591Z-11.965A-13.12
5901	0.00889	manus-atez-5eksen-isY7.393Z-12.229A-11.72
5902	0.00592	manus-atez-5eksen-isY6.19Z-12.464A-10.312
5903	0.00889	manus-atez-5eksen-isY4.981Z-12.668A-8.902
5904	0.00592	manus-atez-5eksen-isY3.768Z-12.844A-7.5 2
5905	0.00592	manus-atez-5eksen-isY2.55Z-12.989A-6.0942

## APPENDIX C

### MAZAK VARIAXIS 630-5X CNC MILLING CENTER

The high-performance vertical machining center VARIAXIS 630-5X is one of the models of Yamazaki Mazak. This model is designed targeting high speed and high accuracy. In the production of wide variety of parts in small- to medium-lot size, shorter cycle time is achieved by reduced idle time which is made possible by super-high speed operation and full usage of the latest tool and high-speed machining technology [34]. Linear guides are used for the X-, Y- and Z-axis slide ways to provide high rigidity to ensure high accuracy in high-speed operation. Positioning accuracy is  $\pm 3 \mu\text{m}$  and repeatability  $\pm 1 \mu\text{m}$  [34]. X, Y and Z are the linear axes. A axis denotes rotational axis around X axis and C axis denotes rotational axis around Y axis.

Machine properties are defined below:

Maximum feed rate is 50 m/min (1969 IPM)	C axis rotation $360^{\circ}$
Maximum speed of spindle $25000 \text{ min}^{-1}$ (rpm)	A axis rotation $150^{\circ} (-120^{\circ} / +30^{\circ})$
Maximum spindle power 30HP	X axis working limit 630mm
Maximum workpiece weight 500kg	Y axis working limit 765mm
Magazine of 30-tool capacity	Z axis working limit 510mm



**Figure C.1 Mazak Variaxes 630-5X milling center**



## APPENDIX D

### PROPERTIES OF DIE MATERIAL

The properties of the steel DIN 2344 which is used in this study is as follows [35];

**Table D.1 Material category**

<b>Class</b>	Tool steel	
<b>Type</b>	Chromium hot work steel	
<b>Designations</b>	<b>France:</b>	AFNOR Z 40 COV 5
	<b>Germany:</b>	DIN 1.2344
	<b>Italy:</b>	UNI KU
	<b>Japan:</b>	JIS SKD61
	<b>Sweden:</b>	SS 2242
	<b>United Kingdom:</b>	B.S. BH 13
	<b>United States:</b>	ASTM A681 , FED QQ-T-570 , SAE J437, SAE J438 , SAE J467 , UNS T20813

**Table D.2 Material composition**

<b>Element</b>	<b>Weight %</b>
C	0.32-0.45
Mn	0.20-0.50
Si	0.80-1.20
Cr	4.75-5.50
Ni	0.3
Mo	1.10-1.75
V	0.80-1.20
Cu	0.25
P	0.03
S	0.03

**Table D.3 Material mechanical properties**

<b>Properties</b>		<b>T (°C)</b>
<b>Density</b> ( $\times 1000 \text{ kg/m}^3$ )	7,76	25
<b>Poisson's Ratio</b>	0.27-0.30	25
<b>Elastic Modulus</b> (GPa)	190-210	25

**Table D.4 Material thermal properties**

<b>Conditions</b>	<b>Thermal Expansion</b>
<b>T (°C)</b>	<b>Coeff. (<math>10^{-6}/^{\circ}\text{C}</math>)</b>
20-100	10.4
20-200	11.5
20-425	12.2
20-540	12.4
20-650	13.1
<b>Conditions</b>	<b>Thermal Conductivity</b>
<b>T (°C)</b>	<b>(W/m-K)</b>
<b>215</b>	28.6
350	28.4
475	28.4
605	28.7

## APPENDIX E

### CALCULATION OF VARIABLE COEFFICIENTS

Coefficient of variables are calculated by using least square methods to derive mathematical model for Ra prediction of curved surfaces of a particular die cavity when only down milling and down and up milling used together.

#### E.1 Mathematical Model for Down Milling

Calculation of variable coefficients of Ra prediction formula when down milling is used within the chosen parameters limits.

According to the Table 6.4, the X and y (Ra) matrixes are

$$X := \begin{matrix} & X_1 & X_2 & X_3 & X_4 & X_5 & X_6 & X_7 \\ \begin{pmatrix} 1 & 100 & 0.034 & 0.15 & 3.4 & 15 & 0.0051 & 0.51 \\ 1 & 130 & 0.034 & 0.15 & 4.42 & 19.5 & 0.0051 & 0.663 \\ 1 & 100 & 0.066 & 0.15 & 6.6 & 15 & 0.0099 & 0.99 \\ 1 & 130 & 0.066 & 0.15 & 8.58 & 19.5 & 0.0099 & 1.287 \\ 1 & 100 & 0.034 & 0.25 & 3.4 & 25 & 0.0085 & 0.85 \\ 1 & 130 & 0.034 & 0.25 & 4.42 & 32.5 & 0.0085 & 1.105 \\ 1 & 100 & 0.066 & 0.25 & 6.6 & 25 & 0.0165 & 1.65 \\ 1 & 130 & 0.066 & 0.25 & 8.58 & 32.5 & 0.0165 & 2.145 \end{pmatrix} \end{matrix} \quad Ra := \begin{pmatrix} 0.941 \\ 0.893 \\ 0.890 \\ 0.885 \\ 1.019 \\ 1.052 \\ 1.083 \\ 1.029 \end{pmatrix}$$

The  $X^T X$  matrix is

$$X^T \cdot X = \begin{pmatrix} 8 & 920 & 0.4 & 1.6 & 46 & 184 & 0.08 & 9.2 \\ 920 & 107600 & 46 & 184 & 5380 & 21520 & 9.2 & 1076 \\ 0.4 & 46 & 0.022 & 0.08 & 2.536 & 9.2 & 0.004 & 0.507 \\ 1.6 & 184 & 0.08 & 0.34 & 9.2 & 39.1 & 0.017 & 1.955 \\ 46 & 5380 & 2.536 & 9.2 & 296.546 & 1076 & 0.507 & 59.309 \\ 184 & 21520 & 9.2 & 39.1 & 1076 & 4573 & 1.955 & 228.65 \\ 0.08 & 9.2 & 0.004 & 0.017 & 0.507 & 1.955 & 0.001 & 0.108 \\ 9.2 & 1076 & 0.507 & 1.955 & 59.309 & 228.65 & 0.108 & 12.603 \end{pmatrix}$$

The inverse of  $X^T X$  matrix is

$$\left( X^T \cdot X \right)^{-1} = \begin{pmatrix} 1367.53 & -11.69 & -24810.11 & -6435.45 & 212.13 & 55.02 & 116753.47 & -998.26 \\ -11.69 & 0.1 & 212.13 & 55.02 & -1.84 & -0.48 & -998.26 & 8.68 \\ -24810.11 & 212.13 & 496202.26 & 116753.47 & -4242.62 & -998.26 & -2335069.44 & 19965.28 \\ -6435.45 & 55.02 & 116753.47 & 32177.26 & -998.26 & -275.12 & -583767.36 & 4991.32 \\ 212.13 & -1.84 & -4242.62 & -998.26 & 36.89 & 8.68 & 19965.28 & -173.61 \\ 55.02 & -0.48 & -998.26 & -275.12 & 8.68 & 2.39 & 4991.32 & -43.4 \\ 116753.47 & -998.26 & -2335069.44 & -583767.36 & 19965.28 & 4991.32 & 11675347.22 & -99826.39 \\ -998.26 & 8.68 & 19965.28 & 4991.32 & -173.61 & -43.4 & -99826.39 & 868.06 \end{pmatrix}$$

And the  $X^T Ra$  vector is,

$$X^T \cdot Ra = \begin{pmatrix} 7.792 \\ 894.97 \\ 0.3893 \\ 1.5871 \\ 44.7048 \\ 182.3185 \\ 0.0794 \\ 9.1148 \end{pmatrix}$$

As the least square estimate of  $\beta$  is

$$\beta = (X^T X)^{-1} X^T Ra$$

$$\left( X^T \cdot X \right)^{-1} \cdot \left( X^T \cdot Ra \right) = \begin{pmatrix} 2.4694 \\ -0.0141 \\ -31.776 \\ -7.746 \\ 0.2479 \\ 0.073 \\ 171.3542 \\ -1.3542 \end{pmatrix}$$

As a result of the least square calculations, the mathematical model for down milling is obtained as;

$$\begin{aligned} Ra = & 2.47 - 0.0141x_1 - 31.8x_2 - 7.75x_3 \\ & + 0.248x_4 + 0.073x_5 + 171x_6 - 1.35x_7 \end{aligned} \quad (E.1)$$

## E.2 Mathematical Model for Down and Up Milling

Calculation of variable coefficients of Ra prediction formula when down and up milling is used together within the chosen parameters limits.

According to the Table 6.10, the X and y (Ra) matrixes are,

$$X := \begin{matrix} & \begin{matrix} X_1 & X_2 & X_3 & X_4 & X_5 & X_6 & X_7 \end{matrix} \\ \begin{pmatrix} 1 & 100 & 0.034 & 0.15 & 3.4 & 15 & 0.0051 & 0.51 \\ 1 & 130 & 0.034 & 0.15 & 4.42 & 19.5 & 0.0051 & 0.663 \\ 1 & 100 & 0.066 & 0.15 & 6.6 & 15 & 0.0099 & 0.99 \\ 1 & 130 & 0.066 & 0.15 & 8.58 & 19.5 & 0.0099 & 1.287 \\ 1 & 100 & 0.034 & 0.25 & 3.4 & 25 & 0.0085 & 0.85 \\ 1 & 130 & 0.034 & 0.25 & 4.42 & 32.5 & 0.0085 & 1.105 \\ 1 & 100 & 0.066 & 0.25 & 6.6 & 25 & 0.0165 & 1.65 \\ 1 & 130 & 0.066 & 0.25 & 8.58 & 32.5 & 0.0165 & 2.145 \end{pmatrix} \end{matrix} \quad Ra := \begin{pmatrix} 1.121 \\ 1.137 \\ 1.231 \\ 1.144 \\ 1.217 \\ 1.216 \\ 1.262 \\ 1.313 \end{pmatrix}$$

The  $X^T X$  matrix is

$$X^T \cdot X = \begin{pmatrix} 8 & 920 & 0.4 & 1.6 & 46 & 184 & 0.08 & 9.2 \\ 920 & 107600 & 46 & 184 & 5380 & 21520 & 9.2 & 1076 \\ 0.4 & 46 & 0.022 & 0.08 & 2.536 & 9.2 & 0.004 & 0.507 \\ 1.6 & 184 & 0.08 & 0.34 & 9.2 & 39.1 & 0.017 & 1.955 \\ 46 & 5380 & 2.536 & 9.2 & 296.546 & 1076 & 0.507 & 59.309 \\ 184 & 21520 & 9.2 & 39.1 & 1076 & 4573 & 1.955 & 228.65 \\ 0.08 & 9.2 & 0.004 & 0.017 & 0.507 & 1.955 & 0.001 & 0.108 \\ 9.2 & 1076 & 0.507 & 1.955 & 59.309 & 228.65 & 0.108 & 12.603 \end{pmatrix}$$

The inverse of  $X^T X$  matrix is

$$(X^T \cdot X)^{-1} = \begin{pmatrix} 1367.53 & -11.69 & -24810.11 & -6435.45 & 212.13 & 55.02 & 116753.47 & -998.26 \\ -11.69 & 0.1 & 212.13 & 55.02 & -1.84 & -0.48 & -998.26 & 8.68 \\ -24810.11 & 212.13 & 496202.26 & 116753.47 & -4242.62 & -998.26 & -2335069.44 & 19965.28 \\ -6435.45 & 55.02 & 116753.47 & 32177.26 & -998.26 & -275.12 & -583767.36 & 4991.32 \\ 212.13 & -1.84 & -4242.62 & -998.26 & 36.89 & 8.68 & 19965.28 & -173.61 \\ 55.02 & -0.48 & -998.26 & -275.12 & 8.68 & 2.39 & 4991.32 & -43.4 \\ 116753.47 & -998.26 & -2335069.44 & -583767.36 & 19965.28 & 4991.32 & 11675347.22 & -99826.39 \\ -998.26 & 8.68 & 19965.28 & 4991.32 & -173.61 & -43.4 & -99826.39 & 868.06 \end{pmatrix}$$

The  $X^T Ra$  vector is

$$X^T \cdot Ra = \begin{pmatrix} 9.641 \\ 1108.4 \\ 0.4862 \\ 1.947 \\ 55.8843 \\ 223.927 \\ 0.0982 \\ 11.2934 \end{pmatrix}$$

According to the least square estimate the  $\beta$  is [22]

$$\beta = (X^T X)^{-1} X^T Ra$$

$$\left( X^T \cdot X \right)^{-1} \cdot \left( X^T \cdot Ra \right) = \begin{pmatrix} -0.57 \\ 0.0133 \\ 41.4323 \\ 7.7069 \\ -0.3495 \\ -0.0606 \\ -181.7708 \\ 1.6146 \end{pmatrix}$$

As a result of the least square calculations, the mathematical model for down and up milling is obtained as;

$$Ra = -0.57 + 0.0133x_1 + 41.4x_2 + 7.71x_3 - 0.349x_4 - 0.0606x_5 - 182x_6 + 1.615x_7 \quad (E.2)$$